2022

Role of biological clocks in ant behavioral plasticity and parasitic manipulation of ant behavior

Biplabendu Das
University of Central Florida

ROLE OF BIOLOGICAL CLOCKS IN ANT BEHAVIORAL PLASTICITY AND PARASITIC MANIPULATION OF ANT BEHAVIOR

by

BIPLABENDU DAS
B.S., Indian Institute of Science, 2016
M.S., Indian Institute of Science, 2017

A dissertation submitted in partial fulfillment of the requirements
for the degree of Doctor of Philosophy
in the Department of Biology
in the College of Sciences
at the University of Central Florida
Orlando, Florida

Spring Term
2022

Major Professor: Charissa de Bekker

ABSTRACT

Living organisms exhibit daily rhythms as a way to anticipate predictable fluctuations in their environment. Such daily rhythmicity is the phenotypic outcome of oscillating genes and proteins, driven by an endogenous biological clock. Clock-controlled behavioral rhythms are inherently “flexible” since their phase, amplitude, and period can change throughout an animal’s life hallmarked by changes in so-called chronotype. How this inherent plasticity of clock-controlled rhythms is linked to plasticity of behavior is still an open question in biology. Characterizing the various mechanistic links between plasticity of the animal clock and behavioral state will not only shed light on the molecular underpinnings of animal behavior, but also lead to novel chronotherapeutic interventions to treat human disorders that affect the behavioral state such as bipolar disorder and Alzheimer's. While clock-controlled behavioral plasticity is crucial to a species’ survival and fitness, it has also been hypothesized to be a target for manipulative parasites that need to induce timely changes in host behavior to facilitate growth and transmission. Using the Florida carpenter ant *Camponotus floridanus* as a model, this dissertation attempts to bridge some of the existing knowledge gaps in sociobiology, chronobiology, and parasitology.

In the first chapter, we have identified a mechanistic link between plasticity of the *C. floridanus* clock and its behavioral state. Subsequently, in chapter two, we have provided evidence showing that *Ophiocordyceps camponoti-floridani*, a fungal parasite

that induces timely changes in *C. floridanus* behavior targets the pre-existing links between host behavior and chronobiological plasticity we have found in chapter one. In the final chapter, we characterize how the clock of *O. camponoti-floridani* functionally differs from the clock of a non-manipulating fungal parasite, *Beauveria bassiana*, and put forward a regulatory mechanism via which the manipulating parasite's clock might be inducing timely changes in host behavior.

For maa, babu, and bultu.

ACKNOWLEDGMENTS

I would like to thank my advisor, Charissa de Bekker, for introducing me to the fascinating world of biological rhythms and for giving me the scientific freedom to grow into an independent researcher. I would like to thank my dear friend and collaborator, Ian Will, without whose guidance and support this dissertation would not have been possible. I would also like to thank my committee members Josh King, Laurie von Kalm, and Sarah Bengston for being supportive and kind throughout my journey as a graduate student; Ken Fedorka, who was very kind to me as graduate coordinator; Bob Fitak, who let me ramble on about network analyses; Brianna, Zaynah, Roos, and Rowan, who have toiled alongside me and also taught me how to be a better mentor. Finally, I would like to thank all the amazing people within and outside our lab who have helped me collect ant colonies for my experiments.

To maa, babu, and bultu, I owe everything. Graduate school has allowed me to meet some of the most supportive people – Ian, Vero, Leo, Bryan, Nick, and Thienthanh – all of whom I can gladly call family.

And last, but not the least, I would like to thank Alicia for being a true friend and a loving partner for the last three years.

TABLE OF CONTENTS

LIST OF FIGURES

LIST OF TABLES

LIST OF ADDITIONAL FILES

GENERAL INTRODUCTION

Living organisms exhibit daily rhythms in physiology and behavior as a way to anticipate predictable fluctuations in their environment [1, 2]. Such predictable daily rhythms are ubiquitous in living organisms, from unicellular cyanobacteria to the multicellular blue whale [3, 4]. These rhythms are emergent properties of endogenous molecular clocks that entrain to external time cues, also known as Zeitgebers. A Zeitgeber can be both abiotic (e.g., light and temperature cycles) and biotic (e.g., presence of food and predators) [5, 6]. At the cellular level, clocks of fungi and animals consist of an autoregulatory Transcription-Translation Feedback Loop (TTFL) that requires around (*circa*) 24 hours (*dia*) to complete one cycle, and hence is called a circadian clock. The clock drives daily oscillations in gene expression and protein abundances that in turn drive behavioral rhythms such as locomotion, even in the absence of external cues [3]. The circadian TTFL is considered to be an ancient timekeeping mechanism conserved in plants, animals and fungi; insects are no exception [1, 7]. In the insect model organism, *Drosophila melanogaster*, the TTFL consists of the activator complex CLK-CYC (BMAL1-CLOCK in mammals) that binds to and activates transcription of the repressor gene *Period* (*Per*) (Fig. 1A). PER heterodimerizes with TIM (CRY in mammals), translocates into the nucleus and inhibits the activator complex, thus closing the feedback loop [8-10]. This core loop is further coupled with multiple phosphorylation-dephosphorylation cycles, that are necessary for a functional 24-hour clock. In most studied model organisms so far, light is usually the strongest Zeitgeber that synchronizes and entrains the cell-autonomous clocks within an organism [11, 12]. However, there is evidence that temperature cues and social behaviors could be more potent than photic entrainment in highly social animals such as bees [13-15]. Regardless of the entrainment

pathway, the output of an entrained clock can be studied at multiple levels of biological organization, from rhythmic expression of genes at the molecular level (e.g., clock-controlled genes) to daily rhythms in behavior at the organismal level (e.g., locomotion). In social insects, such as ants and bees, clock-controlled rhythms can be observed at the colony level as well, in the form of synchronized social behaviors such as group-foraging (Fig. 1B). Clock-controlled behavioral rhythms are "plastic"; the peak times (phases) of several daily rhythms including sleep and hunger have been found to vary among individuals. These characteristic daily timings, also referred to an individual's chronotype, show predictable changes with age [16-18]. For example, an average human reaches their latest chronotype (*night-owl*-like) during the late teenage years. As they age, the "lateness" steadily decreases, reaching their earliest chronotype (*early-bird*-like) during late adulthood. Insects also show age-correlated changes in behavioral rhythms [19]. Ants and honeybees, two independently evolved social insect lineages, live in societies where young individuals specialize on intranidal tasks including brood care which they perform around-the-clock with no apparent daily rhythms in activity levels. As brood-tending ants age, they show changes in physiology and behavioral traits, eventually transitioning into rhythmically active forager-like ants that perform the bulk of extranidal tasks foraging for food [20-23]. In addition to age-correlated changes, the timing of daily behavior can also be affected by infectious diseases. For example, the parasite that causes sleeping sickness in humans, *Trypanosoma brucei*, is capable of altering mammalian activity rhythms (studied in mice) most likely through disruption in clock-controlled gene expression [24]. A lot is still unknown about how rhythmic processes at the organismal and colony/group level emerge from simple cellular oscillators, or how the timing of an organism's daily activities is affected by age or disease-causing agents. Understanding the role of parasite-host clock interactions in infectious disease

outcomes has the potential to improve treatment of human diseases through discovery of novel ways to disrupt parasite growth and transmission, as well as devise better biocontrol strategies by understanding the daily variation in parasitic virulence and host immunity [25, 26].

Parasites are always engaged in an evolutionary arms race with their host species. One result of such evolutionary process is a high diversity of parasitic infection strategies and host defense mechanisms that exist in nature. Thus far, it is well established that the internal clocks of living organisms drive daily rhythms in immune function [25, 27, 28]. For example, innate defenses in mammals have been found to peak during the active phase while repair mechanisms peak during the rest phase [27]. Previous studies have shown that parasites also have intrinsic clocks, and that parasite clocks can entrain to and even disrupt host rhythms in order to maximize within-host survival and between-host transmission [29-31]. This tug-of-war between parasite and host rhythms gets even more interesting when the parasite's transmission depends on adaptively changing host behavior. It has been hypothesized that such parasitic manipulation of host behavior is achieved, at least partially, by breaking into the neural pathways that allow for behavior to be plastic. In the words of Webster and Adamo, "If the mind is merely a machine, then it can be controlled by any entity that understands the code and has access to the machinery" [32, 33]. An emerging model system to study parasitic manipulation of host behavior are the *Ophiocordyceps* fungi that infect ants. For my dissertation, I have focused on one such *Ophiocordyceps*-ant pair that is native to Central Florida, involving the carpenter ant *Camponotus floridanus* (host, also referred to as Cflo throughout the document) and their specialist manipulator *Ophiocordyceps camponoti-floridani* (parasite; *Ocflo*). In controlled laboratory experiments, we found no apparent behavioral changes in infected *C. floridanus* in the early stages (one-two weeks post infection) [34]. However, during the final stages of the

infection, two to four weeks post infection, the infected ant displays characteristic behavioral changes, consistent with field and laboratory observations from other *Ophiocordyceps*-ant pairs [35]. The "manipulated" state is characterized by enhanced locomotory activity (ELA or *hyperactivity*), increased wandering behavior, and severe convulsions ([34, 35]; personal observations). In the final stages of this "manipulated" state, the convulsing ant shows a "summiting" behavior where they bite into a substrate, lock their mandibles into a "death-grip", and die shortly after [36]. Once the ant dies, the fungus utilizes the ant tissues as carbon source to grow a stalk, from which a fruiting body emerges that disseminates spores necessary for the next round of infections - the cycle continues. There is evidence that suggest that the "manipulated" biting outside the nest is adaptive to the fungus and that the location of biting is light-dependent [37, 38]. When offered the choice between a shaded (experimental) and an unshaded (control) plot, new biters preferred unshaded control plots with higher light levels [37]. Among the ants that did bite in the shaded areas, the majority did so at the borders, and usually at higher elevations suggesting potential phototropism [37]. Additionally, the biters in the shaded plots showed significantly lower fruiting body growth, the latter being necessary for completion of the parasite's life cycle. It has been suggested that such spatial preference is an extended phenotype of the parasite, allowing an optimal micro-climate for fungal growth and dispersal [39]. Light, therefore, seems to be an important abiotic cue that ensures that the manipulated ants end up in the right place, at the right time.

Field observations in Thailand showed that the "manipulated" biting is highly synchronized to solar noon [36]. Controlled lab studies with two completely different *Ophiocordyceps*-ant pairs revealed a similar time-of-day synchronized "manipulated" biting [34, 35]. Even though a near-solar noon biting has been observed in the field for "manipulated" *C.*

floridanus ants (n=4), laboratory infections produced a synchronized biting right before lights turned on (pre-dawn) [34]. It has been suggested that a difference in entrainment conditions inside the lab compared to naturally occurring cues might be responsible for a difference in daily timing of synchronized biting. Regardless, the conserved nature of the synchronized, timely manipulation observed in different *Ophiocordyceps*-ant pairs – in both field and lab conditions – strongly suggest an underlying role of biological clocks. As such, it has been proposed that the ant's clock is adaptively manipulated by the fungal parasite to induce changes to circadian timing rather than a complete loss of clock-controlled rhythms [25, 26, 40]. Multiple lines of evidence from recent transcriptomics and behavioral work provides further support for this hypothesis. First, a time-course transcriptomics study has revealed that ant-manipulating *Ophiocordyceps* sp. have the genetic components for an intrinsic clock [30]. *Ophiocordyceps* clock-controlled genes included putative protein tyrosinases with known function in behavior manipulation [30, 35, 41]. The importance of fungal clocks in virulence have been fairly well established in the fungus *Botrytis cinerea* that infects the plant *Arabidopsis thaliana*; the virulence of *B. cinerea* peaks at dusk when *A. thaliana* is the most susceptible [42, 43]. Furthermore, there is transcriptomic evidence suggesting that a caterpillar's phototransduction and circadian entrainment pathways are involved in the phototactic "summitting" behavior induced by baculoviruses [44, 45]. Second, recent work from our lab showed that *Ophiocordyceps*-infected ant hosts display a loss of daily rhythm in extranidal foraging prior to manipulated biting [46]. Third, in a recently published comparative transcriptomics study, we have shown that differential expression of two insect clock gene homologs are conserved during manipulated biting in two independently evolved *Ophiocordyceps*-ant systems [34, 35]. Despite these various lines of evidence that suggest a role of biological clocks in parasitic behavioral manipulation, the hypothesis has not

been empirically tested yet, and represents an existing knowledge gap. Studying the *Ophiocordyceps*-ant system has the potential to not only further our understanding of how parasite-host rhythms interact during infectious diseases but also to identify putative mechanisms by which a parasite could alter host behavior.

For the first part of my dissertation, I used time-course RNASeq to characterize the daily rhythms in gene expression of two distinct ant behavioral castes – extranidal foragers and brood-tending nurses. The study revealed putative mechanisms that likely underlie this chronotypic plasticity in social insects. The findings from this study have already been published in a peer-reviewed journal and are provided verbatim as Chapter one in this dissertation. For the second half of my dissertation, I aimed to test the hypothesis that clock-controlled processes in ant hosts are being targeted by *Ophiocordyceps* in order to induce timely changes to ant behavior. However, it is also likely that disruption of host clock and its output is a general hallmark of infectious diseases and not an adaptive strategy used solely by parasitic manipulators [47]. To test both the hypotheses, I used a non-manipulating fungal parasite, *Beauveria bassiana* to contrast against the behavior modifying parasite *O. camponoti-floridani* to tease apart host changes that are manipulation specific as compared to general infections. The unpublished findings are presented in Chapter two and Chapter three of my dissertation. The generalist entomopathogen, *B. bassiana*, is a widely used biocontrol agent, and has been fairly well-studied through functional genetic testing [48]. Despite this, very little is known about the biological clock of *B. bassiana*, and no study till date has quantified the daily fluctuations in the transcriptome of *B. bassiana*, which is necessary to shed light on the different molecular functions that are likely under clock control. The dissertation, therefore, will shed new light on the role of biological clocks in *B. bassiana*'s pathogenicity and success as a generalist

entomopathogen. But most importantly, the findings from Chapters two and three in my dissertation aims to extend our understanding of the role biological clocks play in behavioral plasticity and infectious disease outcomes, especially behavior modifying diseases.

CHAPTER ONE:
ANT CLOCKS AND BEHAVIORAL PLASTICITY

Introduction

Living organisms exhibit adaptive rhythms in physiology and behavior as a way to anticipate predictable daily fluctuations in their environment [1, 2, 49]. Such daily rhythms are ubiquitous and have been discovered in both unicellular and multicellular organisms [50-55], including eusocial Hymenopterans such as ants and bees [56-62]. These rhythms are driven by endogenous molecular feedback loops that are capable of entraining to external time cues, known as Zeitgebers, which can be both abiotic (e.g., light and temperature cycles) and biotic (e.g., presence of food and predators) [63-66]. In the majority of model organisms studied thus far, light appears to be the strongest Zeitgeber [12, 65]. However, it has been suggested that in Hymenopterans with complex social behaviors, temperature cues and social environment could be more potent Zeitgebers than light [13-15, 20, 67]. Though, a more thorough molecular understanding of the Hymenopteran clock and its role in the social organization of insect colonies is needed to confirm this.

Our knowledge of the molecular underpinnings of the Hymenopteran clock is limited [60-62, 68-70]. This is in stark contrast with our vast molecular understanding of the circadian clock of *Drosophila melanogaster*, which has been extensively studied and is often used as a reference model for insect circadian clocks in general (reviewed in [5, 7, 71]). At the cellular level, the circadian clock consists of an autoregulatory transcription-translation feedback loop (TTFL) that requires around (circa) 24 hours (dia) to complete one cycle. The circadian TTFL is considered to be an ancient timekeeping mechanism conserved in plants, fungi and animals [1, 7,

72]. In the insect model organism *Drosophila*, the TTFL consists of the activator complex CLOCK-CYCLE (BMAL1-CLOCK in mammals) that binds to and activates transcription of the repressor gene *Period* (*Per*). Upon translation in the cytoplasm, PER heterodimerizes with TIMELESS (CRYPTOCHROME in mammals), translocates into the nucleus and inhibits the CLK-CYC activator complex, thus closing the feedback loop [3, 73]. This loop is further coupled with multiple auxiliary phosphorylation-dephosphorylation cycles, that are necessary for a functional 24-hour clock [3, 73]. Several kinases (e.g., Shaggy, Double-time, Nemo, Casein Kinase-2 and Protein Kinase A) and phosphatases (e.g., Protein phosphatase 1 and Protein phosphatase 2A) involved in such auxiliary cycles have been discovered in *Drosophila* (reviewed in [71]). Once entrained, the circadian clock drives daily oscillations in gene expression and protein production that in turn bring about rhythms in physiology (e.g., metabolism and immune function) and behavior (e.g., locomotion and feeding) [74].

In addition to being endogenous and entrainable, circadian clocks are also inherently plastic; the phase, amplitude and period length with which circadian processes oscillate can change with an organism's age or social environment [18, 75-79]. Such changes give rise to phenotypes that differ in their exact timing of activity onset relative to sunset or sunrise, known as "chronotypes" [80-83]. Social insects, which exhibit complex social organization and a decentralized division of colony labor, provide a striking example of plastic chronotypes which appear to be tightly associated with an individual's behavioral role or caste identity within the colony [21, 59, 61, 69, 84]. In ants and bees, broadly two distinct behavioral castes emerge from division of colony labor among non-reproductive "workers": 1) foragers that perform the majority of outside-nest tasks such as gathering food in an environment with daily cycling abiotic conditions and 2) nurses that perform inside-nest tasks, including brood care, in dark nest

chambers with little to no abiotic fluctuations [85]. In most species studied so far, isolated ants and bees in a forager-like state show robust daily rhythms in activity whereas brood-tending nurses display "around-the-clock" activity patterns with no apparent rhythmicity [20-22, 86]. In honeybees, foragers coerced into tending brood will begin to show "around-the-clock" activity whereas brood-tending nurses develop robust locomotory rhythms upon removal from the colony [61, 68, 87]. Similarly, in carpenter ant workers, the presence or absence of rhythmic activity state is tightly linked with their social context and caste identity in the colony [21, 59, 88]. For example, in the carpenter ant *Camponotus rufipes,* nurses showed a rapid development of rhythmic activity patterns when isolated from the colony and placed under cycling light-dark conditions [21]. This rhythmic activity persisted under constant darkness conditions in the absence of brood [21]. Similarly, isolated individuals of the ant species *Diacamma indicum,* showed rhythmic activity under LD cycles in the absence of eggs and larvae, but transitioned to nurse-like "around-the-clock" activity in their presence [20]. As such, 24h-rhythms in locomotory behavior appear to be regulated by an individual's social context and behavioral role in the colony [20, 21, 67, 89]. This is in line with the finding that social cues, such as colony odor or substrate-borne vibrations, can be potent Zeitgebers in social insects and can even override photic entrainment [14, 15].

The molecular aspects of plastic timekeeping and its role in driving behavioral plasticity that gives rise to colony-wide division of labor in ants, and other social insects, are largely unexplored. Exposing the mechanisms of plastic timekeeping in ants, and how they connect to behavioral phenotypes, could be essential in our understanding of eusocial behavior and regulation of colony functioning. A first step in this direction has been made by Rodrigues-Zas and colleagues, who investigated 24h-rhythms in gene expression in honeybee forager and nurse

brains through a time-course microarray study [62]. However, this study identified only 4% of all protein coding genes as rhythmic, which seems almost certainly a vast under-representation considering the abundance of clock-controlled genes that have been found in other organisms [90-96]. No other genome-wide reports that assess daily rhythms in gene expression seem to exist for Hymenoptera despite the availability of newer high-throughput sequencing techniques and improved rhythm detection software [97, 98]. As such, a major knowledge gap regarding the inner workings of social insect clocks, and especially those of ants, remain. This greatly limits our ability to investigate how biological clocks could be interacting with social cues to produce functionally distinctive behavioral castes with their own characteristic chronotypes.

Our current study aims to address this knowledge gap by investigating rhythmic gene expression, throughout a 24h-day, in brains of *Camponotus floridanus* nurse and forager ants. The Florida carpenter ant, *C. floridanus*, produces large colonies with several thousand workers, organized in both behavioral and morphological castes. This species is considered an urban pest [99] and is frequently used in a wide variety of social insect studies (e.g., [100-109]). To collect forager and nurse ants of *C. floridanus*, we conducted a time-course experiment on a single medium-to-large colony, kept in a complex behavioral setup that allowed us to quantify daily rhythms in colony activity and identify forager-nurse castes based on behavior. We subsequently used the brains of collected foragers and nurses for RNASeq to fulfill three primary objectives: (1) to investigate the extent of rhythmic gene expression for both castes, (2) to characterize the similarities and differences in their daily transcriptomes, and (3) to identify putative mechanisms that could allow brood-tending nurse ants, known to show arrhythmic behavior, to possess a functional timekeeping machinery. Given that we sampled ants under LD cycle, we use the term "diurnal" throughout the article to refer to 24h-rhythms, in behavior and gene expression, since

we cannot distinguish internally- and externally-driven rhythms. We found that nurse brains harbored a reduced number of diurnal genes as compared to foragers. Yet, we discovered that several genes with robust diurnal expression in forager brains were not entirely arrhythmic in nurses. Rather, these genes oscillated with 12-hour and 8-hour periodicities (the core clock gene *Period* being one of them). We discuss the possibility that such plasticity in clock and clock-controlled gene expression could facilitate swift nurse to forager transitions and vice-versa. Furthermore, we used functional enrichments of gene ontology annotations to identify biological processes that are seemingly under clock-control in *C. floridanus* brains, and highlight the ones enriched for genes that cycled at different periodicities in the two ant castes. Additionally, we report on genes that were expressed at vastly different levels in the brains of the two ant castes, throughout the day. The protein products of several of these differentially expressed genes have been discovered in the trophallactic fluid of *C. floridanus* [106, 110]. As such, we discuss the possibility that division of labor and the regulation of behavioral chronotypes in ant societies is trophallaxis-mediated.

Methods

Camponotus floridanus collection and husbandry

Our study aimed to investigate daily gene expression differences in the brains of foragers and nurses. To prevent potential inter-colony variation in the degree of division of labor [111-113] from obscuring inter-caste differences, we used a single colony of *C. floridanus*. We collected a queen-absent colony of *C. floridanus* containing several thousand workers and abundant brood (eggs, larvae and pupa) from the University of Central Florida Arboretum in late April of 2019. This colony represents a typical medium-sized *C. floridanus* colony [114] that allowed us to study division of labor in an ecologically-relevant manner since (1) queenless colonies of *C. floridanus* as small as <50 individuals already demonstrate forager-nurse caste differentiation [85], and (2) post-collection, we used this colony for experimentation as quickly as possible (i.e., within three weeks) to minimize any potential effects of queen-absence on overall colony behavior. Upon collection, we housed the colony in a fluon coated (BioQuip) plastic box (dimensions 42 x 29 cm, Rubbermaid) with a layer of damp plaster (Plaster of Paris) covering the bottom. We provided 15% sugar solution and water *ad libitum* and fed crickets to the colony every 2-3 days. We also provided the colony with multiple light-impervious, humid test-tube chambers (50 mL, Fisher Scientific) which they readily moved their brood into and used as a nest. Until the start of the experiment, we kept the colony in this setup inside a climate-controlled incubator (I36VL, Percival) at 25ºC, 75% relative humidity (rH), and a 12h:12h light-dark (LD) cycle.

Experimental setup and timeline

To allow for visible behavioral division of labor between morphologically indistinguishable forager and nurse ant castes (see definitions below), we built a formicarium consisting of a nest box and a foraging arena (42 x 29 cm each, Rubbermaid). Both boxes had a layer of damp plaster covering the bottom. We carved multiple grooves into the plaster of the nest box to imitate nest chambers and kept the box covered at all times to ensure completely dark conditions. We placed the nest in a temperature-controlled darkroom at constant temperature and humidity (25ºC, 70% rH). The foraging arena was placed inside a climate-controlled incubator (I36VL, Percival) under a 12h:12h LD cycle without twilight cues. Lights ramped from zero to >2000 lux within a minute when lights were turned on at Zeitgeber Time, ZT24 (or, ZT0, which indicates the same time of day) and turned off within the same short time at ZT12 (Additional File 9). We maintained constant temperature (25ºC) and humidity (75% rH) inside the incubator to ensure that the LD cycle was the primary rhythmically occurring cue, i.e., Zeitgeber, for circadian entrainment (Additional File 9). Abiotic factors in the foraging arena and nest box were monitored using HOBO data loggers (model U12, Onset) that logged light levels, temperature and humidity at 30 second intervals (Additional File 9). Food was provided *ad libitum* on an elevated circular feeding stage in the foraging arena to distinguish active feeding bouts from general extranidal visits (Additional File 10A). Feeders were replenished, and fresh frozen crickets were provided, every day between ZT2 and ZT4, throughout the experiment. The nest box was connected to the foraging arena with a 1.5m long plastic tube (i.e., *Tunnel*, Additional File 10A), which allowed ants to visit to the foraging arena at any time of the day.

Once the formicarium was set up, we transferred the entire colony along with brood into the foraging arena. To incentivize the colony to move their brood into the dark nest box, we kept the foraging arena under constant light for three consecutive days. This also aided in the resetting of their biological clocks to allow for synchronized entrainment to the 12h:12h LD cycle. After 5 days of initial entrainment, we identified and marked foragers for three consecutive days (Day 6-8, Fig. 1, see below for details on mark-and-recapture). This was followed by another four days of entrainment (Pre-sampling entrainment, Day 9-12, Fig. 1) before we sampled nurse and forager ants at two-hour intervals, spanning an entire LD cycle on day 13 (see below for sampling details).

Colony activity monitoring

The extranidal or outside nest activity of the colony (called *activity* from here on) was used as a proxy for detecting rhythmicity in colony behavior. Before sampling ants for RNASeq, we analyzed the activity data to (a) confirm colony entrainment to the LD cycle, (b) identify peak activity hours for forager identification and painting, and (c) confirm pre-sampling entrainment after foragers had been marked. We monitored colony activity during the entire experimental period by recording time-lapse videos of the foraging arena using a modified infra-red enabled camera (GoPro Hero 6) at 4K resolution, set to capture one frame every 30 seconds at a wide field of view. To facilitate night-time recording, we installed a low intensity near-infrared light (850 nm, CMVision YY-IR30) above the foraging arena. We quantified extranidal activity throughout the experiment by counting the number of ants in the foraging arena on the feeding stage (feeding activity) and off the feeding stage (foraging activity) at one-hour intervals. The activity data can be found in Additional File 11.

Identification of Camponotus floridanus behavioral castes

To measure and compare their daily rhythms in gene expression in forager and nurse brains, we sampled these behaviorally distinct castes using an approach similar to recent work that aimed to measure their trophallactic fluid protein levels [115]. We defined foragers as individuals that perform outside-nest (extranidal) tasks, including foraging for food. To identify foragers, we used a mark and recapture strategy. For three consecutive nights (Day 6-8, Fig. 1), we collected ants from the foraging arena during peak hours of extranidal activity (ZT13 to ZT16) as well as during relative dawn (ZT23 to ZT24). We marked new captures with a dab of white paint (Testors Enamel Paint) on their abdomen. Recaptures were marked with a second dab of white paint on their thorax. After painting, the ants were released back into the foraging arena. Previous studies have shown that such mark-recapture efforts can be used to successfully identify reoccurring foragers [116] and estimate forager abundance in ant colonies [117, 118]. Since peak foraging hours took place during the night-time, we installed a 660 nm red lightbulb (Byingo LED) in the darkroom and wore a red headlamp (Petzl Tikka) to provide us with enough visibility to perform the mark-recapture, while simultaneously minimally disturbing the ants. We identified and marked more than a hundred foragers at the end of the three-day forager identification phase (109 doubly marked, and 39 singly marked). Post forager identification, the whole colony was left undisturbed and allowed to recover from potential stress for four consecutive days of pre-sampling entrainment, prior to sampling ants for RNASeq.

We defined nurses as ants that remained inside the dark nest chambers (intranidal) and cared for brood. Extranidal workers, defined as foragers in this study, do not usually tend brood or frequent brood piles since ant colonies spatially organize themselves to reduce contact

between foraging individuals and brood [119, 120]. Additionally, such proximity networks are stable over time and do not change in the absence of a queen [121]. As such, we identified nurses as unmarked individuals in the colony that were unlikely to have gone outside the nest and were in direct contact with the brood. To confirm that the bulk of brood care inside the nest was performed by unmarked ants, and not marked foragers, we performed qualitative intermittent behavioral observations for a total of 1-2 hours per day during the pre-sampling entrainment period that followed mark-recapture (Days 9-11, Fig. 1). We observed the nest chambers under the same red light (660 nm) that illuminated the darkroom. Monitoring behavior inside the nest confirmed that marked "foragers" were less likely to be in direct contact with the brood (i.e., walking on the brood pile or grooming brood) and were not seen to be involved in brood relocation within the nest chambers. As such, we identified nurses as "unmarked" individuals found in direct contact with the brood or involved in brood care including relocation.

Ant sampling and brain dissections

After identifying foragers and nurses and 12 days of colony entrainment to the 12h:12h LD, we collected ants for RNASeq under the same light-dark regime. We sampled ants from the colony every 2 hours over a 24-hour period, starting two hours after lights were turned on (ZT2) (Additional File 10B). At each sampling time point, we collected three foragers and three nurses from the colony and transferred them into individually labelled cryotubes (USA Scientific) for immediate flash freezing in liquid nitrogen. The whole process, from collection to flash freezing, took less than 60 seconds per sampled ant. Since *C. floridanus* foraging activity is predominantly nocturnal, we sampled foragers from inside the dark nest box during the light phase, and from the foraging arena during the dark phase (Additional File 10B). Nurses were always collected

from inside the nest box. For sampling under dark conditions, we used the same intensity red-light as described for the mark-recapture and behavioral observations described above. Using this sampling regime, we collected 72 ants, which were stored at -80ºC until brain dissection.

To compare transcriptome-wide daily gene expression patterns in the brain tissue of foragers and nurses, we performed brain dissections of individual flash-frozen ants in ice-cold Hanks' balanced salt solution (HBSS) buffer under a dissecting microscope. Prior to dissection, we removed both the antennae and pinned down the head of the ant using a pair of sharp forceps inserted into the antennal "sockets". Next, using small scissors we made an incision around the head and removed the head capsule using another pair of forceps to expose the intact brain. Finally, we carefully extracted the brain from the head and removed any remains of other tissues attached to the brain. This clean, dissected brain was quickly transferred into a cryotube (USA Scientific) kept on dry ice. To preserve RNA integrity and quality of the ant brains, we performed all the above steps as swiftly as possible: brain dissections of individual foragers took an average of 4.6 (±0.7) mins, whereas for a nurse it took 4.5 (±0.5) mins. For each behavioral caste, at each sampling time point, we pooled three individually dissected brain samples for RNA extraction and sequencing (Additional File 10C). Immediately after dissection of all three forager/nurse brains for each time point, the cryotube was transferred to and kept in liquid nitrogen while we dissected the remaining ant brains. The resulting 24 samples were again stored at -80ºC until RNA extraction and library preparation. This sampling approach was designed to adhere to current recommendations for genome-wide time course studies using non-model systems [97, 122]. By pooling triplicates, we have accounted for intra-colony variation while still being able to choose a high sampling frequency (every 2h) and read depth per sample

(≥ 20M per sample, see below) in order to maximize accurate detection of the majority of cycling transcripts in *C. floridanus* brains [122].

RNA extraction, library preparation and RNASeq

To obtain time course transcriptomes for each of the behavioral castes, we extracted total RNA to prepare sequencing libraries for Illumina short-read sequencing. Two frozen steel ball bearings (5/32" type 2B, grade 300, Wheels Manufacturing) were added to each cryotube containing the pooled brain tissues to homogenize them using a 1600 MiniG tissue homogenizer (SPEX) at 1300 rpm for 30 sec while keeping the samples frozen. We isolated total RNA from the disrupted, frozen brain tissues by dissolving the material into Trizol (Ambion) followed by a wash with chloroform (Sigma) and a purification step using RNeasy MinElute Cleanup columns and buffers (Qiagen) [123]. For each library preparation, we used 500 ng total RNA to extract mRNA with poly-A magnetic beads (NEB) and converted this mRNA to 280-300 bp cDNA fragments using the Ultra II Directional Kit (NEB). Unique sequencing adapters were added to each cDNA library for multiplexing (NEB). The quantity of extracted RNA and cDNA libraries were measured using Qubit (Invitrogen), whereas the quality and integrity were assessed using an Agilent Tapestation. All twenty-four cDNA libraries were sequenced as 50 bp single-end reads using two lanes on an Illumina HiSeq1500 at the Laboratory for Functional Genome Analysis (Ludwig-Maximilians-Universitat Gene Center, Munich). Read data are available under BioProject PRJNA704762. After sequencing, we removed sequencing adapters and low-quality reads from our RNASeq data with BBDuk [124] as a plug-in in Geneious (parameters: right end-low quality trim, minimum 20; trim both ends - minimum length 25 bp) (Biomatters). Post-trimming, we retained an average of 22 million reads per sample, which is well beyond the

minimal read depth sufficient to identify the majority of high amplitude 24h-rhythmic transcripts in insects [122]. Subsequently, we used HISAT2 [125] to map transcripts to the latest Cflo v7.5 genome [126], followed by normalizing each sample to Fragments Per Kilobase of transcript per Million (FPKM) with Cuffdiff [127].

Data analyses

We confirmed daily rhythms in colony activity with the WaveletComp package [128]. Using wavelet analyses, we investigated the extranidal activity of foragers for the presence of 24h-rhythms in colony behavior, the potential presence of ultradian rhythms, and to infer synchronicity between the number of ants actively feeding or present on the feeding stage (feeding activity), and those present in the remainder of the foraging arena (foraging activity).

We used the rhythmicity detection algorithm empirical JTK-Cycle (eJTK) [129, 130] to test for significant diurnal and ultradian rhythms in gene expression in foragers and nurses using waveforms of period lengths (tau) equal to 24h, 12h and 8h. The algorithm, eJTK, builds on the non-parametric JTK-Cycle [131] by allowing detection of asymmetric sinusoidal waveforms since there is no *a priori* reason to assume that biological rhythms are symmetric [130]. Furthermore, a recent comparative analysis of different rhythmicity detection algorithms suggests that eJTK is a highly robust method for detection of rhythmic features [98]. Only genes that had diel expression values ≥1 FPKM for at least half of all sampled timepoints were tested for rhythmicity. For a set period length, a gene was considered to be significantly rhythmic if it had a Gamma p-value < 0.05. To test if certain genes could be clustered together based on similar temporal peak activity, we used an agglomerative hierarchical clustering framework (method = complete linkage) using the ‘hclust’ function in the ‘stats’ package for R.

Time-course sampling of foragers and nurses enabled us to account for diel fluctuations in expression levels when identifying genes that were differentially expressed between the two ant groups throughout the day (i.e., DEGs). To determine differentially expressed genes, we used the linear modelling framework proposed in LimoRhyde [132], but without an interaction between treatment and time. A gene was considered differentially expressed if treatment was found to be a significant predictor (at 5% FDR) and the difference in mean diel expression between foragers and nurses was at least 2-fold (i.e., abs($\log_2$-fold-change) $\geq$ 1). The more stringent 2-fold-change threshold allowed us to investigate the putative clock-control of only those genes that were more likely to have a biologically relevant difference in gene expression between forager and nurse brains. LimoRhyde is generally used to test if genes of the same periodicity are differentially rhythmic in phase or amplitude, inferred from a significant interaction between treatment and time. However, we did not find significant differences in phase or amplitude for any of the genes that were found to have 24h rhythms in both foragers and nurses (Additional File 12). Therefore, we indicated a gene as differentially rhythmic (i.e., DRGs) if it significantly cycled in both ant castes but with different period lengths.

To perform functional enrichment analyses of significant gene sets, we wrote a customized function that performs a hypergeometric test through the *dhyper* function in R. The code is available on GitHub (https://github.com/debekkerlab/Will_et_al_2020). The function takes the following inputs: (1) user-provided geneset to test enrichment on, (2) user-provided background geneset to test enrichment against, and (3) functional gene annotations (e.g., GO terms) to test enrichment for. Among other things, the function outputs a Benjamini Hochberg-corrected p-value for each annotation term to indicate if it is significantly enriched in the test geneset. We used all genes that were found to be "expressed" ($\geq$ 1 FPKM expression for at least

one sample) in the brains of foragers or nurses as the background geneset for functional enrichment tests. To analyze the functional enrichment of Gene Ontology (GO) predictions, we used the GO term annotations [108] for the most recent *C. floridanus* genome (v 7.5) [126]. We only tested terms annotated for at least 5 protein coding genes and significance was inferred at 5% FDR.

Homologs of known core-clock genes (*cgs*) and clock-modulator genes (*cmgs*) *in C. floridanus* were identified using previously published hidden-markov-models (HMMs) for well-characterized clock proteins of two model organisms: *Drosophila melanogaster* and *Mus musculus* [133]. We used *hmmersearch* to query these HMM profiles against the entire *C. floridanus* proteome (Cflo_v7.5) [126] with default parameters (HMMER v3.2.1 [134]). To identify orthologs shared between *C. floridanus* and flies, mammals or honey bees we used proteinortho5 [135].

All data wrangling, statistical tests and graphical visualizations were performed in RStudio [136] using the R programming language v3.5.1 [137]. Heatmaps were generated using the pheatmap [138] and viridis [139] packages. Upset diagrams were used to visualize intersecting gene sets using the UpsetR package [140]. We used a Fisher's exact test for identifying if two genesets showed significant overlap using the GeneOverlap package [141].

Results and Discussion

Daily rhythms in colony behavior of Camponotus floridanus

We collected forager and nurse ants from a single *C. floridanus* colony, preventing potential inter-colony differences in timing of foraging from obscuring the inter-caste differences in gene expression that we aimed to measure. *Camponotus floridanus* is known to be largely nocturnal both in nature (personal field observations, [99]) and in the lab [104, 105]. Despite this knowledge, we first had to entrain and quantify the colony-level behavioral rhythms of *C. floridanus* to be able to reliably investigate the daily gene expression underlying their seemingly clock-regulated behavioral activity. Therefore, we recorded extranidal visits of a large *C. floridanus* colony, housed in a darkened nest, that we attached to a foraging arena subjected to a 12h:12h LD cycle (see Methods section for more details). Subsequently, we counted the number of foraging ants throughout the day that were actively feeding or present on the feeding stage (Fig. 1, "feeding" or feeding activity) as well as in the remainder of the foraging arena (Fig. 1, "foraging" or general foraging activity). We defined the colony's total foraging activity (Fig. 1, "Total activity") as the sum of feeding and foraging at any given time. The first signs of initial colony entrainment were visible through the early establishment of a day-night rhythm in foraging (Fig. 1, Day 1-5). In the following 3 days, we performed mark-and-recapture to identify ants of the foraging caste. During this time the foraging rhythm was somewhat less pronounced but managed to stay intact (Fig. 1, Day 6-8). From Day 9 onwards, both feeding and foraging showed pronounced day-night rhythms that persisted during and beyond the sampling day (Fig. 1, Day 9-15). These day-night rhythms followed a consistent pattern with increased foraging activity during the night-time as compared to the daytime, similar to previously reported

locomotory rhythms of isolated *C. floridanus* ants [105]. Thus, based on extranidal activity of the foraging caste, the colony established robust nocturnal activity rhythms as it would in nature by entraining to the light Zeitgeber we provided.

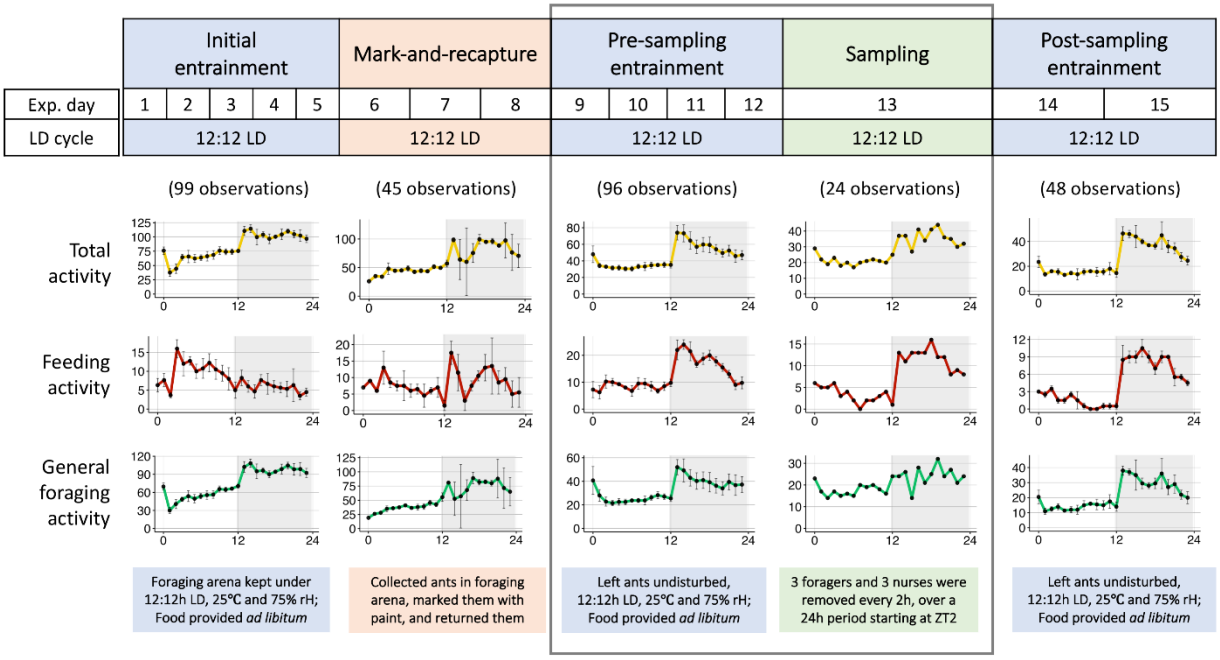

Figure 1: Daily rhythms in colony activity.

The top panel shows the experimental timeline and the bottom graphs show the mean (±SE) daily extranidal activity of the ant colony during each phase of the experiment. During the entire experiment, the foraging arena was kept at 25ºC, 70% rH and under oscillating 12h:12h light-dark (LD) cycles. Undisturbed phases under light-dark cycles are shown in blue, while experimental phases of disturbance are shown in orange (mark-and-recapture of foragers) and green (sampling of ants for RNASeq). For each plot, colored lines connecting the dots represent average activity while black bars represent one standard error around the mean. The y-axis represents number of ants and the x-axis represents Zeitgeber Time (ZT) during the 12h:12h LD cycle. The shaded part of the plots represents the dark phase (ZT12-24). The number of ants actively feeding or present on the feeding stage is plotted as the feeding activity. The general foraging activity is the number of ants present in the foraging arena but not on the feeding stage. The total activity is the sum of feeding and foraging activity, representing the total extranidal activity of the colony at a given time. The number of observations used to calculate the mean (± SE) activity for each phase are shown in parenthesis at the top of the plots. Missing data points during 'Initial entrainment' and 'Mark-and-recapture' were due to inability to get accurate count of ants from video frames and a recording failure, respectively.

To further characterize the behavioral rhythms in the entrained *C. floridanus* colony and to investigate the potential behavioral effects of the disturbance introduced by the mark-recapture, we performed wavelet analyses [128] on the foraging data collected during the four-day period just after mark-recapture and prior to sampling (Fig. 1, Day 9-12). *Camponotus floridanus* ants of the foraging caste showed significant 24h-rhythms in feeding and foraging activity (Fig. 2A). Average wavelet powers indicated that both feeding and foraging activity profiles comprised of significant waveforms with a period length close to 24 hours (Fig 2A). Neither feeding nor foraging activity peaked exactly at lights-off (ZT12). Rather, we noticed a sharp increase in both activities about an hour later (~ZT13) (Fig 1, Day 9-12). After peaking around ZT13-15, both feeding and foraging activity continued to decrease throughout the night and reached their daily minimum shortly after lights were turned on (ZT2-4) (Fig 1, Day 9-12). In Central Florida (the location of colony collection), dusk lasts for 84 (± 5) minutes after sunset (Additional File 1A, data retrieved from www.timeanddate.com). In our experimental setup, we chose an abrupt light-dark transition, and hence, did not provide twilight cues. Therefore, the stark increase in extranidal activity within an hour post lights-off, could be indicating an endogenous dusk-entrainment in colony foraging activity. Taken together, the colony activity rhythms that we observed for *C. floridanus* – 24h-rhythmic and predominantly nocturnal, with a dusk-phase – largely resembled previously reported activity patterns [105]. This indicates that the experimental setup that we designed allowed us to collect daily gene expression data related to expected ant daily activity patterns.

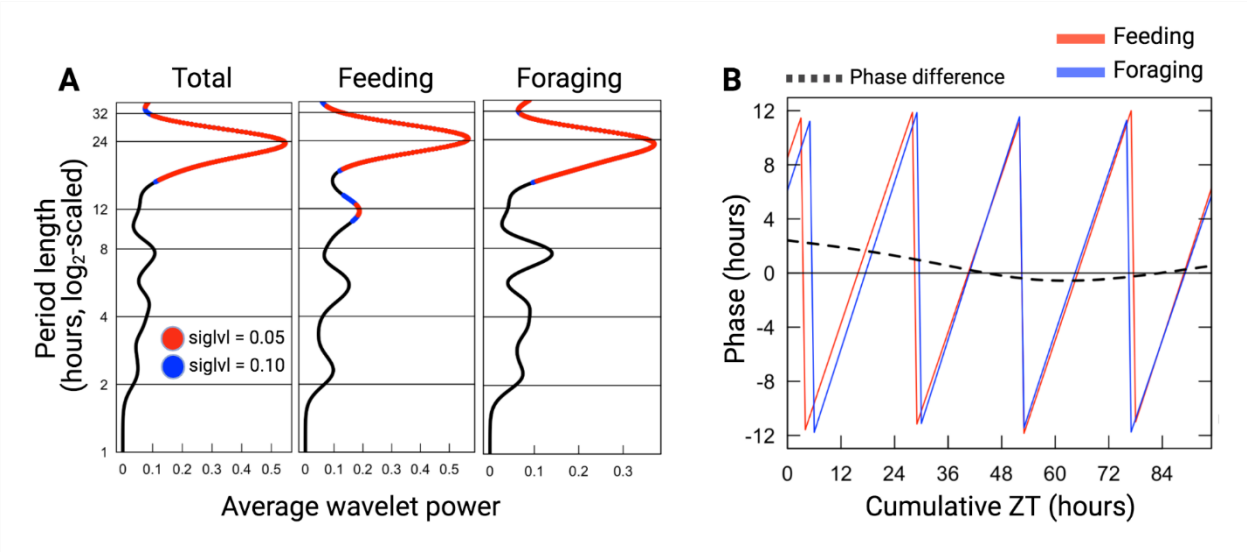

Figure 2: Wavelet analysis of feeding and general-foraging activity rhythms.

(A) Dominant periods identified using wavelet decomposition of each activity profile during the continued entrainment phase (Day 9-12). The x-axis shows the average wavelet power for different period lengths. The y-axis shows the period length (log2-scaled) in hours. Significant period lengths (siglvl < 0.05) are shown in red, and the peak indicates the dominant period having the most power (around 24h for all three activity profiles, and an additional 12h peak observed in feeding bouts); **(B)** The plot shows the phase (on the y-axis) of feeding bouts (Feeding) and general foraging activity (Foraging) during continued entrainment. The dotted line indicates the phase difference of feeding over foraging during the same time period. Positive phase difference indicates that feeding leads foraging. The x-axis shows the cumulative hours passed since disturbance due to mark-and-recapture (Cumulative ZT).

In addition to the dominant 24h-rhythm, we detected a significant circa-12h rhythm in feeding activity (Fig. 2A). Inspection of feeding power-spectra over the four days of continued-entrainment revealed that, while the 24h-rhythm was sustained throughout, the 12h rhythm was only significantly present during the first 36 hours post disturbance. Within this 36h time-period, integration of the 12h and 24h waveforms improved fit (Additional File 1B). A possible explanation for the presence of this short-lived 12h activity rhythm could be that it played a role in catching up with feeding needs of the colony in the initial hours after disturbance. The removal of foragers during mark-recapture most likely desynchronized the colony's daily feeding pattern and might explain the lack of a clear diurnal activity in colony feeding and a

diminished overall 24h foraging pattern during the mark-recapture period (Fig 1; Day 6-8). As such, we enquired if the circa-12h rhythm in feeding could be important to re-establish a rhythmic colony feeding behavior that is synchronous to the colony's foraging activity. To this end, we calculated the phase difference of the 24h-wavelets for feeding-over-foraging throughout the four days post mark-recapture (Fig. 2B). At the start of pre-sampling entrainment (i.e., right after disturbance by mark-recapture), feeding was found to lead general foraging by more than two hours. Approximately 36 hours into the pre-sampling entrainment period, the phase difference reduced to zero; 24h-rhythms in feeding and foraging aligned. Subsequently, the phase difference between feeding and foraging remained close to zero (Fig. 2B). This data suggests that, indeed, after three consecutive nights of disrupted feeding, the colony attempted to get back on track through a short initial phase shift between feeding and foraging. Once synchrony between the phases of the two activities was restored, it was maintained. The intermittent 12h feeding peaks observed during the first 36h after mark-recapture (Additional File 1B) likely contributed to restoring this synchrony.

General patterns of gene expression in Camponotus floridanus brain tissue

After twelve days of LD entrainment, we collected three *C. floridanus* foragers and nurses from the colony every 2 hours, over a 24-hour period (Fig. 1, Day 13). Individuals that were collected in the foraging arena and paint-marked as part of our mark-recapture efforts were collected as foragers. Unmarked individuals that interacted with the brood inside the dark nest chambers were collected as nurses. We subsequently used RNA-Seq to obtain the transcriptome profiles of forager and nurse brain tissue.

Of the 13,808 protein coding genes annotated in the *C. floridanus* genome [107], 8% (1130 genes) were not expressed (i.e., FPKM = 0) and 19% (2640 genes) were only lowly expressed in forager and nurse brains (i.e., $0 < \text{FPKM} \leq 1$) throughout the day (Additional File 2, sheet 1). The majority of genes involved in olfactory and gustatory functions in *C. floridanus* were among these lowly expressed genes (93% of 363 genes involved in sensory perception of smell and 73% of 26 genes involved in sensory perception of taste) (Additional File 2, sheet 2). Notably, majority of the genes involved in hormone activity (69% of 16), metallopeptidase activity (86% of 110), and nucleotide binding (85% of 27) were found to be enriched among the genes that showed either no or low expression (Additional File 2, sheet 2). The clear overrepresentation of certain gene functions among genes that were either lowly or not expressed necessitated the use of a reduced background gene set for subsequent enrichment analyses that consists of only those genes that were actually expressed. This, to avoid obtaining gene function enrichments that merely reflect brain tissue specific gene expression. We classified genes to be expressed in *C. floridanus* brains if mRNA levels were greater than 1 FPKM for at least one time point, for either behavioral caste, during the 24h sampling period.

We found 71% (i.e., 9843 genes in foragers and 9872 genes in nurses, Additional File 2, sheet 3) of all protein coding genes to be expressed in ant brains. Of these genes, 166 were uniquely expressed in the forager brains and 195 in nurses. One *odorant receptor 4-like*, two *odorant receptor 13a-like*, and two other uncharacterized odorant receptor genes were among those uniquely expressed in forager brains, along with several proteases. In addition to significant enrichments in olfaction and proteolysis-related biological processes, uniquely expressed genes in foragers were also enriched in the cellular component nucleosome and included several histone-related genes (Additional File 2, sheet 4). In comparison, genes

uniquely expressed in nurses were enriched in redox and lipid metabolic processes and included several putative *cytochrome P450* and *lipase 3-like* genes (Additional File 2, sheet 4). This is in line with the canonical behavioral and physiological differences that characterize foragers and nurses in a social insect colony. A fine-tuned olfactory and gustatory repertoire in foragers is essential for trail-following and other general foraging tasks. In contrast, metabolic processes have been previously found to be upregulated in intranidal nurse workers that are usually tasked with larval feeding and brood care [142]. This indicates that the expression data that we obtained is likely a good representation of the gene expression profiles that are characteristic for both castes.

Diurnal rhythms in gene expression

We used the non-parametric algorithm empirical JTK Cycle (eJTK) [129, 130] to detect diurnal (24h) rhythms in gene expression in forager and nurse ant brains. Of the 10,038 genes expressed in *C. floridanus* brains, 42% (i.e., 4242 genes) had significant diurnal expression patterns in either foragers or nurses (Additional File 3, sheet 1 and 2). The number of putative diurnal genes in foragers was almost three times higher (i.e., 3569 genes; Fig 3A and B, indicated with "for-24h") as compared to nurses (i.e., 1367 genes; Fig 3A and C, indicated with "nur-24h"). Only 16% of all identified diurnal genes cycled in both behavioral castes with a 24h rhythm (i.e., 694 genes; Fig 3A and D, indicated with "for-24h-nur-24h"), which represents half of all the diurnal genes that we identified in nurses. The reduced number of diurnal genes in nurses is consistent with the previous time-course microarray study done in honeybees (541 probes in forager bees and 160 probes in nurses were found to have 24h-rhythms) [62]. This suggests that a reduced circadian control at the level of gene expression in "around-the-clock" active nurses as compared

to rhythmically active foragers is likely a convergent pattern since bees and ants have evolved eusociality independently.

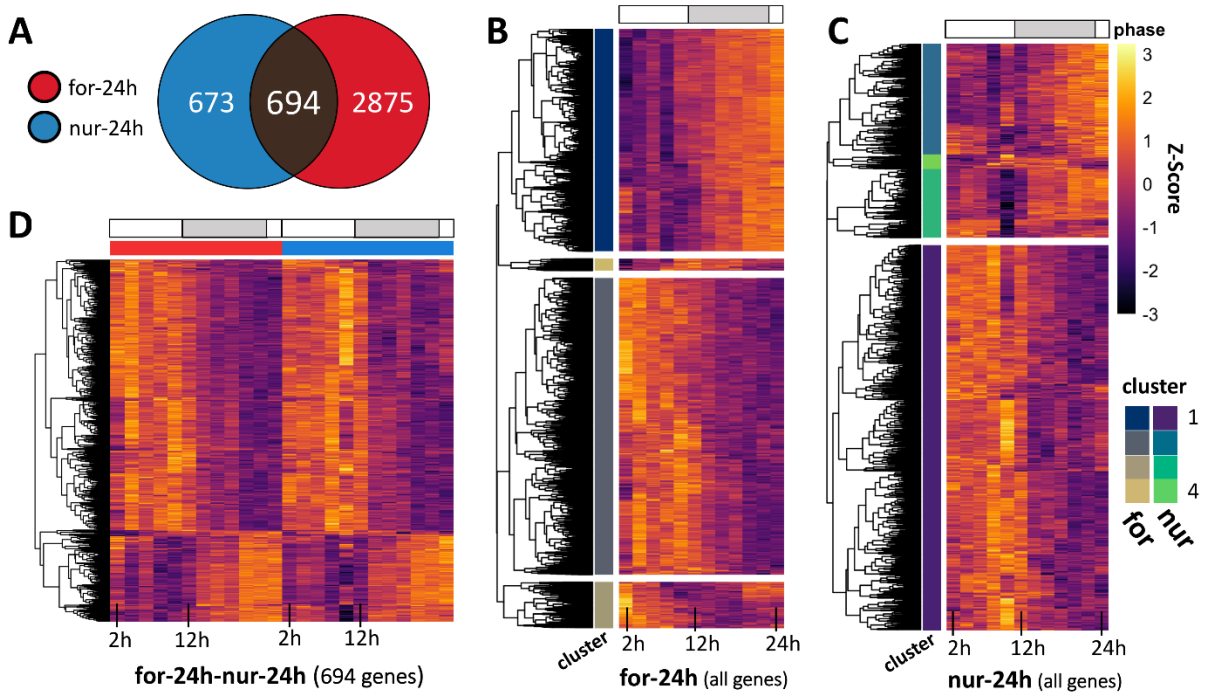

Figure 3: Diurnal rhythms of gene expression in the ant brain

(**A**) Venn-diagram showing the number of genes significantly oscillating every 24h in forager (for-24h) and nurse (nur-24h) brains. The heatmaps show the daily expression (z-score) patterns of all identified 24h-oscillating genes in **(B)** foragers (for-24h), **(C)** nurses (nur-24h), and **(D)** both foragers and nurses (for-24h-nur-24h). Each row represents a single gene and each column represents the Zeitgeber Time (ZT) at which the sample was collected, shown in chronological order from left to right (from ZT2 to ZT24, every 2h). The grey bar above the heatmaps runs from ZT12 to ZT24 and indicates the time during the light-dark cycle in which lights were off. Both for-24h and nur-24h genes were hierarchically clustered into four clusters. The cluster identity of each gene is indicated in the cluster annotation column.

After identifying putative 24h cycling genes in the two behavioral groups, we asked if they contained functional annotations with coordinated temporal peak activity (i.e., are certain biological functions “day-peaking” or “night-peaking”) and if such a temporal division of clock-controlled processes can be found in both foragers and nurses. To answer these questions, we

used an agglomerative hierarchical clustering framework to group the diurnal genes in foragers and nurses into four gene clusters (Additional File 3, sheet 3 and 4). We followed this analysis by identifying significantly enriched gene ontology (GO) terms for each identified gene cluster.

The choice of four clusters was aimed to demarcate, if possible, potential day-, night-, dawn-, and dusk-peaking genes. Using this method, we identified that more than half of all diurnal genes in foragers showed a peak activity during early-to-mid daytime (1916 genes, Fig. 3B, for-24h_Cluster2). The majority of the remaining genes showed peak expression activity around late night-time (1417 genes, Fig. 3B, for-24h_Cluster1). Additionally, one of the two smaller clusters of genes that cycled with a 24h rhythm in foragers (74 genes, Fig. 3B, for-24h_Cluster4) appeared to peak at dusk with an acrophase around ZT12-14. Among these dusk-peaking genes we identified the putative insect melatonin receptor *trapped in endoderm* (*tre1; MTNR1a* in mammals), which has been reported to be central to the dusk/dawn entrainment pathway in humans (Table 1) [143-145]. The genes in nurse brains that showed 24h rhythms also primarily clustered into two groups – day-peaking (909 genes, Fig 3C, nur-24h_Cluster1) and night-peaking genes (261 genes, Fig 3C, nur-24h_Cluster2) – with only a few genes in the remaining two clusters (Cluster 3, 162 genes; Cluster 4, 35 genes).

Table 1: Clock components of Camponotus floridanus and their gene expression patterns in forager and nurse brains.

Homologs of key insect clock components present in *Camponotus floridanus* (*Cflo*)			Periodicity of daily gene expression		One-to-one ortholog of the *Cflo* gene in	
Drosophila gene	*Cflo homolog*	*Function*	*Forager*	*Nurse*	*mice or humans*	*honeybees*
Clock	LOC105257275	core-clock	12h	-	*Npas2*	*Clock*
Period	**LOC105256454**	**core-clock**	**24h**	**8h**	**-**	***Per***
Vrille	LOC105252510	core-clock	8h	-	-	*Ataxin-2* homolog
Double-time	LOC105255207	modulator	24h	-	*Ck1d/e*	*Ck1*
Casein kinase 2 alpha	LOC105256631	modulator	24h	24h	*Ck2a*	*Ck2a*
Shaggy	**LOC105258655**	**modulator**	**24h**	**8h**	***Gsk3b***	***Sgg***
Nemo	LOC105248529	modulator	24h	-	*Nlk*	*Nlk2*
Protein phophatase 1b	**LOC105251553**	**modulator**	**24h**	**8h**	***Pp1b***	***Pp1b***
Pp1	**LOC105250191**	**modulator**	**24h**	**8h**	**-**	**-**
Rhodopsin	LOC105252466	modulator	24h	24h	*Opn4*	*Lop1*
mAchR	LOC105253861	output	24h	-	-	*mAchR*
DopEcR	**LOC105257836**	**output**	**24h**	**8h**	***Gpr52***	***DopEcR***
Pigment dispersing factor	LOC105256952	output	24h	-	-	*Pdf*
Pdf receptor	LOC105252917	output	24h	-	-	*Pdfr*
Protein kinase A	LOC105249574	output	24h	-	*Prkaca/b*	*Pka*
Lark	LOC105259208	output	24h	24h	*Rbm4*	*Lark*
Protein kinase C	**LOC105255087**	**output**	**24h**	**8h**	***Prkci***	***Pkc***
Trapped in endoderm 1	LOC105250997	output	24h	-	*MT1*	*Tre1*
Slowpoke	LOC105258647	output	24h	-	*Slo*	*Kcnma1*

The table above lists the *C. floridanus* homologs of several *Drosophila* core-clock, clock-modulator and clock-output genes. The periodicity (tau) of rhythmic gene expression in the brain, if any, is indicated for both foragers and nurses. The one-to-one ortholog of the identified *C. floridanus* gene in mammals and honeybees is also provided. A dash in the periodicity column indicates that no significant daily rhythms were detected for the *C. floridanus* gene, whereas a dash in the ortholog columns indicates that no one-to-one orthologs of the *C. floridanus* gene was detected. The genes that show differential rhythmicity, oscillating at two distinct periodicities, in the two ant castes are shown in bold.

Despite the relatively smaller number of day-peaking and night-peaking diurnal genes in nurses, we found functional enrichments comparable to those found in foragers. The night-peaking gene clusters in foragers and nurses were both enriched in genes with the annotated GO terms: regulation of transcription (DNA-templated), signal transduction and protein phosphorylation (Additional File 3, sheet 5). This indicates that a significant number of night-peaking diurnal genes in nurse and forager brains seem to be involved in cell-cell communication, gene expression, and protein modification. The day-peaking diurnal gene clusters in both behavioral groups were enriched for genes involved in metabolism (glycosylphosphatidylinositol (GPI) anchor biosynthesis) (Additional File 3, sheet 5). In addition, the diurnal gene clusters in foragers were enriched for multiple other biological processes that were not found to be enriched in nurses. The day-peaking genes in foragers were enriched for GO terms that concerned response to stress, as well as tRNA, mRNA and translational processes, and terms involved in post protein processing such as folding and transport (Additional File 3, sheet 5). Night-peaking genes in foragers were additionally enriched in terms such as regulation of transcription by RNA polymerase II, multicellular organism development, protein homooligomerization, microtubule-based movement, G protein-coupled receptor signaling pathway, and ion transmembrane transport (Additional File 3, sheet 5). This temporal segregation of clock-controlled processes in foragers appears to be in line with findings from previous studies done on the fungus *Neurospora crassa*, mammals and flies [92, 94, 146].

However, while the daily transcriptome of rhythmic foragers revealed the expected temporal separation, nurse gene expression showed a much more limited temporal organization. This provides further evidence for a reduced diurnal control in "around-the-clock" active nurses as compared to rhythmically active foragers.

The question that remains is if the shared functional enrichments among the 24h rhythmic genes in both ant castes encompass the same exact genes or if they are different but with similar functions. To answer this question, we analyzed the functional annotations of the 694 diurnal genes that were shared between foragers and nurses. Hierarchical clustering revealed that these genes predominantly peaked during the daytime (Fig. 3D) and that the shared day-peaking genes were significantly enriched in the functional annotation GPI anchor biosynthesis (genes *Pig-b, Pig-c, Pig-g, Pig-m,* and *Mppe*) (Additional File 3, sheet 5). However, the relatively smaller set of shared night-peaking diurnal genes was not enriched in any functional annotations. Using a Fisher exact to test for significant overlap between genesets, we found that the night-peaking activity of regulation of transcription (DNA-templated) (Odds-ratio = 0.55; p-value = 0.89), signal transduction (Odds-ratio = 7.48; p-value = 0.06) and protein phosphorylation (Odds-ratio = 2.12; p-value = 0.21) are mostly due to different sets of diurnal genes in foragers and nurses, but with similar functions. In contrast, GPI anchor biosynthesis activity appears to be driven by the same day-peaking diurnal genes in both ant castes.

The molecular underpinnings of timekeeping in nurse ants, and other animals with "around-the-clock" activity, is still elusive [60, 62, 147]. To find candidate genes presumably involved in daily timekeeping in *C. floridanus* nurses, we queried the diurnal genes that they shared with foragers for known components of the insect clock (Additional File 4). The shared day-peaking gene cluster contained one known clock output gene (i.e., *Lark*) and two genes

known to modulate the circadian clock – *Casein kinase 2 alpha* (*Ck2a*) and the light-dependent *Rhodopsin* (*Rh6*; orthologous to mammalian *Opn4*) (Table 1, Fig. 4). Along with other members of the opsin gene family, the *Rh6* gene in *Drosophila* has been shown to also have light-independent functions in thermosensation (in larvae) and hearing (in adults) [148, 149]. The auditory role of opsins, likely mediated by mechanotransduction [150], could be especially relevant for circadian entrainment in social insects. Ants and bees are known to use vibroacoustic means such as "drumming" behavior (i.e., vibrations produced by tapping the nest substrate with their head and gaster) to communicate within dark nest chambers [151-154]. Moreover, there is recent evidence that substrate-borne vibrations are potent social Zeitgebers capable of entraining the circadian clock of newly emerged honey bees housed in the dark [15]. These substrate-borne vibrations could potentially play a similar role in the social entrainment of nurse ants through the light-independent involvement of a rhodopsin-mediated mechanosensory pathway [150], while extranidal foragers might also make use of its light-dependent functions.

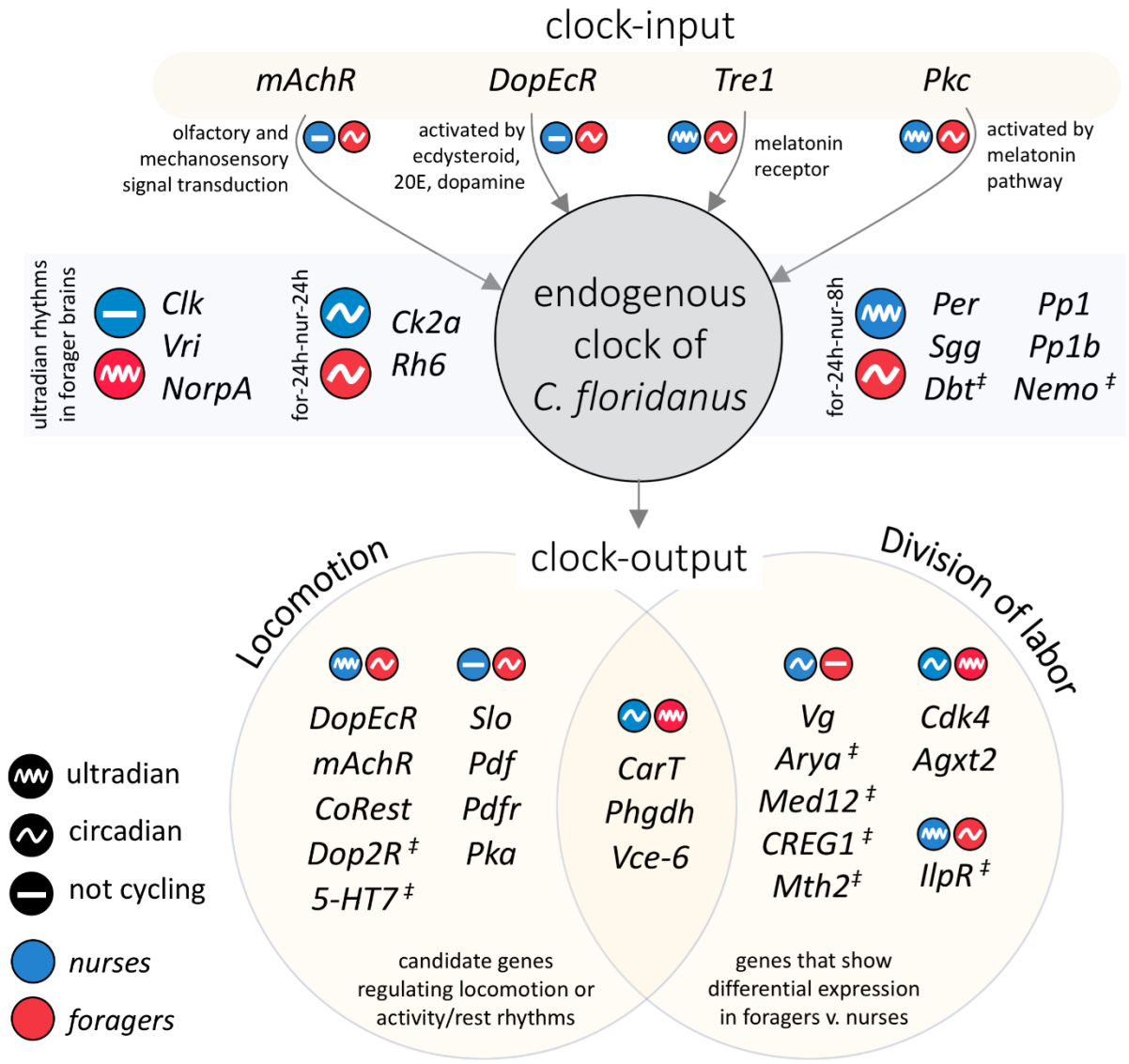

Figure 4: Potential links between chronobiological plasticity and behavioral division of labor in C. floridanus.

The infographic shows differences in rhythmic expression in forager and nurse brains for several genes involved in entrainment of the endogenous clock (clock-input), proper functioning of the endogenous clock, and the clock-controlled pathways (clock-output) that likely regulate locomotion and division of labor in ants. The symbol "‡" indicates that gene expression for that gene shows a trend of rhythmic expression in one of the ant castes (Additional File 5) but was not significant ($p \geq 0.05$). Ultradian rhythms include both 8h and 12h oscillations. The following genes have been abbreviated in the figure but not in the text: *Venom-carboxylesterase-6* (*Vce-6*), *Arylphorin-subunit-alpha* (*Arya*)

.

In addition to *Rh6,* the kinase *Ck2a* showed robust 24h rhythms and a near-perfect alignment in gene expression between the behavioral groups (Additional File 3, Fig. 4). *Ck2a* encodes the catalytic subunit of the circadian protein, Casein Kinase 2 (CK2). In *Drosophila,* CK2 appears to regulate rhythmic behavior by phosphorylating the core clock proteins PERIOD (PER) and TIMELESS (TIM) [155-158]. This CK2-mediated phosphorylation is perceived as a rate-limiting step in the circadian clock, important for a functional 24h transcription-translation feedback loop [158]. The central role of CK2 in regulating the endogenous clock in other organisms suggests a potential role of *Ck2a* in maintaining a functional 24h oscillator in both, "around-the-clock" active nurses and rhythmically active foragers. However, other homologs of genes encoding core clock proteins, such as PER, were not present among the diurnal genes that were shared between foragers and nurses (Table 1, Additional File 3).

Ultradian rhythms in gene expression

"Ultradian rhythms" in gene expression refer to significantly oscillating expression patterns around the second and third harmonic of 24h-rhythms (i.e., genes cycling with periodicities of 12 hours and 8 hours, respectively). Such rhythms can be found in a wide range of species [159-165], and examples in which organisms switch from diurnal to ultradian gene expression due to changes in environmental circumstances have been reported [166]. When we visually inspected the expression of several genes that exhibited diurnal rhythmicity in foragers but not in nurses, we noticed that the expression of multiple such genes in nurses was relatively dampened but seemed to oscillate at a frequency higher than 24 hours. As such, we used eJTK to detect if any genes were expressed with significant ultradian rhythms (Additional File 6). We identified a comparable number of genes that cycled with a 12h period in forager and nurse brains (i.e., 148

and 193, respectively), and 2 genes that showed 12h period in both castes (Fig. 5A). In foragers, the core-clock gene *Clock* (*Clk*) was present among the 12h oscillating genes (Table 1, Fig. 4). However, we did not detect diurnal or ultradian rhythmicity in *Clk* expression in nurses (Table 1). As for genes that oscillated with a robust 8h rhythm, we discovered 229 such genes in forager brains and about twice as many (550 genes) in nurses. Only three genes showed an 8h cycling pattern in both behavioral castes (Fig 5A).

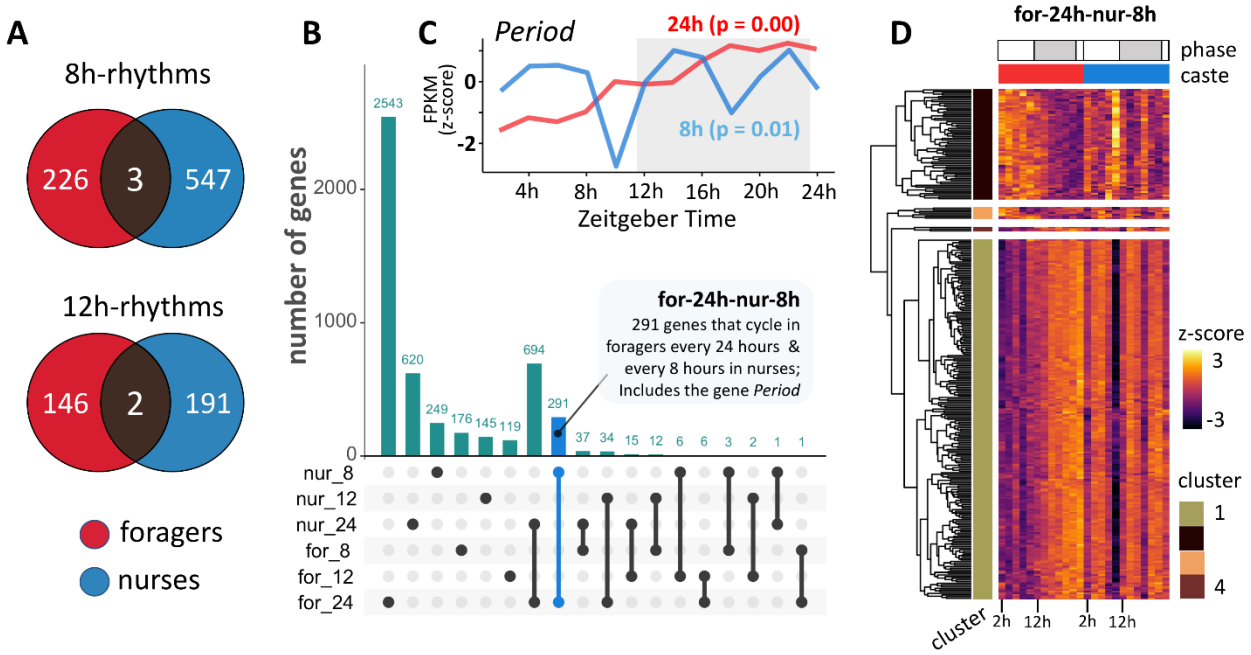

Figure 5: Ultradian rhythms and caste-associated differential rhythmicity in gene expression.

(**A**) Venn-diagrams showing the number of genes with significant ultradian expression in the ant brain, oscillating every 8-hour (8h-rhythms) and 12-hour (12h-rhythms); (**B**) Upset plot showing the number of genes uniquely expressed in, and shared between, diurnal (24h) and ultradian (8h and 12h) gene sets. Each bar represents a unique intersection between the six diurnal and ultradian genesets (e.g., for-24: 24h-oscillating genes in foragers, nur-12: 12h-oscillating genes in nurses, etc.). A gene is binned only once, and as such, belongs to only one intersection. Dark circles indicate the gene sets that are part of a particular intersection. For example, the first circle indicates that there are 2543 genes that are uniquely cycling in foragers with a 24h period (for-24). Similarly, the blue bar indicates that there are 291 genes that have a significantly diurnal expression in foragers but cycle every 8-hours in nurses (for-24h-nur-8h); **(C)** Caste-associated differential rhythmicity in the expression of the core clock gene *Period* is shown. The expression

of *Per* cycles every 24-hours in forager brains (red) and every 8-hours in nurses (blue); p-values obtained from eJTK are provided in parenthesis. The Zeitgeber Time is indicated on the x-axis, while the y-axis shows the normalized (Z-score) gene expression. The dark phase of the 12h:12h light-dark cycle is represented in grey (dark phase begins at ZT12); **(D)** Heatmap showing the daily expression of all genes in the for-24h-nur-8h geneset, for nurses and foragers. Caste identity is indicated above the heatmap as a column annotation (red-foragers and blue-nurses). The for-24h-nur-8h geneset was clustered into four groups, and the cluster identity of each gene is indicated as row annotations ("cluster"). The majority of 8h-cycling genes in nurses, including the *Per* gene, belong to Cluster 1 and show a night-time peak in forager heads.

Having identified ultradian rhythms in gene expression, we asked if genes that oscillated in a diurnal manner in forager brains, but not in nurses, were cycling in an ultradian manner in nurses. Indeed, we found that 325 (out of 2875) genes that cycled every 24h in foragers were not arrhythmic in nurses but differentially rhythmic genes (DRGs) that showed robust 8h (291 genes) or 12h (34 genes) rhythms ("for-24h-nur-8h" and "for-24h-nur-12h", respectively; Fig. 5B). Remarkably, several components of the insect clock were among the 291 DRGs that cycled every 24h in foragers and every 8 hours in nurses: *Period* (*Per*), *Shaggy* (*Sgg*; *Gsk3b* in mammals), *Protein phosphatase 1b* (*Pp1b*), and *Protein phosphatase 1 at 13C* (*Pp1-13c* or *Pp1*) (Fig. 4, Table 1). This suggests that gene expression in nurse ant brains is, perhaps, not as arrhythmic as previously reported [69]. Instead, certain clock components in nurses seem to be cycling at a different harmonic compared to foragers, which could be partly facilitating the swift behavioral caste changes between foragers and nurses that have been observed in other studies [20, 21, 167]. As such, we continued our investigation into the genes that cycled every 24h in foragers and every 8h in nurses by asking if these DRGs play putative functional roles in regulating known clock-controlled processes as well as behavioral plasticity in ants.

Plasticity of rhythmic gene expression in ant brains

In *Drosophila*, the circadian clock regulates daily rhythms in transcription via rhythmic binding of CLK and RNA Polymerase (Pol) II to the promoters of clock genes including *Per*, *Doubletime (Dbt; Ck1* in mammals*)* and *Shaggy (Sgg, Gsk3b* in mammals*)* [74, 168]. The kinase SGG regulates nuclear accumulation of the PER/TIM repressor complex [158, 169, 170], whereas DBT regulates its stability [171-173]. In addition to DBT, several other kinases (e.g., NEMO, CK2, and PKA) [171, 174-176] and a few phosphatases (e.g., PP1 and PP2a) [177, 178] have been identified as regulators of PER and PER/TIM stability in *Drosophila*. In the fruit fly *Drosophila*, the expression of *Per* and several other clock and clock-controlled genes peak during the night-time [168]. Similar to *Drosophila*, we observed a night-time peak in *Per* expression for *C. floridanus* foragers, which is also consistent with previous findings in fire ants and honeybees [60, 167]. Additionally, the phase of diurnal *Per* expression in *C. floridanus* foragers is consistent with the phase of oscillating PER abundance previously reported for the species [105]. For instance, the expression of *Per* and its protein product, both, peak at lights on (ZT24/ZT0). This is followed by a sharp decrease of *Per* at ZT2 which could explain, in part, the gradual decline in PER abundance during the day-time that has been reported by Kay and colleagues [105].

In our study, the daily changes in the expression of *Sgg*, *Dbt*, *Nemo*, *Pp1b* and *Pp1* mirrored the differentially rhythmic expression patterns of *Per* in the two ant castes (Fig. 5C, Table 1). Even though the 8h rhythms of *Dbt* (p=0.11) and *Nemo* (p=0.11) in nurse brains were not statistically significant, their expression patterns showed a strong phase coherence with *Per* (Additional File 5). Having core clock components that simply cycle at a different harmonic,

versus not showing any rhythmicity at all, could indeed explain the ability of "around-the-clock" nurses to rapidly develop forager-like rhythmic activity, in behavior and gene expression, when their social context changes [20, 21, 167]. Furthermore, hierarchical clustering of the DRGs that cycled every 24h in foragers and every 8h in nurses revealed that most of these DRGs clustered with *Per* (i.e., largely in-phase with the expression pattern of *Per* in foragers and nurses) (Fig. 5D, Additional File 7, sheet 1). Therefore, we hypothesized that the DRG-cluster in nurses that oscillated every 8h with a phase similar to *Period* would be enriched for some of the same biological processes performed by 24h cycling genes in foragers discussed above. Indeed, we found that the *Per*-like DRG-cluster was significantly enriched in functional annotations that we also identified in the night-peaking diurnal gene cluster of foragers; the GO terms: transcriptional regulation (DNA-templated), transcriptional regulation by RNA Pol II, protein phosphorylation and GPCR signal transduction (Additional File 7, sheet 2).

Moreover, the *Per*-like DRG cluster contained the muscarinic acetylcholine receptor gene *mAchR* and the insect dopamine/ecdysteroid receptor *DopEcR*, which have both been found to be clock-controlled in *Drosophila* [92, 179, 180]. The *mAchR* gene has a putative role in olfactory and mechanosensory signal transduction [181, 182]. Therefore, its differential clock-controlled regulation in foragers and nurses could be contributing to caste-specific behavioral phenotypes (Fig. 4). The same could be true for *DopEcR*, which modulates insect behavior by responding to dopamine, ecdysone and 20-hydroxyedysone [183-186]. In fact, dopamine is a known regulator of foraging activity in ants (reviewed in [187, 188]) and dopamine signaling has been found to be important in entraining the insect circadian clock as well as mediating clock-controlled behavioral phenotypes such as locomotion [189-191]. Studies in mammals suggest that certain dopaminergic oscillators are highly tunable and capable of generating 12 rhythms in locomotor

activity, independent of the circadian clock, and this independent 12h-clock coordinates metabolic and stress rhythms [192, 193]. Although we have not yet identified any biological oscillator that produces 8h rhythms, such ultradian rhythms in gene expression has been found in both fungi [159] and animals [194]. Our finding that a set of genes, enriched for several biological processes, that oscillate in a diurnal manner in forager brains can switch to ultradian oscillations in nurses suggests that mechanistic links between chronobiological and behavioral plasticity in ants exist (Fig. 4).

It is not clear if the 8h rhythms in ant brain gene expression are endogenously produced or socially regulated, and what the functional aspects of such rhythms are, if any. However, the social insect literature does point to one likely role for the ability of nurses to track 8h periods: brood translocation. Workers of the carpenter ant species *Camponotus mus* have been observed to show daily rhythms in brood translocation behavior to move their brood between different temperature conditions. The measured time between the two daily brood translocations was exactly 8 hours [57, 195, 196]. This suggests that the 24h rhythm in thermal preference in *C. mus* nurses could be coupled with an 8h oscillator that drives the observed daily timing of temperature-dependent brood translocation. Brood translocation is important for larval development, and hence, has implications for colony fitness [58]. As such, 8h rhythms in behavioral outputs could have important adaptive functions. To begin to understand the potential roles for ultradian rhythms in the functioning of ant colonies, behavioral and molecular studies aimed at linking 8h transcriptional rhythms and brood translocation could provide a good first step.

Plasticity in behavioral output pathways

In flies, rhythmic activity patterns in total darkness have been related to the signaling pathway mediated by the neuropeptide Pigment Dispersing Factor (PDF) [74, 197-200]. PDF binds to the PDF receptor (PDFR) and triggers a signal transduction that increases cAMP levels and activates the protein kinase PKA [176]. A deficiency in PKA resulted in loss of fly locomotory rhythms even when *Per* oscillation was intact [201]. Moreover, PDF plays a central role in circadian timekeeping by mediating light input to the circadian clock neurons in the brain, coordinating pacemaker interactions among neurons, regulating the amplitude, period, and phase of 24h-oscillations, and mediating output from the clock to other parts in the central brain [202-210]. Neurons that express PDF are present in the *C. floridanus* brain as well and could be mediating time-of-day information to brain regions involved in activity rhythms [105, 211-213]. In line with this, we found robust diurnal rhythms in *Pdf*, *Pdfr* and *Pka* gene expression in the brains of *C. floridanus* foragers (Fig. 4, Table 1). However, nurse ants, which generally reside in dark nest chambers and demonstrate a lack of 24h-rhythms in locomotion, did not exhibit diurnal nor ultradian rhythmicity in *Pdf*, *Pdfr* and *Pka* expression (Fig. 4, Table 1). The absence of locomotory rhythms in nurse ants could, thus, also be the result of a non-oscillatory PDF signaling pathway.

Links between division of labor and chronobiological plasticity

Past research has identified several genes and pathways that could be underlying behavioral division of labor [142, 214-218]. However, the extent of clock control over these key elements has not been explored yet. As such, we identified genes that were differentially expressed between the two ant castes throughout the day and determined if these differentially expressed

genes (DEGs) showed any diurnal or ultradian oscillations. Of the 10,038 expressed genes in the brains of *C. floridanus*, only 81 were significantly differentially expressed between the two behavioral groups based on our stringent cut-off criteria (fold change ≥ 2, q-value < 0.05; Additional File 8, sheet 1). However, we should note that as many as 2439 genes displayed a fold-change greater than zero at 5% FDR (Additional File 8, sheet 1), which is consistent with the number of DEGs reported in prior studies that have compared gene expression in nurse and forager ants [142, 218]. Of these 81 DEGs, 34 were significantly higher expressed in forager brains, and the remaining 47 were higher expressed in nurses (Fig. 6; Additional File 8, sheet 1). The 34 genes that were higher expressed in foragers comprised of several genes with unidentified functions and did not contain any significantly enriched GO terms. In contrast, the 47 genes that were higher expressed in nurses contained five maltase and five alpha-amylase genes which resulted in a significant enrichment for the GO terms carbohydrate metabolic process and catalytic activity (Additional File 8, sheet 2). This suggests that nurses might be metabolically more active than foragers, which is in line with previous findings from another ant species [142].

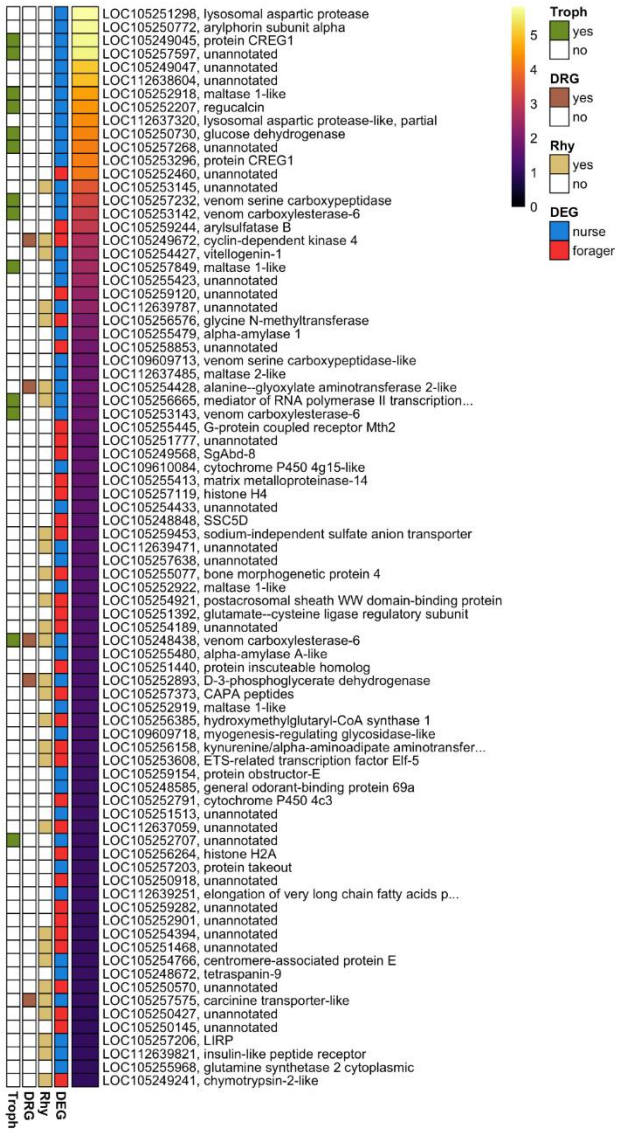

Figure 6: Differentially expressed genes between forager and nurse ant brains.

Heatmap showing absolute (abs) log2-Fold-Change (log_2FC) values for all 81 DEGs ($q < 0.05$ and $abs(log_2FC) \geq 1$), ordered from highest to lowest fold-change. The DEG column indicates if the gene is significantly higher expressed in foragers (red) or nurses (blue). For each DEG, the *C. floridanus* gene numbers and their blast annotations are provided. Genes with no blast annotation or annotated as uncharacterized protein are indicated as "unannotated". The Rhy (rhythmic) column indicates genes that are significantly rhythmic in at least one of the ant castes. The DRG column indicates genes that are significantly rhythmic in both castes but oscillating at different periodicities. Genes that code for proteins previously found in the trophallactic fluid of *C. floridanus* are indicated in the Troph column.

Looking for oscillating genes among the DEGs that we identified in *C. floridanus*, we found that more than one-third (i.e., 28 of the 81 DEGs) were expressed rhythmically in either forager or nurse brains (Fig. 6). The set of 81 DEGs was significantly overrepresented in genes that show ultradian (8h or 12h) oscillations in daily expression (Odds-ratio = 2.18; p-value = 0.006). Of these clock-controlled DEGs, five genes oscillated at different periodicities in the two ant castes, providing further support for potential links between chronobiological and behavioral plasticity in *C. floridanus*. One of these differentially rhythmic genes, *Cyclin-dependent kinase 4* (*Cdk4*), was higher expressed and cycled every 12h in forager brains, while it cycled with an overall lower expression in nurse brains every 24h (Fig. 6, Additional File 8, sheet 1). The other four differentially rhythmic DEGs, *Alanine—glyoxylate aminotransferase 2-like* (*Agxt2*), *D-3-phosphoglycerate dehydrogenase* (*Phgdh*), *Carcinine transporter-like* (*CarT*) and *Venom carboxylesterase-6*, showed a higher overall expression in nurse brains where they cycled every 24h, while foragers exhibited an 8h oscillation in expression (Fig. 6, Additional File 8, sheet 1).

The results of our study, and previous findings with regards to *venom-carboxylesterase-6*, warrant speculation on the potential role of *venom-carboxylesterase-6* in mediating the links between chronobiological and behavioral plasticity. *Venom-carboxylesterase-6*, a gene that is both differentially expressed and differentially rhythmic in *C. floridanus* brains, is an abundant protein found in the trophallactic fluid of this species [106, 110]. In fact, we found that more than a quarter (13 out of 47) of all genes that were higher expressed in nurses encoded such orally transferred proteins, including all three copies of *venom-carboxylesterase-6* (Fig. 6). The protein encoded by *venom-carboxylesterase-6* is a JH esterase (JHE). JHEs are enzymes that degrade JH in insect hemolymph, thus, regulating JH titers and caste-associated behaviors in ants [110, 219]. The peak expression of the 24h cycling *venom-carboxylesterase-6* in nurse brains was around

ZT12-14, which corresponds to the peak time of colony foraging that we found in *C. floridanus* (Fig. 1, Additional File 4 and 6). As such, a *venom-carboxylesterase-6* mediated dip in JH levels could be contributing to a lower propensity of nurses to engage in extranidal tasks during peak colony foraging hours. In line with this reasoning, we found that the lowest dip in forager *venom-carboxylesterase-6* expression, and likely corresponding increased levels of JH, occur at ZT12, the onset of peak foraging activity (Fig. 1, Additional File 4 and 6). We should note that expression of trophallactic fluid genes in the brain is somewhat unexpected, and that the expression of such genes could potentially result from remnant fat body cells during brain dissections. In our study, the expression levels of trophallactic fluid genes showed consistent differences between the two castes throughout the 24h-day. Therefore, we suspect that the results are not an artefact of our dissections because they were conducted in the same way for the two castes. One would expect a more random distribution of trophallactic signals in our dataset if they were due to fat body cell contamination. However, if the signal originates in the brain or fat body cells remains unclear at this time and future studies using time-course single-cell RNA-Seq could be used to uncover tissue-specific daily expression profiles.

Even though not much is known about the role of circadian clocks in regulating behavioral plasticity in ants, previous studies have identified several genes and protein products that seem to be central regulators of behavioral plasticity in social insects [220]. Caste-specific differences in larval storage proteins, especially Vitellogenin (Vg) and Arylphorin subunit alpha, and JH have been consistently found across social insects. In bees, for example, high *Vg* levels and low JH titers correlate with nurse-like behaviors [221], whereas downregulation of *Vg* results in increased JH titers and a behavioral state characteristic of forager bees [222]. Similarly, nurses of the fire ant *Solenopsis invicta* show significantly higher *Arylphorin subunit alpha* expression

as compared to the foragers [223]. Consistent with these previous findings, we found *C. floridanus* nurse brains to have significantly higher *Arylphorin-subunit-alpha* (50-fold) and *Vg* (6-fold) expression as compared to foragers (Fig. 6, Additional File 8, sheet 1). Additionally, our data showed that *Vg* expression is significantly oscillating every 24h in nurse brains. Although not significant, *Arylphorin subunit alpha* also showed a *Vg*-like oscillatory expression in nurse brains (tau = 24h, p = 0.09) (Additional File 5). However, forager brains showed no such rhythms in *Vg* or *Arylphorin subunit alpha* expression. As such, our study provides further support for a role of *Vg* and *Arylphorin subunit alpha* in behavioral division of labor and highlights a putative clock-control of these genes in nurse brains (Fig. 4). The functional role, if any, of a rhythmic *Vg* expression in ant physiology or behavior remains to be explored.

Conclusion

The study presented here is providing a first look at the clock-controlled pathways in ants that could underlie caste-associated behavioral plasticity and sheds new light on the links between molecular timekeeping and behavioral division of labor in social insects. Understanding how an ant's biological clock can predictably interact with its environment to produce distinct, yet stable, caste-associated chronotypes, lays the foundation for further molecular investigations into the role of biological clocks in regulating polyphenism in ant societies.

To produce high-interval time course data that reflects the transcriptional differences between forager and nurse ants throughout a 24h day, we used an experimental setup that allowed us to reliably sample each ant caste and obtain their diurnal brain transcriptomes. The colony activity data that we collected had high enough resolution to even identify how the colony is able to quickly get back on track with regards to food collection efforts after a disturbance. More importantly, we found a reduced circadian time keeping in nurses as compared to foragers. This was evidenced by the vastly different number of genes that oscillated every 24h in each ant caste, and the temporal segregation of clock-controlled processes, which is detectable in both castes but to a lesser extent in nurses. Our findings are, therefore, in line with the results of a previous study done in honeybees, which indicates that a difference in 24h-rhythmic gene repertoire between foragers and nurses could be a more general phenomenon within eusocial Hymenoptera, and likely contributes to the caste-specific differences observed in behavioral activity rhythms.

Moreover, many genes that showed a diurnal expression in forager brains were expressed in an ultradian manner in nurses, instead of being entirely arrhythmic. Among the differentially

rhythmic genes were essential components of the core and auxiliary feedback loops that form the endogenous clock of insects, as well as genes involved in metabolism, cellular communication and protein modification (Fig. 4). The ability of core clock and clock-controlled genes to oscillate at different harmonics of the circadian rhythm, and to switch oscillations from one periodicity to the other due to age or colony demands, might explain why chronotypes associated with ant behavioral castes are stable in undisturbed conditions, yet highly plastic and responsive to changes in their social context. However, it remains to be seen if the caste-associated differential rhythmicity that we observed is a general phenomenon across ant and other eusocial societies, or a species-specific trait. In addition, the potential for an actual adaptive function for maintaining both diurnal and ultradian rhythms in ant colonies will have to be further explored.

Finally, we found that the genes differentially expressed between forager and nurse brains are enriched in genes that show ultradian rhythms (periodicity = 8h or 12h). Additionally, several of these differentially expressed genes showed robust 24h rhythms in nurse brains, including known regulators of JH titers in insects: *Vg* and *venom-carboxylesterase-6* (Fig. 4). Given the central role of Vg and JH in regulating division of labor in social insects, we propose that a mechanistic link between plasticity of the circadian clock and division of labor likely exists.

CHAPTER TWO:
ANT CLOCKS AND PARASITIC MANIPULATION

Introduction

In the first chapter, we demonstrated that plasticity of the ant's clock and clock-controlled rhythms seems to be tightly linked to its behavioral plasticity. The ease with which ants display behavioral plasticity, although beneficial to the host, could make them susceptible to parasite hijacking. Parasites that modify host behavior in order to successfully grow and transmit are found in a wide variety of taxa. Field studies and laboratory experiments on different behavior modifying diseases indicate that manipulating parasites might be targeting the host's biological clock to induce to some of the behavioral changes in its host. For example, flies infected with the fungus *Entomophthora*, caterpillars infected with baculoviruses, and ants infected with the fungus *Ophiocordyceps* and the trematode *Dicrocoelium* show altered, or even loss of, daily activity-rest rhythms (REFS). Furthermore, parasite-adaptive behaviors shown by infected hosts, such as summitting and attachment to substrate before death, seems to be highly synchronized to a specific time of day (REFS). Although the phenotypic evidence for a role of clocks in behavior modifying diseases seems to be emerging across different host-parasite systems, empirical evidence of the same on a molecular level is currently elusive.

An emerging model system to study parasitic manipulation of host behavior are the *Ophiocordyceps* fungi infecting ant hosts, and we focus primarily on one such parasite-host pair that is native to central Florida (USA): the carpenter ant *Camponotus floridanus* (host; *Cflo*) and their specialist manipulator *Ophiocordyceps camponoti-floridani* (parasite; *Ocflo*). As we layout in the General Introduction at the beginning of this dissertation, the *Ocflo*-induced "manipulated"

state in ants is associated with enhanced locomotory activity (or hyperactivity), increased wandering behavior, and severe convulsions. The characteristic manipulation phenotype is observed in the final stages of this disease: the infected ant shows a seemingly phototactic summiting behavior, and upon reaching a relatively elevated position, bites into a substrate with locked jaws, dying shortly after (REF). The amount of light received at the final location of the manipulated ant seems to be important for *Ocflo* fruiting body growth, whereas the elevated position has been hypothesized to be important for spore dispersal, and therefore, transmission of *Ocflo* [37, 38, 224]. Taken together, the specific manipulation of ant behavior by *Ocflo* provides a growth and transmission site that appears to be adaptive for the fungal parasite.

Moreover, the manipulated biting appears to be highly synchronized to a specific time of day across multiple *Ophiocordyceps*-ant species interactions, observed in field conditions as well as in controlled laboratory experiments [26, 34-36]. This time-of-day specific manipulation of host behavior demonstrates that in the final stages of the disease, *Ocflo*-infected ants do have some form of functional timekeeping machinery. It has been hypothesized that the fungal parasite might be driving at least some aspects of this timekeeping in the diseased ant (REFs). Different lines of evidence suggest that *Ophiocordyceps* fungi could be hijacking the timekeeping machinery of the ant to induce timely manipulation of host behavior. First, like most fungi, *Ophiocordyceps* has a biological clock that is functionally similar to the endogenous oscillators found in animals and plants [30]. Second, several candidate fungal manipulation genes or effectors (e.g., small secreted proteins) seem to be under clock control in *Ophiocordyceps* [30]. And third, using a network-based meta-analysis, we have identified a possible molecular link between ant's clock and behavioral plasticity that is likely targeted by the manipulating parasite to induce timely changes to the ant's behavior and clock-controlled

processes [225] (Fig. 7). In the latter study, we set out to understand the regulatory links between the behavior plasticity genes in *C. floridanus* (a set of 81 genes differentially expressed between forager and nurse brains; Chapter one) [226] and its clock-controlled genes. To do so, we mapped the behavior plasticity genes and the 24h-rhythmic genes on to the gene co-expression network (GCN) of *C. floridanus* brains (Fig. 7). We found that most behavioral plasticity genes were primarily located in only two modules of highly co-expressed genes. Although the two behavioral plasticity modules did not contain an overrepresentation of rhythmic genes, both were connected to modules that showed an overrepresented for 24h-rhythmic genes (Figure 7). This suggests that behavioral plasticity and clock-controlled rhythms are co-regulated in the brain of *C. floridanus*. Next, we wanted to know what happens to the ant's GCN during active manipulation by *O. camponoti-floridani*. We mapped the ant genes differentially expressed at the final manipulated biting stages of *Ophiocordyceps*-infection [227] on to the ant's GCN, we found that the disease-associated DEGs reside in exactly the same modules as those containing behavior plasticity genes (Figure 7). This puts forward the data-driven hypothesis that the manipulating parasite, *Ocflo*, might be targeting this pre-existing co-regulatory link between the host clock and behavior in order to induce timely manipulation [225]. One of the goals of the current study, therefore, was to empirically test this apriori hypothesis by sampling *Ophiocordyceps*- infected ants over a 24h day to investigate what happens to the daily expression of their clock genes, clock-controlled genes and behavioral plasticity genes, and if the parasite does in fact affect the host's pre-existing links between behavioral plasticity and clock.

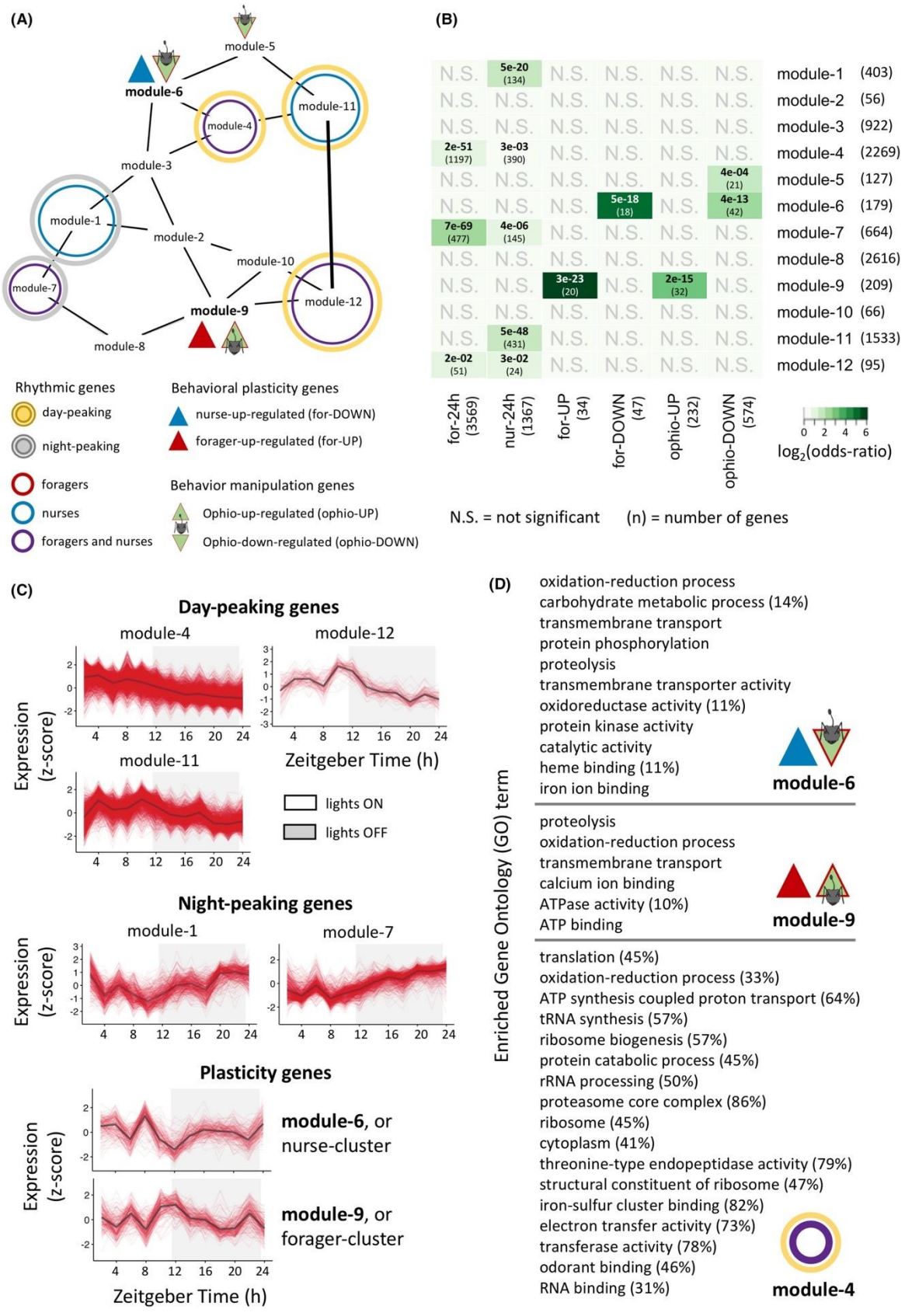
(A)
module-5
module-6
module-11
module-4
module-3
module-1
module-2
module-10
module-7
module-12
module-9
module-8
Rhythmic genes
day-peaking
night-peaking
foragers
nurses
foragers and nurses
Behavioral plasticity genes
nurse-up-regulated (for-DOWN)
forager-up-regulated (for-UP)
Behavior manipulation genes
Ophio-up-regulated (ophio-UP)
Ophio-down-regulated (ophio-DOWN)
(B)
module-1 (403)
module-2 (56)
module-3 (922)
module-4 (2269)
module-5 (127)
module-6 (179)
module-7 (664)
module-8 (2616)
module-9 (209)
module-10 (66)
module-11 (1533)
module-12 (95)
for-24h (3569)
nur-24h (1367)
for-UP (34)
for-DOWN (47)
ophio-UP (232)
ophio-DOWN (574)
log2(odds-ratio)
N.S. = not significant
(n) = number of genes
(C)
Day-peaking genes
module-4
module-12
module-11
Expression (z-score)
Zeitgeber Time (h)
lights ON
lights OFF
Night-peaking genes
module-1
module-7
Plasticity genes
module-6, or nurse-cluster
module-9, or forager-cluster
(D)
Enriched Gene Ontology (GO) term
oxidation-reduction process
carbohydrate metabolic process (14%)
transmembrane transport
protein phosphorylation
proteolysis
transmembrane transporter activity
oxidoreductase activity (11%)
protein kinase activity
catalytic activity
heme binding (11%)
iron ion binding
module-6
proteolysis
oxidation-reduction process
transmembrane transport
calcium ion binding
ATPase activity (10%)
ATP binding
module-9
translation (45%)
oxidation-reduction process (33%)
ATP synthesis coupled proton transport (64%)
tRNA synthesis (57%)
ribosome biogenesis (57%)
protein catabolic process (45%)
rRNA processing (50%)
proteasome core complex (86%)
ribosome (45%)
cytoplasm (41%)
threonine-type endopeptidase activity (79%)
structural constituent of ribosome (47%)
iron-sulfur cluster binding (82%)
electron transfer activity (73%)
transferase activity (78%)
odorant binding (46%)
RNA binding (31%)
module-4

Figure 7 Gene co-expression network (GCN) in Camponotus floridanus ant brains.

(A) The annotated gene co-expression network summarizes our overrepresentation analyses and identifies different modules of interest that are putatively important for the interplay of rhythmicity, behavioral plasticity and parasitic behavioral manipulation. The connectivity patterns between the gene modules are shown; thick edges indicate correlations ≥0.8, thinner edges indicate correlations between 0.6 and 0.8, and no edges indicate correlations <0.6. (B) The heatmap summarizes the pairwise Fisher's exact tests used to annotate the ant brain GCN. Box colors represent odds ratio, and the Benjamini–Hochberg corrected p-values are shown together with the number of overlapping genes between module–geneset pairs in parenthesis. Non-significant overlaps are indicated as N.S., and the total number of genes in each module or geneset is shown in parenthesis as well. (C) Daily expression pattern of all genes in each of the rhythmic and plasticity modules are shown. Each red line represents the expression of a single gene, every 2 h over a 24-h day in forager brains. The black line represents the module's median gene expression. The x-axis shows the time of day or Zeitgeber Time (ZT) in hours, whereas the y-axis shows normalized gene expression as z-scores calculated from log2-transformed expression data. White background indicates the light phase (lights on at ZT24/ZT0), and grey background indicates the dark phase (lights turned off at ZT12). (D) The significantly overrepresented Gene Ontology (GO) terms in the behavioral plasticity/manipulation modules (Modules 6 and 9) and the correlated rhythmic modules (Modules 4 and 12). Module 12 is not depicted since it was only overrepresented in one GO term (i.e. membrane). The number in parenthesis indicates the percentage of all genes annotated with the GO term found in the module, if it was higher than 10%. The figure presented here was published in de Bekker and Das (2022) [225].

A synchronized timely change (increase/decrease) in the daily expression of behavioral plasticity genes can have multiple effects on the rhythmic properties of co-regulated clock-controlled genes, such as (1) loss or complete disruption of daily rhythms, (2) increase or decrease in the degree of synchronization of daily rhythms (e.g., most genes peaking at the same time of day), and (3) general increase or decrease in their average daily expression (differential gene expression). Such changes to host daily rhythms, however, could be a general effect of infectious diseases and not necessarily specific to manipulating parasites such as *Ophiocordyceps* (reviewed in [228]). Another goal of this study, therefore, was to tease apart the changes that occur to the *C. floridanus'* clock and clock-controlled rhythms during infection by its manipulating, specialist parasite (*Ocflo*) as compared to infection by a non-manipulating, generalist parasite (*Beauveria bassiana*). Previous work from our lab has characterized the effects these two infectious diseases have on host's collective behavior, especially its ability to

forage [116]. Trinh and colleagues demonstrated that in the early stages of *Ocflo*-infection, prior to halfway through disease progression – the time point in disease at which only half of the infected ants survive – infected ants in a group perform extranidal (outside nest) visits in a rhythmic manner, similar to uninfected control groups (Fig. 8A) [116]. However, in later stages of the disease, *Ocflo*-infected ants show a loss of daily rhythms in foraging (Fig. 8A). It remains to be seen if this loss of rhythmic activity in group foraging is due to loss of individual locomotory rhythms in the infected hosts, or an inability of infected ants to detect or respond to social cues necessary for synchronizing their activity rhythms, or both. At least for *C. floridanus*, an absence of rhythms in locomotory behavior (e.g. arrhythmicity in nurse ants) does not necessarily mean an absence of functional timekeeping at the molecular level (several core clock and clock modulating genes oscillate every 8h in nurses; see Chapter one for more details) [226]. Unlike *Ocflo*-infected ants, *Beauveria*-infected ants do not show a loss of rhythmic foraging in the latter half of its disease. However, they do show a drastic shift in the daily timing of the foraging peak, shifting from a nocturnal peak during early disease, similar to uninfected controls, to a day-time peak around ZT6 (middle of the subjective day time) in the latter half of the disease (Fig. 8A) [116]. Therefore, the halfway mark in both diseases seem to be a diverging point in their ultimate disease outcome, at least in terms of the parasite's effect on host's activity rhythms, a behavior driven by the host's biological clock, which could be used to discern how daily gene expression is potentially affected by infection with both fungi. As such, in this study, we use the halfway mark of infection for both *Ocflo* and *Beauveria* infections to characterize the changes that occur to the infected host's clock and clock-controlled processes.

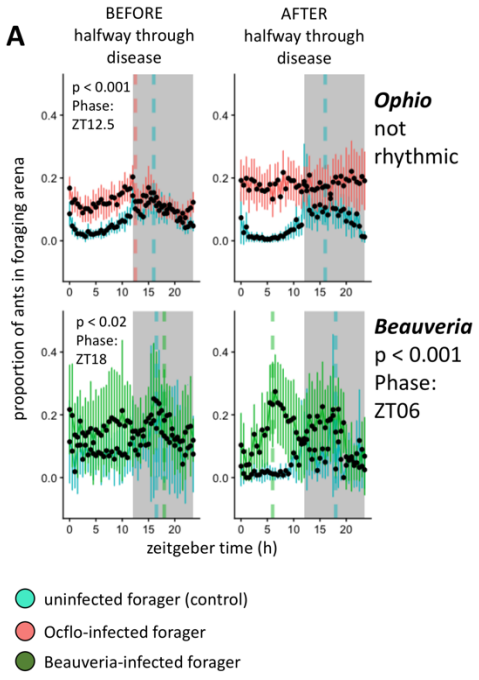

B

Covariate	Model for nonzero data (μ)				Model for zero data (ν)			
	Estimate	SE	*t*	*P*	Estimate	SE	*t*	*P*
Model 1: OI and OC in the foraging arena								
Treatment (T)	0.653	0.121	5.382	**<0.001**	−4.621	0.654	−7.071	**<0.001**
Day	0.069	0.017	4.114	**<0.001**	0.22	0.031	7.036	**<0.001**
ZT	0.023	0.007	3.411	**0.001**	−0.158	0.022	−7.243	**<0.001**
T*Day	0.015	0.018	0.815	0.415	0.105	0.063	1.679	0.093
T*ZT	−0.036	0.008	−4.33	**<0.001**	0.147	0.049	2.981	**0.003**
Model 3: BI and BC in the arena								
Treatment (T)	0.717	0.132	5.418	**<0.001**	−0.411	0.518	−0.794	0.427
Progression (P)	−0.423	0.187	−2.26	**0.024**	2.613	0.389	6.719	**<0.001**
ZT	0.015	0.008	1.891	0.059	0.017	0.023	0.754	0.451
T*P	0.575	0.216	2.657	**0.008**	−1.53	0.599	−2.553	**0.011**
T*ZT	−0.015	0.01	−1.567	0.117	−0.046	0.04	−1.153	0.249
Day*ZT	0.04	0.013	3.041	**0.002**	−0.058	0.028	−2.097	**0.036**
T*Day*ZT	−0.036	0.015	−2.325	**0.02**	0.117	0.045	2.579	**0.01**

Figures and data from Trinh et al. (2021) *Animal Behaviour*

Figure 8 Fungal infections affect ant foraging rhythms, but the effect is parasite-specific.

The changes to infected ant's group foraging rhythm (proportion of ants visiting the foraging arena throughout the day) as observed by Trinh and colleagues (2021) is shown. The top row in (A) shows the average (± 95% CI) activity of *Ocflo*-infected ants (red) before and after the halfway mark in disease as compared to the uninfected controls (blue) monitored in parallel. The bottom row in (B) shows the same for *Beauveria*-infected ants (green). The authors used the rhythmicity analysis software RAIN to detect any significant 24h-rhythms, if present, in foraging rhythms. The results from the rhythmicity analysis for infected ants are shown. A p-value less than 0.05 indicates a significant 24h-rhythm in activity was detected by RAIN, and for such scenarios, the peak time of daily activity (Phase) estimated by the software is shown. Panel (B) provides a different set of results from the same study by Trinh and colleagues, in which they show that, among other things, the daily fluctuations in ant's foraging activity change with disease progression (Day*ZT is significant) for both infections. Also, for either infectious disease, the daily fluctuations in ant foraging activity were significantly different during disease as compared to controls (T*ZT is significant). The figures and all the data were obtained from Trinh et al. (2021) [116] and Trinh (2021) [46], and have been reported here without any additional analyses.

Comparing the two infectious diseases at the halfway mark also allowed us to standardize the comparison since the two fungi have very different incubation periods inside its host. *Ocflo*-infected ants can live for up to four weeks whereas *Beauveria*-infected ants succumb to fungal infection within a week. We collected whole heads of forager ants infected with *Ocflo*

(manipulating) and *Beauveria* (non-manipulating), every 2 hours, over a 24h period. In parallel, we also collected time-matched uninfected foragers to obtain a control, baseline daily gene expression patterns for ant heads. Given that fungal infected ant heads might contain mRNA from both ant and fungi, we performed time-course RNASeq of the entire ant head to be able to quantify changes in the daily transcriptome of both host and parasite during disease (see Chapter 3 for fungal data). By combining time-course RNASeq and comparative network analyses, we aimed to (1) compare and contrast the changes in ant's daily transcriptome caused by the two fungal parasites, (2) identify putative mechanisms via which *Ocflo* might be inducing changes to the host's clock and clock-controlled output, and (3) to test if manipulation of host's daily gene expression is a hallmark of infectious diseases in general or specific to behavior manipulating parasites.

Methods

Collecting Camponotus floridanus colony and experimental setup

We collected a large (several thousand workers), queen-absent colony of *C. floridanus* with abundant brood (eggs, larva, and pupa) from the University of Central Florida Arboretum on 19th March 2021, from inside a decaying saw palmetto. Two days after collection, we split the source colony into two daughter colonies of approximately the same size and moved each into a clean container with talcum-coated walls. Until the start of the experiment, we kept the two daughter colonies under oscillating light-dark cycles (12h:12h) but constant temperature (25 ºC) and relative humidity (75% rH). Given that in natural conditions *Ophiocordyceps* is most likely to infect ants in the foraging caste (ones that perform most of the outside nest activities), we used only forager ants for fungal infections and as controls. To identify the forager ants in a given daughter colony, we replicated the formicarium setup described in Das and de Bekker (2022) in which a foraging arena (container) was connected via a 2 m long plastic tube to another container always kept in dark. The dark container imitated the dark nest chambers of an ant colony. Prior to starting the experiment, each individual daughter colony was moved into its own formicarium setup housed inside climate-controlled incubators. For the first phase of the experiment, the foraging arena of both daughter colonies were exposed to constant light conditions to incentivize ants to move their brood into the dark nest box. The constant light conditions in the foraging arena also aided in resetting the biological clocks of the ants and ensuring that the colony can later synchronize to the strict 12h:12h light-dark (LD) cycles they are exposed to. After 2-3 days of constant light conditions, the foraging arenas were exposed to 12h:12h LD cycles (lights were turned on at noon local time, and lights were turned off at midnight). Throughout the experiment,

the colonies were kept at constant temperature (25 ºC) and relative humidity (75% rH). After three days of initial entrainment to the light-dark cycles, each daughter colony was sugar starved for at least 24h before we performed mark-and-recapture to identify foragers in the colony. Overnight sugar starvation helped with ensuring the colony was actively foraging during our days of mark-and-recapture in which we collected ants in the foraging arena during their active phase (night-time for our nocturnal ants), marked their gasters with a dot of silver paint (Testors) if collected the first time, or marked their thorax with a second dot of paint if collected for the second time. We performed all mark-and-recapture within two hours after lights were turned off (ZT12-ZT14) and two hours prior to lights turning on (ZT22-ZT24/ZT0). We then proceeded to setup smaller experimental colonies – one for controls and one for fungal infections – that contained either infected (with *Ocflo* or *Beauveria*) or uninfected (control) foragers. The experimental setups also ensured that the size of our experimental colonies was standardized. Each of our experimental boxes contained 150 marked forager ants that were either infected with fungi or served as uninfected controls. Additionally, we added 10 brood-tending nurse ants and some brood (10 larva and 10 pupa) to incentivize foraging during the experiment.

Due to logistical constraints, we could setup only two experimental colonies at a given time. For the first run, we constructed two experimental setups, one for infection trials with *Beauveria* and another that served as control. Once *Beauveria*-infected ants were sampled along with the controls for RNASeq, we setup two more experimental colonies – one for *Ocflo* infection and the other served as control – to harvest infected ants at the same two-hour resolution used for *Beauveria*-infected and control ants. For the *Beauveria* infection run, we sampled the 300 foragers (150 for *Beauveria*-infections and 150 for controls) from 445+ marked

ants across the two daughter colonies that had visited the foraging arena at least once. For *Ocflo* infection run, we sampled the 300 foragers from at least 378 marked ants.

Camponotus floridanus ants infected with *Ocflo* can live up to four weeks before they show manipulated biting and ultimate death, whereas *Beauveria* infected ants die within the first week post-infection. To standardize our comparison of the changes in ant daily gene expression during infection by *Ocflo* as compared to *Beauveria*, we sampled infected ants at halfway through disease progression (~50% of infected ants in the colony had died). This is at the time during infection at which disruptions in daily activity rhythms have been observed for *Ocflo*-infected ants (Fig. 8) [116]. For either infection run, we monitored disease progression by performing daily mortality checks and visualizing survival curves of the infected (and control) colonies. For *Beauveria* infections, the disease reached halfway on Day 3 post-infections. Whereas *Ocflo* infections reached the halfway mark on Day 11 post-infections (Additional File 13). As mentioned above, uninfected ants were collected from the control colony in parallel to sampling *Beauveria*-infected ants. All the experimental runs were performed within a month (Apr 15th to May 5th, 2022), under the same controlled climatic conditions (12h:12h LD, 25 ºC, and 75% rH). The climatic conditions of the foraging arena throughout the experiment were monitored using an environmental data logger (HOBO) (Additional File 14).

Monitoring ant foraging behavior and activity

The protocol used to monitor and quantify ant foraging rhythms are detailed in Chapter one (see Methods section: *Colony activity monitoring*) [226].

Fungal culturing and controlled infections

Fungal culturing and controlled infections of ant hosts were performed using the same methods and fungal strains as described in Trinh et al. (2021) [116]. For *Ocflo* infections, we used the *O. camponoti-floridani* Arb2 strain, isolated from a manipulated *C. floridanus* ant cadaver previously collected from the wild [34]. For *Beauveria* infections, we used the *B. bassiana* strain Bb0062 [229]. For both fungi, first we obtained fresh blastospores (i.e., yeast-like single cells) suspended in Grace's Insect Medium (Gibco, Thermo Fisher Scientific) supplemented with 2.5% FBS (Gibco) using established protocols [30, 34, 230]. To infect ants, we injected (*Ocflo*) or pricked (*Beauveria*) ants with freshly harvested blastospores. As shown in Trinh et al. (2021), pricking ants with *Beauveria* reliably caused infections while extending host's survival time as compared to *Beauveria*-injected ants [116]. For *Ocflo* infections, we injected 0.5 µL of the blastospore solution ($2x10^7$ cells/ml) into the ventral side of the thorax between its legs using 10 ml borosilicate capillary tubes (Fisher) fitted onto an aspirator (Drummond Scientific). Whereas for *Beauveria* infections, we dipped the capillary tubes in the blastospore solution ($2x10^7$ cells/ml) prior to pricking the ants on the same ventral side of its thorax. Control ants were neither injected nor pricked.

Sample collection, RNA extraction, and RNA Sequencing

To obtain daily transcriptomes of host ant heads halfway through fungal infection, we sampled three infected (marked) foragers every 2h, over a 24h light-dark period, at 3 days post *Beauveria*-infection and 11 days post *Ophiocordyceps*-infection. To obtain corresponding daily transcriptomes of hosts in an uninfected state, we sampled marked foragers from the control colony run alongside *Beauveria*-infections, in parallel to sampling *Beauveria*-infected ants, using

the same sampling regime. Ants were collected in cryotubes, immediately flash frozen in liquid nitrogen, and stored at -80ºC until further use.

Prior to RNA extractions, for each treatment (control, *Ocflo*-infected, and *Beauveria*-infected ants), we pooled the three heads (antenna removed) harvested at each time point in a frozen cryotube containing two frozen steel ball bearings (5/32" type 2B, grade 300, Wheels Manufacturing). Next, we homogenized the pooled heads using a 1600 MiniG tissue homogenizer (SPEX) at 1300 rpm for 40 sec while keeping the samples frozen. Next, we isolated total RNA from the disrupted head tissues, followed by preparing cDNA libraries for RNASeq using the exact methods discussed in Das and de Bekker (2022) [226]. For each library preparation, we started with 500 ng of total RNA, extracted mRNA with poly-A magnetic beads (NEB), and converted this mRNA to 280-300 bp cDNA fragments using the Ultra II Directional Kit (NEB). Unique sequencing adapters were added to each cDNA library for multiplexing (NEB).

All thirty-six cDNA libraries were first sequenced as 50 bp single-end reads on an Illumina HiSeq1500. Given that fungal infected ant heads might contain mRNA from both ant and fungi, we re-sequenced the twenty-four mixed transcriptomes to obtain enough reads to be able to look at the daily transcriptomes of both ant host and fungal parasite (see Chapter three). The re-sequencing was performed as 75 bp paired-end reads on an Illumina NextSeq 1000. We combined the sequencing reads for the mixed transcriptomes by concatenating the raw reads from the two runs. Since we combined reads from single-end HiSeq run and paired-end NextSeq run, we used only the R1 reads from the latter. Raw read data will be uploaded to the relevant NCBI database prior to submitting this study for publication.

Processing RNASeq data and obtaining normalized gene expression

Prior to any analyses, we first removed sequencing adapters and low-quality reads from our RNASeq data using BBDuk (parameters: qtrim = rl, trimq = 10, hdist = 1, k = 23) [124]. Post-trimming, we used HISAT2 [125] to map transcripts to the relevant genomes. We used the publicly available genomes of *C. floridanus* (Cflo v7.5; [107]), *O. camponoti-floridani* (NCBI ID: 91520; [34]) and *B. bassiana* (ARSEF 2860; [231]). For all control *C. floridanus* samples, we mapped reads to the ant genome [126]. However, for fungal-infected *C. floridanus* samples, we first mapped all reads from the mixed transcriptomes to the respective fungal genomes to ensure that we only retained reads that are not of fungal origin, following which we mapped the remaining reads to the ant genome. Finally, we obtained normalized gene expression from the mapped reads as Fragments Per Kilobase of transcript per Million (FPKM) using Cuffdiff [127].

Data analyses

We used the rhythmicity detection algorithm empirical JTK-Cycle (eJTK) [129, 130] to test for significant diurnal (24h) and ultradian (12h and 8h) rhythms in gene expression. Only genes that had diel expression values ≥1 FPKM for at least half of all sampled timepoints were tested for rhythmicity. For a set period length, a gene was considered to be significantly rhythmic if it had a Gamma p-value < 0.05.

As a proxy for a gene's amplitude, we calculated its coefficient of variation throughout the 24h day. For a given gene, its coefficient of variation provides a normalized score of the variation observed in its expression around the mean. Therefore, using coefficient of variation as a proxy for amplitude allows us to compare the degree of daily fluctuations for any gene, not only the ones classified as rhythmic by a rhythmicity detection algorithm. For a given set of

genes, we tested if the mean amplitude was significantly different between treatment groups using Kruskal-Wallis H test [232], and the post-hoc pairwise comparisons were done using Wilcoxon signed-rank test [233], using the "compare_means" function from the ggpubr package in R [234].

To cluster set of genes according to their daily expression, we used an agglomerative hierarchical clustering framework (method = complete linkage) using the 'hclust' function in the stats package for R.

To determine differentially expressed genes, we used the linear modelling framework proposed in LimoRhyde [132], but without an interaction between treatment and time. A gene was considered significantly differentially expressed if treatment was found to be a significant predictor (at 5% FDR) and the gene showed at least a two-fold change in mean diel expression between controls and *Ocflo*-infected (or *Beauveria*-infected) ants (abs($\log_2$-fold-change) ≥ 1).

To perform functional enrichment analyses, we used an updated version of the custom enrichment function that performs hypergeometric test (previously used in [34] and [226]). The function "check_enrichment" is now publicly available for use via the timecourseRnaseq package on GitHub (https://github.com/biplabendu/timecourseRnaseq) [235]. For a given set of genes, we identified overrepresented Gene Ontology (GO) terms or PFAM domains using the check_enrichment function, and significance was inferred at 5% FDR. If not mentioned otherwise, for functional enrichment tests, we used all genes that were found to be "expressed" (≥ 1 FPKM expression for at least one sample) in the ant heads, for each treatment, as the background geneset. We only tested terms annotated for at least 5 protein coding genes. We used the GO and PFAM annotations [108] for the most recent *C. floridanus* genome (v 7.5) [126].

All data wrangling, statistical tests and graphical visualizations were performed in RStudio [136] using the R programming language v3.5.1 [137]. Heatmaps were generated using the pheatmap [138] and viridis [139] packages. Upset diagrams were used to visualize intersecting gene sets using the UpsetR package [140]. We used a Fisher's exact test for identifying if two genesets showed significant overlap at 5% FDR. We visualized the results of multiple pairwise Fisher's exact test using the GeneOverlap package [141]. All figures were generated using the ggplot2 package [236].

Network analyses

To build the annotated gene co-expression network (GCN), we used the exact protocol detailed in de Bekker and Das (2022) [225] (Additional File). The clustering of genes into co-expressed modules was performed using functions from the WGCNA package [237-239], the gene-gene and module-module correlations were calculated using Kendall's tau-b correlation [240], and the global connectivity patterns of the GCN was visualized using the igraph package [241]. The significance of pairwise overlaps were calculated using Fisher's exact tests and visualized using the GeneOverlap package [141].

Results and Discussion

Validation of sampling time point at halfway through disease progression

In this study, we aimed to look at the daily rhythms in gene expression of infected ants halfway through disease progression since this is where the daily foraging activity of carpenter ants infected with *Ophiocordyceps* and *Beauveria* appears to be disturbed, albeit in a different manner (Fig. 8) [116]. We validated our sampling timepoint by comparing daily foraging activity of the infected ants in each of our treatment groups (*Ocflo*-infected and *Beauveria*-infected ants) to that of Trinh and colleagues [116]. We did so by counting the number of ants present in the 12h:12h LD exposed foraging arena, every 2h, throughout the experiment (after initial infections and prior to sampling). The entrainment cues (temperature, humidity, and light levels) presented in the foraging arena were consistent across the two infection runs (Fig. 9). Therefore, any time-of-day specific differences that we found in *Ocflo*-infected as compared to *Beauveria*-infected ants are likely to be the result of infection differences and not due to differences in their external environment in terms of temperature, humidity, or light. The uninfected controls were also exposed to entrainment cues identical to the ones shown for the two infection runs, and the environmental data is provided as a supplementary file (Additional File 14).

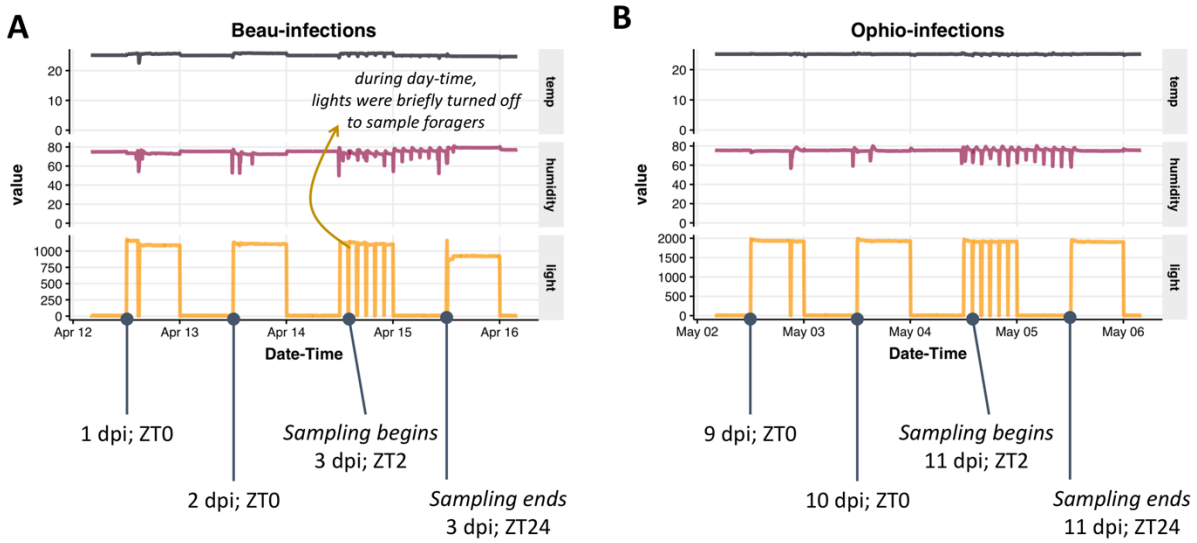

Figure 9 Environmental conditions in the foraging arena during infection run.

The abiotic conditions (light intensity, temperature, and relative humidity) in the foraging arena of the experimental setup are shown for ants infected with (A) *Beauveria bassiana* (Beau) and (B) *Ophiocordyceps camponoti-floridani* (Ophio). Data is shown for two days prior to sampling, the sampling day, and one day after sampling.

We quantified the daily foraging activity of the *Ocflo*-infected and *Beauveria*-infected ants in parallel to uninfected controls. As shown in Figure 9A, *Ocflo*-infected ants maintained daily foraging rhythms until 6 to 7 days post infection (dpi), and by 10 dpi their foraging levels showed no apparent daily rhythm. This loss of rhythmicity coincided with the halfway point of infection during which only half of all ants infected with *Ocflo* survived (i.e., lethal time (LT) 50%), which is consistent with our prior knowledge (Fig. 8A) [116]. The mortality data for all treatment groups is provided as a supplementary file (Additional File 13). As such, we sampled *Ocflo*-infected ants on 11 dpi. Corresponding samples of *Beauveria*-infected ants at halfway through disease were sampled on 3 dpi. Uninfected control ants were sampled in conjunction

with *Beauveria*-infected ants. Both their daily foraging activities prior to sampling are shown in Figure 9B.

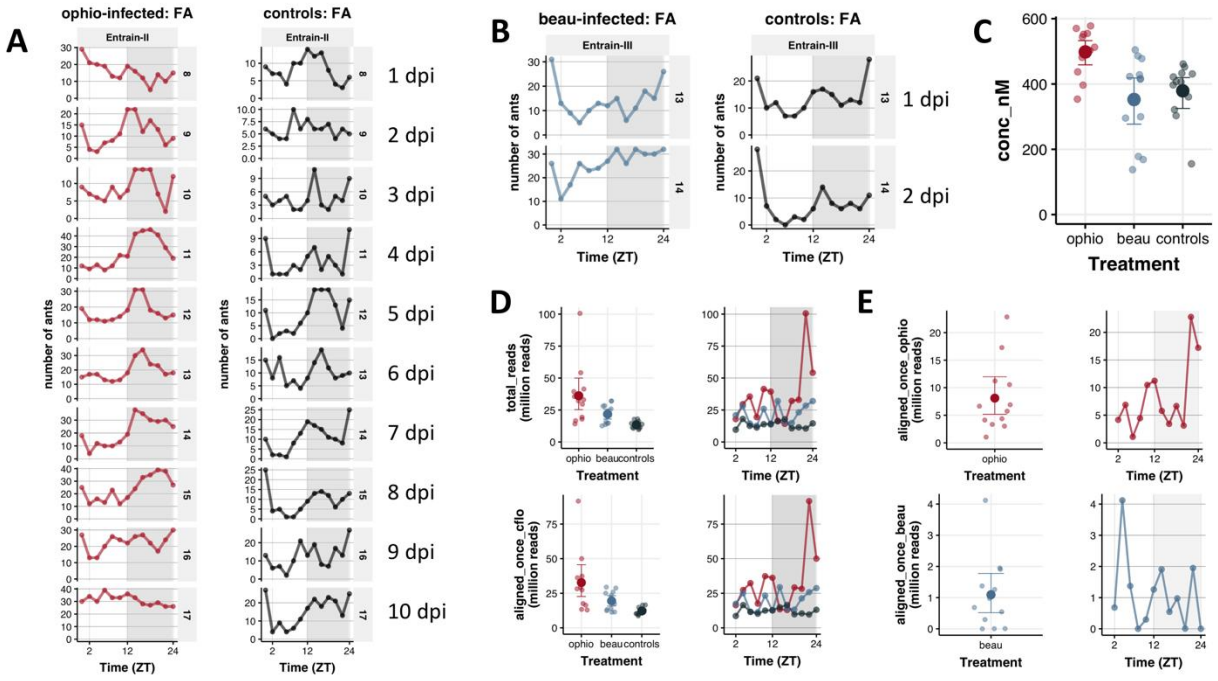

Figure 10 Ant activity rhythms and quality of time-course transcriptomes

The daily foraging activity of ants infected with (A) *Ophiocordyceps camponoti-floridani* (red) and (B) *Beauveria bassiana* (blue) during the entrainment period post infections and prior to sampling are shown. For each infection run, the daily foraging activity of the uninfected controls that were monitored in parallel are also shown (black lines). Once sampled, total RNA was extracted from the whole heads of infected ants and uninfected controls for RNASeq. For each treatment group, (C) shows the concentration (in nM) of extracted total RNA from each sample (lighter circles), along with the mean (darker circles) and 95% confidence intervals (CI) for each treatment group. (D) shows the total number of reads (in million) obtained for each sample, along with their mean and 95% CI (top row), as well as the number of reads that uniquely mapped to the *C. floridanus* genome (bottom row). Given that sequencing the infected ant heads resulted in mixed transcriptomes containing both ant and fungal reads, (E) shows the number of reads from the respective mixed transcriptomes that mapped to the *O. camponoti-floridani* and *B. bassiana* genome.

Quality of transcriptomes and possible sources of variation

To obtain RNA for sequencing, we pooled three technical replicates (whole heads), per treatment group, for each time point of sampling. What we aimed to obtain in the process is the average

gene expression for a given treatment group, for each time point. Given that we were working with only one value per time point, per treatment, we wanted to ensure that time-of-day specific patterns that we find in our analyses were not introduced by differences in sample processing and sequencing. Therefore, we checked the concentration of cDNA libraries used, number of reads sequenced per sample, and number (and percent) of reads mapping to the *Cflo* genome.

The concentrations of all cDNA libraries were comparable (controls = 379 ± 25 nM, *Ocflo*-infected ants = 498 ± 20 nM, and *Beauveria* -infected ants = 352 ± 38 nM; mean ± standard errors) (Fig. 10C). Performing RNASeq, we aimed to produce more reads for infected individuals than for controls since we needed to account for the portion of fungal reads in the mixed transcriptomes that we would obtain [35]. As such, we obtained 13.4 (± 0.8) million reads for control ants, 36.1 (± 0.7) million reads for *Ocflo*-infected ants, and 21.8 (± 0.2) million reads for *Beauveria*-infected ants. On an average, 12.2 (± 0.8) million reads for control ants, 32.7 (± 6.2) million reads for *Ocflo*-infected ants, and 19.5 (± 2) million reads for *Beauveria*-infected ants mapped uniquely to the ant genome (Fig. 10D). This is consistent with the advised coverage depth to reliably detect daily rhythms in gene expression [122]. As such, our environmental conditions, sampling time point and sample processing for RNASeq should have resulted in a dataset that would allow us to investigate infection-related differences in daily gene expression in *C. floridanus* ants.

Fungal gene expression inside ant heads

We found substantial amounts of *Ocflo* mRNA in the ant heads at halfway through disease progression (8.1 ± 1.8 million reads from the mixed transcriptome mapped uniquely to the *Ocflo* genome) (Fig. 10E). Whereas for *Beauveria*-infected ants, we did not find much fungal mRNA

in ant heads at the same disease stage (only 1.1 ± 0.3 million reads mapped uniquely to *Beauveria* genome). This difference in fungal load inside ant heads might be reflective of the different strategies employed by the two fungal parasites to ensure successful infection in its ant host. *Beauveria* is a generalist necrotrophic parasite that kills its ant host within in a week, and as such might not require entry into the ant's head for ensuring infection and eventual transmission. In comparison, *Ocflo* behaves as a hemibiotroph, growing inside its alive host for weeks and requiring timely manipulation of the host's behavior for successful transmission (reviewed in [228]). It has been shown previously that *Ophiocordyceps* do grow into its host's head and mandibular tissues [36], and the proximity of fungal growth inside the head, around the ant brain, has been hypothesized to be important for successful manipulation of ant behavior [242]. We further investigate *Ocflo* daily gene expression during infection and how it compares to the daily expression exhibited in culture (i.e., non-infective state) in Chapter three of this dissertation.

General patterns of daily gene expression in ant heads

We defined genes to be "expressed" in *C. floridanus* ant heads if their mRNA levels were greater than 1 FPKM for at least one time point during the 24h sampling period. Of the 13,808 protein coding genes annotated in the *C. floridanus* genome [107], we found similar number of genes to be expressed in ant heads during infection as in healthy controls (73%, 75%, and 72% of *C. floridanus* genes were expressed in control, *Ocflo*-infected, and *Beauveria*-infected ants, respectively), and their pairwise overlaps were significant (Fisher's exact test: odds ratio > 957 and $p < 0.001$). Of interest were 246 genes uniquely expressed in ant heads during *Ocflo* infection (not expressed in controls or *Beauveria*-infected ants), given that only 41 such uniquely expressed genes were found in *Beauveria*-infected ants and 76 genes were uniquely expressed in

control ants (Fig. 11A). The two distinct sets of uniquely expressed genes, in healthy controls and in *Ocflo*-infected ants, were significantly enriched in the same olfactory processes (genes annotated with the Gene Ontology (GO) terms olfactory receptor activity, odorant binding, sensory perception on smell) (Fig. 11B; Additional File 15A). Therefore, it seems that while several olfactory genes usually expressed in healthy ants are deactivated during *Ocflo* infections, a distinctly different set of olfactory genes is activated simultaneously. In terms of daily fluctuations, most of the genes uniquely expressed in *Ocflo*-infected ants showed a synchronized peak at ZT14 (two hours after lights are turned off) (Fig. 11C-D). Eleven of these uniquely expressed genes were also classified as significantly 24h-rhythmic in *Ocflo*-infected ant heads including a putative serotonin receptor (*5-hydroxytryptamine receptor 3A*-like) and an anti-apoptotic protein coding gene (*death-associated inhibitor of apoptosis 1* like) (Fig. 11E). Although neither of the odorant receptor genes were classified as significantly rhythmic, the shapes of their daily expression profiles were almost identical to that of the significantly rhythmic genes (Fig. 11E-F). Neither our environmental data nor sequencing statistics indicate an abnormality for *Ocflo*-infected ant samples collected at ZT14 (Fig. 8-8). Moreover, such a degree of time-of-day synchronization of daily expression was not observed for the uniquely expressed olfactory genes in controls, which were kept under the same conditions (Fig. 11G). Therefore, this synchronized timely peak observed for uniquely expressed genes in *Ocflo*-infected ants is most likely a biological signal and not an experimental artefact.

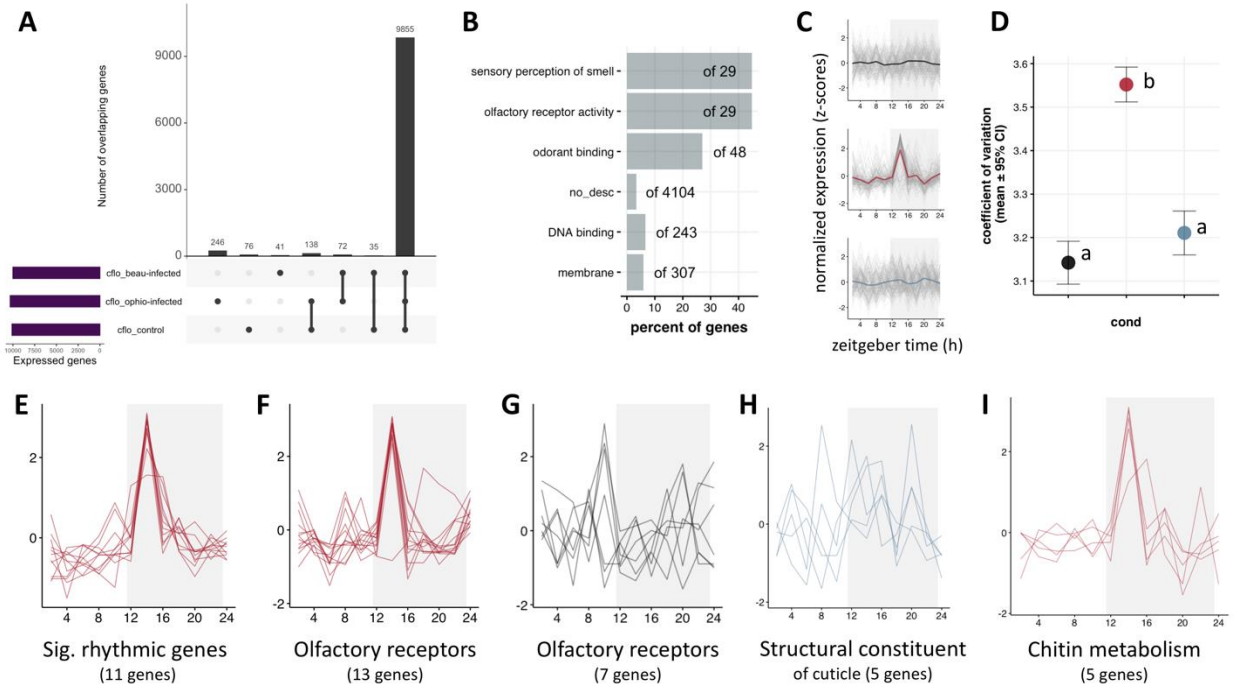

Figure 11 Uniquely expressed ant genes during Ocflo infections are involved in olfaction.

The panel (A) shows the number of genes expressed in ant heads during *Beauveria* infections (cflo_beau-infected), *Ocflo* infections (cflo_ophio-infected) and in uninfected control heads (cflo_control), as well as the number of genes intersecting between these three gene sets. Panel (B) shows the overrepresented GO terms in the 246 genes expressed uniquely during *Ocflo* infections. The bars represent the percent of genes annotated with a given GO term that is found in the test gene set as compared to all such genes in the background gene set (in this case, all genes in the ant genome). Panel (C) shows the daily expression of the 246 genes uniquely expressed during *Ocflo* infections, for each treatment group, as a "stacked zplot". For a stacked zplot, the y-axis always represents the z-score normalized gene expression, and the x-axis represents zeitgeber time (in hour). Each grey line in the plot represents the expression of one gene, whereas the colored lines represent the median expression of all the genes used to build the stacked zplot. Throughout this manuscript, the color black is used to indicate data from uninfected foragers (control), red for *Ocflo*-infected foragers, and blue for *Beauveria*-infected foragers. Panel (D) shows the average (± 95% CI) amplitude of the same 246 genes shown in (C) for the three treatment groups. Colors have the same meaning. Different letters indicate significantly different amplitudes ($p < 0.05$). Additionally, stacked zplots are shown for (E) uniquely expressed genes during *Ocflo* infections that are also classified as significantly rhythmic, (F) olfactory genes uniquely expressed in *Ocflo*-infected ants, (G) olfactory genes uniquely expressed in uninfected controls, (H) genes annotated with the GO term structural constituent of cuticle that are expressed during *Beauveria* infections but not in controls, and (I) genes annotated with the GO term chitin metabolism that are expressed during *Ocflo* infections but not in controls.

In ants, like other insects, odorant receptors are known to regulate acceptance and avoidance behavior based on sensory perception of odor, e.g., response to pheromones in ant

colonies. Additionally, colony odors can be a strong zeitgeber to entrain the clocks of social insects, even stronger than light-dark cycles [15]. Therefore, timed activation of the ant's olfactory-mediated entrainment pathway can be a possible strategy for fungal parasites to regulate the phase of the ant's clock and clock-controlled behavioral output. The 13 uniquely expressed olfactory genes in *Ocflo*-infected ants contained the odorant receptors *OR10a*, *OR43a*, *OR85d*, an *OR2*-like gene, and two copies of *OR13*-like genes. Whereas the seven olfactory genes uniquely expressed in controls, but not during *Ocflo*-infection, contained copies of *OR13a*-like, *OR82a*-like, *OR82a*, *OR4*-like, and *OR4* genes. Although not much is known about the function of these odorant genes in social insects, a previous study in the fruit fly *D. melanogaster* has shown that differences in expression levels of *OR10a* and *OR43a* correlate with differences in fly response (attraction v. repulsion) to an aversive odor (benzaldehyde) [243]. Therefore, a synchronous daily peak expression of olfactory genes in *Ocflo*-infected ant heads might correlate with a drastically reduced or heightened sensitivity of infected ants to certain colony odors in a time-of-day specific manner.

Next, we explored the function of genes that showed expression in ant heads only during infection but not in uninfected controls. When we considered the 113 genes expressed in ant heads during *Beauveria* infection but not in controls (i.e., 41 uniquely expressed during *Beauveria*-infection + 72 expressed during *Beauveria*- and *Ocflo*-infection; Fig. 11A), we found an overrepresentation of genes annotated with the GO term structural constituent of cuticle (five out of 43 such genes), including two abdominal endocuticle structural glycoproteins *SgAbd-3* and *SgAbd-8* (Additional File 15B). Upon penetration of the host's epicuticle, fungal entomopathogens are known to lyse the endocuticle of their host using mechanical and chemical (cuticle degrading enzymes) means [244, 245]. Activation of significant number of host genes

important for structural integrity of the endocuticle might be indicative of host's heightened response to such endocuticular tissue damage caused by a necrotrophic fungus such as *Beauveria*. We checked to see if a similar response to cuticular damage can be detected in *Ocflo*-infected ants by performing functional enrichment on the 318 genes expressed in *Ocflo*-infected ants but not in controls. We did not find a significant enrichment for structural component of cuticle even though two (*larval cuticle protein LCP-17* and an uncharacterized protein coding gene) of the five genes expressed during *Beauveria* infections were also expressed during *Ocflo* infections. Instead, we found a significant overrepresentation of chitin metabolic genes putatively involved in muscle integrity (fibrillar forming *collagen alpha-1(I) chain*), assembly and functioning (*titin* homolog), and mucosal protection against infectious agents (*mucin-3a*) (Additional File 15B). Unlike signs of endocuticular damage we found in *Beauveria*-infected ants, genes activated in *Ocflo*-infected ants suggest a host response to muscle degradation, consistent with previous findings [242]. Exploring time-of-day effects, we found that the chitin metabolic genes expressed in *Ocflo*-infected ant heads show a synchronized daily expression peak at ZT14 (Fig. 9D), with a waveform almost identical to that of the olfactory genes uniquely expressed during *Ocflo* infection (Fig. 11H-I). However, similar to the olfactory genes discussed above, none of the chitin metabolism genes were classified as significantly rhythmic.

Taken together, the data suggests that in *Ocflo*-infected forager ants, the olfactory pathway might be playing a role in setting the phase of the host ant's clock and its rhythmic output. In the next section, we have attempted to answer this question, at least partially, by testing (1) if a significant number of 24h-rhythmic genes in *Ocflo*-infected ants show a daily peak (or trough) in expression at ZT14, (2) how the distribution of the phases (peak time-of-day) of significantly rhythmic genes compared across the three treatment groups, and (3) if the

functions of rhythmic genes that show a waveform similar to the uniquely expressed olfactory genes during *Ocflo*-infection are known to be under clock-control in ants.

Daily rhythms in gene expression: forager heads vs. dissected brains

We identified rhythmic gene expression in ant heads using the non-parametric algorithm empirical JTK Cycle (eJTK) [129, 130]. Of the approximately ten thousand genes expressed in *C. floridanus* forager heads, 8.4% (852 genes) showed significant 24h-rhythmic expression in uninfected controls (Additional File 16A). At halfway through *Ocflo* infection, however, only 2.9% (294 genes) of all expressed genes showed significant 24h-rhythms (Additional File 16B). Additionally, 6.7% (673 genes) showed significant diurnal rhythms at halfway through *Beauveria* infection (Additional File 16C).

To validate our data, we compared the 24h-rhythmic genes identified in uninfected forager heads (this study) to those previously identified in forager brains (Chapter one) [226]. We expected to see a reduced yet significant overlap in rhythmic genes between the brain and the head due to any of the following scenarios. First, even if a gene is rhythmic in every cell in the ant head, it might be oscillating with different phases in different tissues. Therefore, if there is enough tissue-specific variation in the phase of a rhythmic gene, we might not see a synchronous daily rhythm for the gene's expression by sampling the entire head. Second, certain genes might be only rhythmic in the brain, and not in the surrounding muscle or gland tissues, which could dampen the amplitude of oscillating genes to the level where they are not readily detected. However, in the case that we do see rhythmic expression for a given gene in both ant brains and heads, we can be certain that it oscillates in both and is suggestive of a relatively high synchronization of its daily expression across different tissues inside ant heads.

A total of 334 genes that were found to be 24h-rhythmic in both ant brains and whole heads. This overlap was significant (Fisher's exact test: odds-ratio = 1.27, $p < 0.001$). However, no significant overlaps were found for genes oscillating every 12h or 8h in ant heads and ant brains. The reduced overlap for ultradian rhythms at the two different scales (brain tissue and whole heads) might be caused by the same reasons we discussed above. Indeed, gaining ultradian rhythms in whole ant heads as compared to brain tissue alone is difficult to interpret. They might be due to 24h-rhythmic genes that cycle with significantly different phases in different tissues, therefore, seeming ultradian when their expression is detected together. As such, we focused our attention on characterizing the changes that occur to the 24h-rhythmic gene expression of ants during infectious disease as compared to controls and interchangeably use the terms "rhythmic" and "24h-rhythmic" throughout.

Changes in ant daily gene expression during infection: Differentially Rhythmic Genes

We wanted to explore the changes that occur to the rhythmic properties of genes that oscillate strongly enough to be rhythmic in both, brains (Chapter one) and whole heads (this study) of foragers. The daily transcriptomes of forager heads and brains were sampled using the same experimental design, sampling resolution, and entrainment conditions, but the experiments were conducted a year apart using two different ant colonies. In the former study, comparison of the daily transcriptomes of forager and nurse ant brains revealed a set of caste-associated differentially rhythmic genes (DRGs): 281 genes including the core clock *Period* and several clock modulators such as *Sgg, Dbt, Nemo, Pp1, Pp1b* that highly synchronized switch from oscillating every 24h in forager brains to oscillating every 8h in nurses (see Figure 3 in Chapter

one) [226]. Therefore, it appears that plasticity of ant's rhythmic (behavioral) state, and associated caste identity (task specialization) in the colony, is linked to synchronized changes in the daily expression of these 281 rhythmic genes. In this section, we wanted to test if the genes oscillating in both brains and heads show any signs of disease-associated differential rhythmicity (i.e., synchronized changes in daily expression as a result of disease), and if so, do these disease-associated DRGs show a significant overlap with the caste-associated DRGs we have identified in Chapter one.

Among the 334 genes that show robust 24h oscillations in both ant brains and heads, hierarchical clustering revealed a set of 166 genes that show highly synchronized changes in their daily expression (Cluster-1, Fig. 12A-B). One could argue that we could have explored Cluster-2 as well, given that it also seems to show synchronized changes in daily expression. However, we chose to explore the genes in Cluster-1 because this is the largest cluster for which we found evidence of synchronized changes. The size of the cluster matters since our eventual goal was to test the possibility that disease-associated DRGs, if any, significantly overlapped with the caste-associated DRGs or not. As the cluster size would decrease, the chances of a false negative for a Fisher's exact test would increase. That is why we decided to explore the 166 genes in Cluster-1. These 166 genes show a dawn peak in the forager brains (ZT22-24), whereas in forager heads we found a dusk peak (ZT12-ZT16) (Fig. 12A-B). The phase difference for these 166 genes between forager heads and brains could be, in part, due to the presence of tissue-specific variation in the phase of these genes throughout the entire head. Although these genes show a dawn phase in the brains, at the scale of the head, the various tissue-specific phases seem to integrate and produce a bell-shaped curve peaking around dawn. Regardless of the reasons for which these 166 genes show a phase shift between forager brains and heads, the fact that they

can show a highly synchronized change in their daily rhythm is what motivated us to look at what happens to these genes during disease. Indeed, we found a highly synchronized change in the shape of daily expression for these 166 genes during disease, as compared to controls (Fig. 12B). Furthermore, when we compared these 166 genes to the 281 caste-associated DRGs (for24-nur8), we found a significant overlap (Fisher's exact test; odds ratio = 5.7, $p < 0.001$). Taken together, these two finding suggests that the core set of caste-associated DRGs in *C. floridanus*, which usually functions as molecular links between behavioral plasticity and plasticity of the clock, also shows synchronized changes in its daily expression during disease. Furthermore, the synchronized change at halfway through disease shows parasite-specific difference that might have a biological meaning. For example, the expression of these 166 differentially rhythmic genes peak around ZT14 in both uninfected forager heads and foragers infected with *Ocflo*, but switches from smooth fluctuations in controls to a synchronized sharp peak (activation) in *Ocflo*-infected ants (Fig. 12B). The same genes, however, do not show a clear peak around ZT14 in *Beauveria*-infected ants. Instead, their daily expression shows a sharp dip (deactivation) at ZT6 with no apparent daily fluctuations during the rest of the 24h day (Fig. 12B).

This set of 166 disease-associated DRGs (brain-head-rhy24-cluster1) showed a significant overrepresentation for genes involved in protein phosphorylation and GPCR signaling pathway (Fig. 12E). The phosphorylation genes included *casein kinase 1*, both conventional and atypical *protein kinase C*, serine/threonine-protein kinase *SIK3*, *Calcium/calmodulin-dependent protein kinase II* (*CaMKII*), and *mitogen-activated protein kinase 1* (*MAPK1*; synonymous to *extracellular signal-regulated kinase 2* or *ERK2*). Whereas genes involved in GPCR signaling included a *dopamine D2-like receptor* and *tyramine receptor 1* (*TAR1*). In summary, key

regulators of signal transduction (PKCs), insulin signaling pathway (serine/threonine protein kinases), synaptic plasticity (CAMKs), and social behavior (ERK2 and dopamine/tyramine receptors) show synchronized change in their daily expression during infectious disease, albeit in a parasite-specific manner.

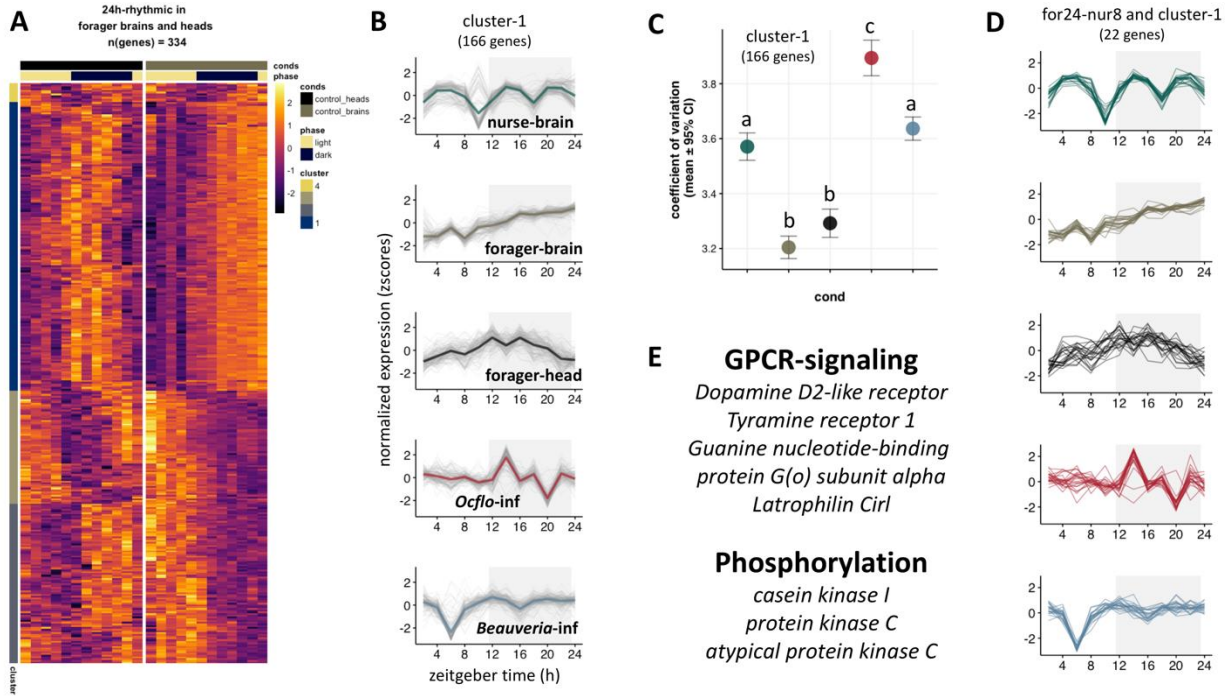

Figure 12: Genes that show 24h-rhythmicity in forager heads and brains show a synchronized change in daily expression during fungal infections, in a species-specific manner.

The heatmap in panel (A) shows the daily expression (z-score) patterns of 334 genes identified as significantly oscillating every 24h in both forager heads and brains. Each row represents a single gene and each column represents the Zeitgeber Time (ZT) at which the sample was collected, shown in chronological order from left to right (from ZT2 to ZT24, every 2 h). These 334 genes were hierarchically clustered into four clusters, and the cluster identity of each gene is indicated in the cluster annotation column on the left of the heatmap. Panel (B) shows the stacked zplots for all 166 genes in Cluster-1 of the heatmap in (A). The data for nurse brains and forager brains were obtained from Das and de Bekker (2021) (also available in Chapter one). We have used the colors green and grey, respectively, to indicate the data for nurse and forager brains throughout the manuscript. In panel (C) we have plotted the mean (± 95% CI) amplitude of these 166 genes in Cluster-1. Different letters indicate significantly different amplitudes ($p < 0.05$). Panel (D) shows the stacked zplots for the 22 genes that were overlapping between the 166 genes in Cluster-1 and the 281 differentially rhythmic genes (for24-nur8) identified in Das and de Bekker (2021). Finally, in

panel (E) we have highlighted two GO terms that were overrepresented in the 166 genes in Cluster-1, and some of the genes that contributed to the respective enrichment.

We additionally asked how changes to the degree of daily fluctuation of these 166 disease-associated DRGs might correlate with the parasite-specific disease outcome we see in infected ants. To obtain a standardized metric for the degree of daily fluctuation observed for a gene, we calculated its coefficient of variation throughout the 24h day, which we refer to as the amplitude. For a given gene, its coefficient of variation provides a normalized score of the variation observed in its expression around the mean. Therefore, using coefficient of variation as a proxy for amplitude allows us to compare the degree of daily fluctuations for any gene, not only the ones classified as rhythmic by a rhythmicity detection algorithm. It appears that in uninfected conditions, nurse ants show a significantly higher amplitude of daily expression in these DRGs as compared to foragers (Wilcoxon signed-rank test: p-value < 0.001; Fig. 12C). As such, significant differences in the amplitude of these DRGs, in addition to differences in periodicity, seem to correlate with different behavioral state (nurse v. foragers). Given that the DRGs show a synchronized peak (or a trough) in infected foragers, we expected to see an increase in the amplitude of daily fluctuations in both diseased states as compared to uninfected foragers, which is what we found (Wilcoxon signed-rank tests: p-values < 0.001; Fig. 12C). Furthermore, the disease-associated DRGs showed a significantly higher amplitude in *Ocflo*-infected ant heads as compared to *Beauveria*-infected ones as well as nurse brains (Wilcoxon signed-rank tests: p-values < 0.001; Fig. 12C). The amplitude of these genes in *Beauveria*-infected ants were not significantly different than that of nurses (Wilcoxon signed-rank tests: p-values = 0.056; Fig. 12C). Therefore, it seems that the disease-associated changes to the behavioral state of the ants are associated with not only changes to the shape, but also the

amplitude, of these 166 genes. Taken together, this suggests that in ants infected with *Ocflo*, the peak time of daily expression of several essential clock components (*CK1* and *PKCs*) and behavioral regulators (dopamine and tyramine receptors) still mimics that of controls, albeit with a significantly higher degree to daily fluctuation. During *Beauveria* infections, such an expression peak around ZT14 is lost, and rather a sharp dip at ZT6 is observed. As we discussed previously, although *Beauveria*-infected ants seem to maintain robust foraging rhythms in the second half of the disease, the peak time of their daily foraging activity shifts from a night-time peak (usually between ZT12-16) to the middle of the day, at ZT6 (Fig. 8). It is unclear, but the possibility remains that the sharp deactivation of these 166 disease-associated DRGs at ZT6 might underlie the altered foraging peak seen in *Beauveria*-infected ants. It also remains to be seen what drives this synchronized activation and deactivation, respectively, of these 166 disease-associated DRGs during *Ocflo* and *Beauveria* infections.

Changes in ant daily gene expression during infection: Temporal division of clock-controlled processes

Of the 24h-rhythmic genes found in *Ocflo*-infected ant heads, a majority showed a daily peak at ZT14 (two hours post lights-off), which was close to the phase of rhythmic genes in control heads (around ZT16) (Fig.12A-B). During *Beauveria*-infection, however, most 24h-oscillating genes in the infected ant's head showed a peak expression at ZT6 (middle of the light phase) (Figure 12C). The shift in the average phase of rhythmic genes in ant heads during infection with *Ocflo* (Watson test statistic = 1.4, $p < 0.001$) and infection with *Beauveria* (Watson test statistic = 7.7, $p < 0.001$), as compared to controls, were both significant. The phase shift in host's clock-controlled genes was significantly higher during *Beauveria* infection as compared to *Ocflo*

infection (Watson test statistic = 3.7, $p < 0.001$). This finding is consistent with the difference in clock-controlled activity rhythms that Trinh and colleagues found for ants infected with *Ocflo* versus *Beauveria*. As we have discussed previously, *Ocflo*-infected ants seem to maintain daily rhythms in foraging – a clock-controlled process – until the halfway mark in disease but lose such rhythmic activity in the second half of the disease. Given that the incubation period of *Ocflo* inside its host is relatively long (around three to four weeks), and that we have sampled *Ocflo*-infected ants exactly at the halfway mark in disease progression, we have most likely sampled infected ants that are in the process of transitioning from a seemingly rhythmic phenotype to an arrhythmic one. In other words, several clock-controlled processes in the host might still be oscillating in a rhythmic manner with a phase similar to uninfected controls. The latter, at least, seems likely since we found a similar phase of rhythmic gene expression in both uninfected controls and *Ocflo*-infected ants. In comparison, the disease progresses relatively faster in *Beauveria*-infected ants; infected ants succumb to the fungal infection within a week. Therefore, our sampled ants at the halfway mark might already give us a glimpse of what is about to happen to the infected ants in the latter half of the disease. The fact that we find that majority of the clock-controlled genes in *Beauveria*-infected ants peak at ZT6, the same time of day at which their daily activity peaks during the latter half of the disease, suggests that by the halfway mark in its disease, *Beauveria* likely causes a drastic phase shift in most host processes under clock control, including activity rhythms. The vastly different rate of disease progression of these two infectious diseases in ants, therefore, seems to be associated with the different degrees to which the host's temporal division of clock-controlled processes is affected at the halfway mark in the disease. Future studies on other infectious diseases in ants, with varying rates of disease progression would be necessary to confirm our speculation.

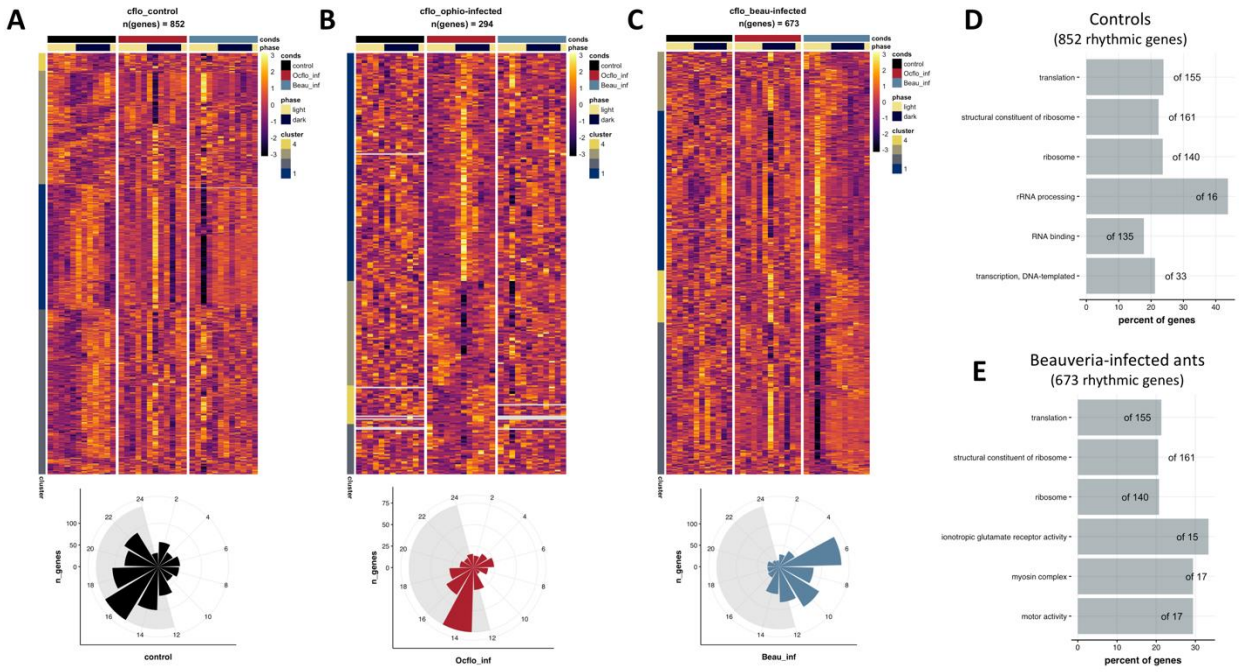

Figure 13: Clock-controlled biological processes are disrupted during Ocflo infections but keep oscillating during Beauveria infections, albeit with a drastic phase shift.

The heatmaps show the daily expression profiles of genes identified as 24h-rhythmic in (A) uninfected controls, (B) *Ocflo*-infected ants, and (C) *Beauveria*-infected ants, whereas the phase plot at the bottom shows the distribution of the phases (time-of-day of peak expression) of the identified rhythmic genes. The corresponding daily expression of the same genes for the other two conditions are also shown as a reference. For example, (B) shows the daily expression pattern of the 294 genes that were identified as significantly rhythmic in *Ocflo*-infected ant heads. For comparison, the daily expression of these 294 genes in uninfected controls and *Beauveria*-infected ants are also shown. At the bottom of the heatmap, the distribution of the phases for these 294 rhythmic genes are shown. Panels (D) and (E), respectively, show the GO terms overrepresented in the genes identified as 24h-rhythmic in controls and *Beauveria*-infected ants. No enriched GO terms were found for genes rhythmic in *Ocflo*-infected ants. Uninfected control = cflo_control, *Ocflo*-infected ants = cflo_ophio-infected, and *Beauveria*-infected ants = cflo_beau-infected.

Next, we wanted to find out if the identity of the genes that are under clock control in uninfected foragers, and the processes they regulate, changed drastically at the halfway mark in either infectious disease. We expected to see a drastic change in the clock-controlled rhythms for *Ocflo*-infected ants since both previous work [116] (Fig. 9) and activity data collected during this study (Fig. 10) showed a loss of foraging rhythms at this disease stage. However, for *Beauveria*-

infected ants, we expected to see less drastic changes to the repertoire of rhythmic genes, at least for ones underlying locomotion, since *Beauveria*-infected ants tend to maintain rhythmic activity even in the latter half of the disease, although with a large phase shift. Using pairwise Fisher's exact tests, we found that the set of 24h-oscillating genes in control forager heads did not significantly overlap with those identified as 24h-rhythmic in *Beauveria*-infected or *Ocflo*-infected ants. Although not significantly overlapping, the rhythmic genes identified in uninfected controls and *Beauveria*-infected ants showed a higher overlap (63 genes) than those between controls and *Ocflo*-infected ants (12 genes) (Supp. Fig. 2A). Only three genes (*centromere-associated protein E, neither activation not afterpotential protein C* (*ninaC*), and *selenoprotein P-like*) were classified as rhythmic in all three conditions, and all three displayed a similar night-time peak in daily expression. Indeed, majority of the genes (780 genes in controls, 591 genes in *Beauveria*-infected ants, and 263 genes in *Ocflo*-infected ants) were classified as rhythmic in one treatment group but not the other.

Even though the identity of the rhythmic genes seems to change drastically in both disease conditions, their functions might be comparable. However, we did not find any enriched GO terms in among the 294 rhythmic genes in *Ocflo*-infected ants. In contrast, the rhythmic genes in controls and during *Beauveria*-infections did contain overrepresented gene functions for similar translation-related processes (Fig. 13D-E). This overlap was found to be significant (Fisher's exact test: odds-ratio = 118, p-value < 0.001) (Fig. 12D-E). Therefore, it seems that although the clock-controlled genes shift from a night-time peak activity in uninfected controls to a mid-day peak (at ZT6) during *Beauveria* infection, the rhythmic genes in *Beauveria*-infected ants show a significant functional overlap with those oscillating in controls. The disease

phenotype of *Beauveria*-infected ants is likely due to the drastic effects *Beauveria* has on the host's temporal division of clock-controlled processes.

In addition to translation-related processes, the rhythmic genes in *Beauveria*-infected ants were overrepresented in motor activity. The five genes involved in motor activity showed a synchronized daily expression in *Beauveria*-infected ants with a sharp dip observed around ZT6, similar to the disease-associated DRGs discussed previously (Supp. Fig. 2C, Fig. 12B). These motor related genes included a *myosin heavy chain*, a *dilute class unconventional myosin*, a *paramyosin*, and *ninaC*. In *Drosophila*, these genes seem to be involved in muscle contraction [246], transport of pigment granules in photoceptors [247], general muscle integrity and function [248, 249], and photoreceptor cell function [250, 251]. Given that these genes seem to link photoreception to muscle function, it remains to be seen if the sharp trough in the daily expression of these motor-related genes at ZT6 correlates with an increased motor activity observed for *Beauveria*-infected ants.

In summary, it appears that infection by both, manipulating and non-manipulating, fungal parasites can largely disrupt the identity of the clock-controlled genes in the host's head. Although the identity of the 24h oscillating genes inside ant heads were distinct during infection with the biotrophic, specialist manipulator *Ocflo*, the bulk of the rhythmic genes still showed a night-time peak of daily expression similar to uninfected controls. In comparison, infection by the necrotrophic, non-manipulating fungal pathogen *Beauveria* caused relatively less drastic changes to the ant's repertoire of rhythmic genes but induced a nocturnal to diurnal phase shift in the ant's clock-controlled processes, consistent with its observed disease phenotype (Fig. 8) [116]. This large phase shift in the ant's rhythmic output might be a hallmark of ants succumbing to *Beauveria* infection, and in part, could be responsible for the relatively fast disease

progression observed (*Beauveria* kills its ant host within a week and does not require its host to be alive for extended periods to complete its lifecycle). In comparison, ants infected by *Ocflo* need to survive for more than two to three weeks. This relatively long incubation time of *Ocflo* is likely achieved by its host being able to maintain a control-like temporal structure of clock-controlled processes during disease, at least till the halfway mark. If *Ocflo* aids in this process, by synchronizing to and maintaining its host's rhythms, or not remains to be seen.

Differentially expressed genes

To discuss genes and biological processes that are drastically altered in ant heads during infection by fungal pathogens and characterize the differences between infection by *Ocflo* and *Beauveria*, we identified the genes that were significantly differentially expressed in ant heads between control and diseased conditions (fold change ≥ 2, q-value < 0.05). Of the approximately ten thousand genes expressed in ant heads, 143 were upregulated, and 81 were downregulated at halfway through *Ocflo* infection as compared to controls (Figure 13A). At a similar disease stage in *Beauveria*-infected ants, the opposite trend was found: 80 ant genes were upregulated, and 139 were downregulated as compared to controls (Figure 13B). We found significant overlap between ant genes downregulated during *Ocflo* infection and ones upregulated during *Beauveria* infection (*Ocflo*-DOWN-Beau-UP: 63 genes; odds ratio = 106, q-value < 0.001) (Figure 13D). A smaller, yet significant, overlap was found between genes upregulated during *Ocflo* infection and downregulated during *Beauveria* infection (*Ocflo*-UP-Beau-DOWN: 18 genes; odds ratio = 47, q-value < 0.001) (Figure 13D). The findings suggest that there exist two core sets of ant genes both of which show drastic changes in their expression during fungal infections, but in a parasite-specific manner. Whereas infection by *Ocflo* causes upregulation (or downregulation) in a set of

host's gene, infection by *Beauveria* causes downregulation (or upregulation) in the same set of host genes.

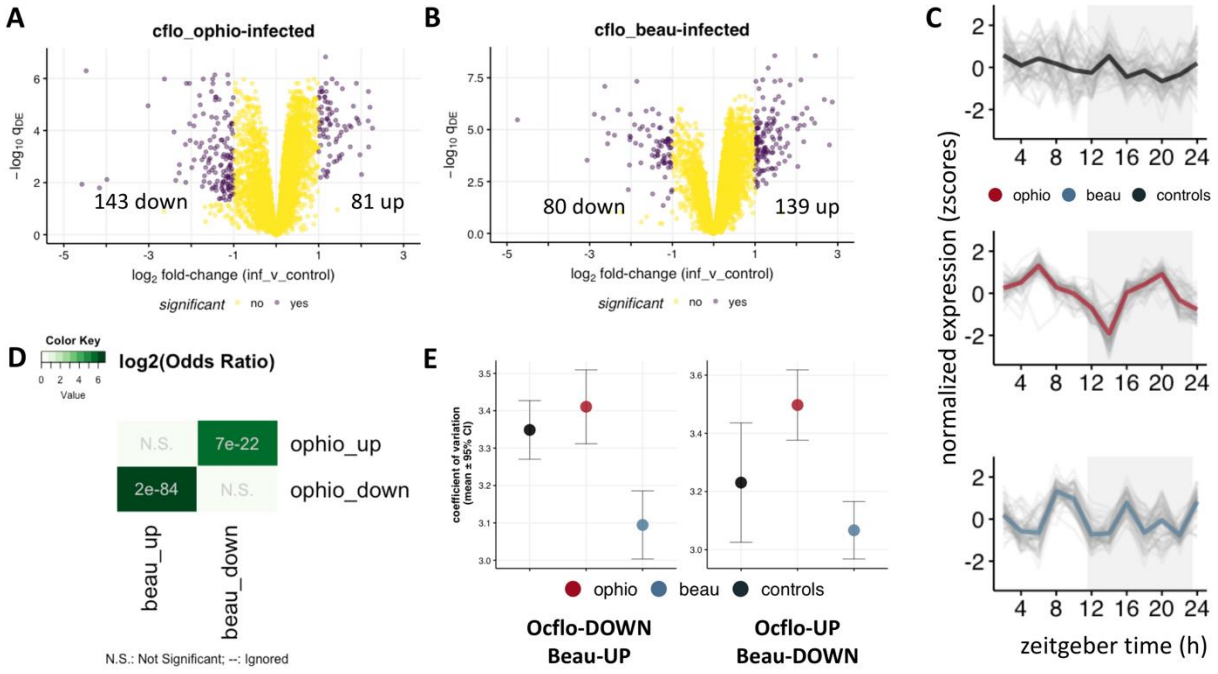

Figure 14: Differential gene expression reveals two core sets of ant genes that are affected during fungal infections, but the direction of the effect is parasite-dependent.

The volcano plots show the results of differential gene expression analysis for (A) *Ocflo*-infected ant heads and (B) *Beauveria*-infected ant heads, as compared to controls. Purple dots indicate genes that were classified as significantly differentially expressed (fold-change ≥ 2, p-value < 0.05). The number of up and down regulated genes during an infectious disease, as compared to controls, are shown. Panel (C) shows the stacked zplots for the 63 genes that were found to be significantly down regulated in *Ocflo*-infected ants but up regulated in ant heads during *Beauveria* infections (*Ocflo*-Down, Beau-UP). Each grey line represents daily expression of one gene, and the colored solid line represents the median daily expression for all genes in the set. The x- and y-axis of the stacked zplot have the same meaning as before. Panel (D) shows the results of pairwise Fisher's exact test. The color of each cell indicates the log2-(odds-ratio) for the overlap between two gene sets and the p-values used to infer significance of overlap are shown. The odds ratio and p-value are only shown for significant overlaps (p-value < 0.05). Panel (E) shows the amplitude of the genes found to be (left) significantly down regulated in *Ocflo*-infected ants but up regulated in *Beauveria*-infected ants (*Ocflo*-DOWN, Beau-UP), and (right) significantly up regulated in *Ocflo*-infected ants but down regulated in *Beauveria*-infected ants (*Ocflo*-UP, Beau-DOWN), as compared to controls, in all three treatment groups. The circles show mean amplitude of the respective genes and the error bars indicate 95% CI.

Looking at the identity of these 63 *Ocflo*-DOWN but Beau-UP genes (downregulated during *Ocflo* infection but upregulated during *Beauveria* infection), we found several genes-of-interest: *bubblegum* (affects neurodegeneration and lifespan in flies; [252, 253]), pheromone-binding protein *Gp-9-like* (regulator of social complexity in ants; [254]), *D-3-phosphoglycerate dehydrogenase* (caste-associated DRG in *C. floridanus*; Chapter one [226]), venom acid phosphatase *Acph-1-like* (a known venom acid phosphatase; [255]), the juvenile hormone esterase *venom carboxylesterase-6* (juvenile hormone esterase that show caste-associated DRG in *C. floridanus*; Chapter one [226]), three copies of *juvenile hormone acid O-methyltransferase* (catalyzes the last step of JH synthesis, can regulate titers of both JH and Vg in insects [256]) . This relatively small set of genes showed significant overrepresentation for *cytochrome p450* genes involved in oxidoreductase activity, iron ion binding, and heme binding.

Furthermore, the *Ocflo*-DOWN-Beau-UP genes showed synchronized daily expression in *Ocflo*-infected ants with a sharp dip at ZT14 and seemingly bimodal peaks (Fig. 14C). In fact, most of the genes downregulated in *Ocflo*-infected ants showed a similar synchronized rhythmicity during *Ocflo* infection with a bimodal peak of daily expression, suggestive of 12h oscillations. In comparison, for *Ocflo*-UP genes, relatively less synchronization of their daily fluctuations was found, although most *Ocflo*-UP genes showed a clear local trough at ZT6. The presence of 12h oscillations in *Ocflo*-DOWN genes during *Ocflo* infections was confirmed as we found a significant overlap of *Ocflo*-DOWN genes with ones classified as 12h-rhythmic in *Ocflo*-infected ants. Of more interest is the timing of the synchronized sharp dip observed around ZT14 for these *Ocflo*-DOWN genes (Fig. 14C, Supp. 3B), the same time of day at which majority of the rhythmic genes and processes in *Ocflo*-infected ants show a peak activity (Fig. 13B). It seems, therefore, that at the halfway mark in *Ocflo* infections, host genes are

significantly downregulated (as compared to controls) in a time-of-day specific manner, and the timing of this downregulation correlates with the peak time of activity for most genes found oscillating in the infected ant head. Taken together, our findings suggest a possible mechanism via which *Ocflo* might be regulating the phase of the host's clock-controlled genes, and the processes they regulate. As we have discussed in the Introduction, *Ocflo* is known to secrete toxins, including several enterotoxins, while inside their ant host, some of which are rhythmically expressed (see Chapter three). We do not have the data to test if during infection, the timing of peak toxin activity, driven by the parasite's clock, correlates with the time at which we observe a sharp deactivation of host genes involved in oxidoreductase activity. However, if we do find that the correlation exists, it would be suggestive that at least some of these mycotoxins likely function to reduce the oxidative stress in the ant host but in a timely manner. Given that the cluster of downregulated genes we have identified in *Ocflo*-infected ants contains several behavior regulatory genes (juvenile hormone esterases), the parasite's ability to manipulate host behavior in a timely manner might have evolved due to pre-existing links between host's behavioral state and response to oxidative stress. In comparison, the relatively fast progression of *Beauveria* infections in ants might be, in part, due to a significantly upregulated host response to oxidative stress. Future studies comparing the changes that occur to the parasites' daily transcriptome during disease, and how the phase of rhythmic fungal effectors compare with the host's response to oxidative stress will be necessary to shed light on our speculations. However, for our argument to hold, the timely changes in the DEGs would need to have time-of-day effects on the host's clock-controlled processes. In other words, there needs to be cross-talk between the host's behavior regulatory genes and clock output, and that's exactly what we have found in Chapter one [226]. In the next section, we demonstrate that even in the

ant heads there is evidence for co-regulation between genes underlying behavioral plasticity and that are under clock control.

Effects of infectious diseases on host gene expression network

Thus far, we have compared our time-course transcriptomics datasets to identify several sets of genes that characterize the disease-associated changes in the host's daily transcriptome. In this section, we take a systems approach to identify the regulatory mechanisms that potentially link these genes of interest. Furthermore, constructing the global network of gene expression in uninfected controls, and characterizing the changes to the network during disease allowed us to ask, for example, if the accelerated disease progression of *Beauveria*, a necrotrophic parasite, is due to substantial changes to the structure of the host's expression network. In comparison, infection by *Ocflo* might cause less drastic but targeted changes to certain parts of the network, with the affected regions potentially being overrepresented for core clock and clock-controlled genes. Most importantly, using network analyses we aimed to integrate all of our findings, from the current study as well as prior studies done in our lab, in order to put forward a hypothesis for the regulatory mechanism via which manipulating parasites such as *Ocflo* might be driving time-of-day specific changes in their host's behavior.

Prior to this study, we published a separate meta-analysis in which we showed that the genes differentially expressed between foragers and nurses (behavioral plasticity genes; Chapter one) were primary located in two modules of the ant's brain gene expression network (Das and de Bekker 2022). Additionally, we discovered that both behavior plasticity modules were connected to at least one rhythmic module of the host. This suggested that in ants, at least in *C. floridanus*, there exists a putative regulatory link between genes underlying behavioral plasticity

(caste-associated DEGs) and clock-controlled (rhythmic) output. Therefore, drastic changes to the expression of these two behavioral plasticity modules, due to changes in the ant's social context or disease state, could induce changes to the rhythmic modules and the different processes they regulate, including rhythmic behavior. In a separate study prior to our meta-analysis, we had identified over a thousand genes that were differentially expressed in ant heads at the manipulated biting stage (infected ants biting down on a substrate with a locked jaw) prior to death. When we mapped the genes differentially expressed in the ant heads during active manipulation (biting) onto the ant's brain gene expression network, we found that most of these manipulation genes were located in exactly the same modules as the behavioral plasticity genes. This led us to hypothesize that, to induce timely behavioral changes in its host, *Ocflo* likely targets existing molecular links between host's behavioral and chronobiological plasticity. Here, we empirically test this hypothesis using the time-course RNASeq data that we have collected for infected ant heads at the halfway mark in both diseases. For our hypothesis to hold, we should observe the following in our data, (1) the presence of molecular links between behavioral plasticity and rhythmic genes (i.e., for-UP or for-DOWN modules connected to rhythmic modules in the gene expression network), and (2) *Ocflo* infections significantly affecting the expression of the behavioral plasticity genes (i.e., *Ocflo*-UP (DOWN) genes and for-UP (DOWN) genes should be located in the same modules).

We constructed and annotated the gene co-expression network (GCN) of control forager heads as per the protocol detailed in de Bekker and Das (2022) which is also provided as a supplementary file (Additional File 18). We built the ant's GCN using the 9591 genes that were expressed (≥1 FPKM) in control ant heads for at least half of all sampled time points. We wanted to use the gene expression network of uninfected controls as the background to identify the

changes that occur in the host's network during infection. But building the ant's network using only genes that are expressed in control conditions did not allow us to map the genes that might be expressed during infection, but not in controls, on to this network, which is a limitation of our analyses. However, the reference network we built should allow us to achieve the goal of identifying the modules that show an overlap with our genes of interest. These 9591 expressed genes were clustered into 22 modules based on co-expression and named accordingly (C1 to C22). The global connectivity patterns of the ant GCN is shown in Figure 14A, where nodes represent the modules or clusters of highly co-expressed genes (Kendall's tau-b correlation ≥ 0.6), and edges between modules indicate a similarity of module-module expression (Kendall's tau-b correlation of at least 0.6 between a module's eigengene expression with another).

Next, we annotated the GCN of forager heads by identifying where in the network our genes of interest are located to understand how these genes regulate each other. In addition to testing our aforementioned hypothesis, annotating the GCN also allowed us to ask, for example, if drastic changes in the expression of a set of genes (DEGs) during disease might be able to induce differential rhythmicity (synchronized changes in the daily expression) of core clock components, clock modulators, or clock-controlled output. To annotate the ant GCN, we identified the module(s) that have a significant overlap with genes displaying (1) significant 24h rhythms in control heads (rhy24h-controls), (2) disease-associated differential rhythmicity (brain-head-rhy24-cluster1, Fig. 12B), (3) caste-associated differential rhythmicity (for24-nur8, discussed in *Changes in ant daily gene expression during infection: Differentially Rhythmic Genes*; Fig. 5D in Chapter one), (4) significant differential expression between control and diseased states (*Ocflo*-UP/DOWN and Beau-UP/DOWN; Fig. 14A-B), and (5) significant

differential expression between foragers and nurses (for-UP/DOWN, also referred to as behavioral plasticity genes; Fig. 6 in Chapter one).

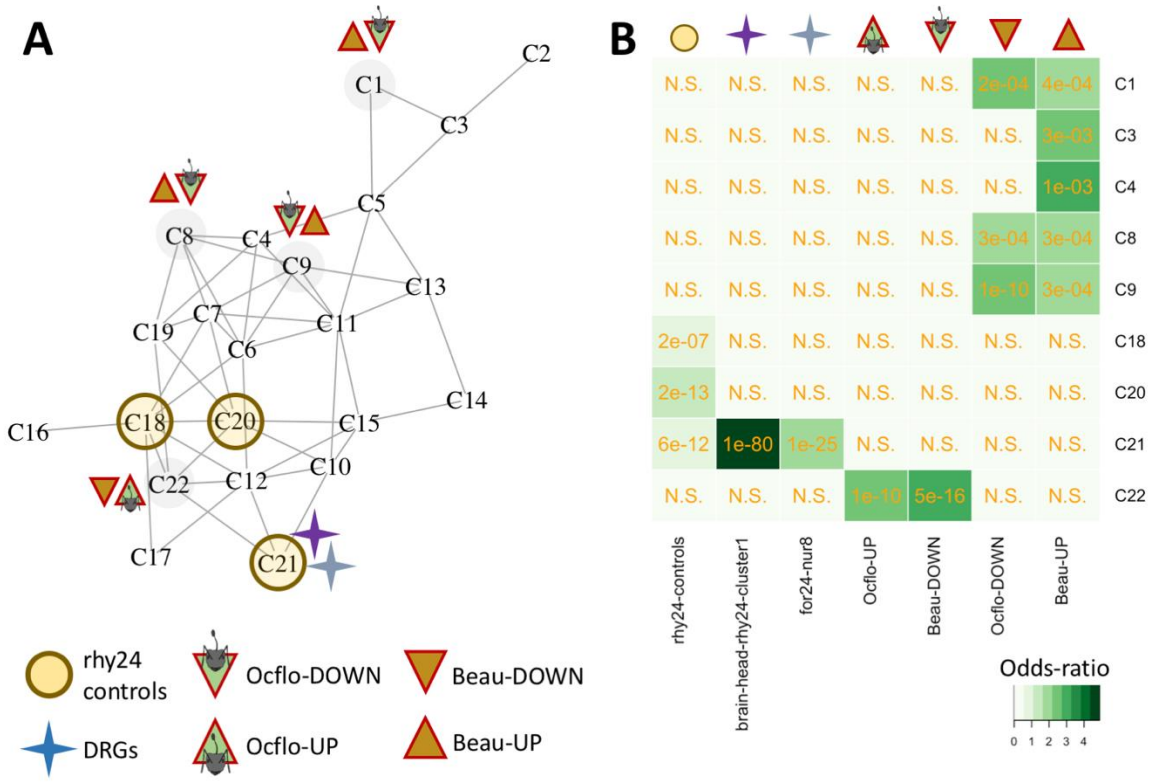

Figure 15 Annotated gene co-expression network of uninfected forager heads.

Panel (A) shows the annotated gene co-expression network (GCN) of uninfected (control) forager heads of *Camponotus floridanus*. The annotations in the network shows the different modules of interest that we have identified as being putatively important for the cross-talk between ant's clock-controlled rhythmicity, behavioral plasticity, and disease-associated differential expression and differential rhythmicity. The nodes, labelled C1 through C22, represent modules of highly co-expressed ant genes, and the edges represent co-expression of connected modules. All edges indicate module-module correlations between 0.6 and 0.8, and no edges between two modules indicate correlations <0.6. The abbreviations have the following meaning: (i) rhy24 controls indicate modules that show an overrepresentation for ant genes that were classified as significantly rhythmic in uninfected controls, (ii) DRGs indicate the modules that show overrepresentation for ant genes that show disease-associated (purple) and caste-associated (light blue) differential rhythmicity (brain-head-rhy24-cluster1 and for24-nur8, respectively), (iii) *Ocflo*-DOWN (or *Ocflo*-UP) identifies the module(s) in the ant's GCN that shows a significant overrepresentation for genes down regulated (or up regulated) in ant heads at halfway through *Ocflo* infections, and (iv) Beau-DOWN (or Beau-UP) identifies the module(s) in the ant's GCN that shows a significant overrepresentation for genes down regulated (or up regulated) in ant heads at halfway through *Beauveria* infections. Panel (B) shows the results of the

pairwise Fisher's exact test that was performed to identify the modules of interest in (A). The respective gene sets have been discussed in detail within the main text.

We found that most of the genes identified as 24h-rhythmic in controls were primarily located in three modules (C18, C20, and C21) (Fig. 15). To validate our annotation, we looked at the identity of the genes clustered into each of the rhythmic modules as we expected to see known insect clock components in these three clusters. Indeed, we found that module C21 contained core clock genes (*Clock* and *Period*), clock modulators (*Doubletime* and *Nemo*), and clock output genes (*mAchR*, *DopEcR*, *Pka*, and *Lark*) (Fig. 15). Additionally, C19 contained the clock modulating kinases *Ck2a* and *Pp1*, whereas C18 contained the gene encoding the major insect photoceptor *Rhodopsin* (Fig. 15). However, we should note that not all of these genes were classified as significantly 24h-rhythmic by eJTK. We believe that this inconsistency is likely due to our choice of an arbitrary p-value cutoff to classify genes into rhythmic and otherwise, and not the absence of rhythmicity, and we briefly explain our reasoning. A network-based identification of rhythmic modules is a powerful tool as it allows us to identify clusters of rhythmic genes using guilt-by-association. As we have discussed previously, the modules in the ant GCN were created on the basis of co-expression, i.e., how similarly do two genes mirror each other's daily expression pattern. Therefore, if a significant number of genes in a module are classified as rhythmic, then the probability that majority of the genes in the module (cluster of highly co-expressed genes) are rhythmic is relatively high. The presence of known clock components in rhythmic modules, therefore, likely suggest that these clock genes are also rhythmic in uninfected controls, consistent with our expectations.

Now that we have identified the rhythmic modules in our ant GCN, we wanted to know if the structure (gene-gene connectivity patterns) of the rhythmic modules changed drastically

during disease or not. For a given infectious disease, we calculated each module's preservation using the Preservation Zsummary score proposed by Langfelder and colleagues [239]. As the author's point out using simulations, a Zsummary score of greater than 10 indicates that there is strong evidence that the structure of the module is preserved, a Zsummary score between 2 and 10 indicates moderate evidence for module preservation, whereas Zsummary < 2 provides no evidence for module preservation. To be stringent, we classified a module to be preserved if it showed Zsummary > 10, but not preserved otherwise. Comparing the ant transcriptome during *Beauveria* infections to controls, we found only three modules that showed a Zsummary > 10, all of which were rhythmic modules (preservation ranking: C21 > C20 > C19). In *Ocflo*-infected ants, however, only two modules showed evidence for preservation, one of which was the rhythmic module C21, also found to be preserved during *Beauveria* infections. Given that C21 contains core clock genes as well as clock modulators, our finding hints at the possibility that during either disease the connectivity patterns of the core feedback loop of the host clock does not get drastically altered. However, ants infected with *Ocflo* do seem to lose their daily foraging rhythms at halfway through disease progression, but *Beauveria*-infected ants do not. This might be due to the fact that we find that all three of the host's rhythmic modules show a high degree of preservation during *Beauveria* infections, at least in their connectivity patterns. However, it does not eliminate the possibility of an altered or differential co-expression, the occurrence of which would explain the altered pattern of clock-controlled foraging rhythm that Trinh and colleagues have observed in ants during late-stage *Beauveria* infections. The loss of locomotory rhythms in *Ocflo*-infected ants, therefore, might be due to drastic rewiring that occurs in either one or both of the rhythmic modules (C18 or C20) which contains the photoreceptor *Rhodopsin* and the kinases *Ck2a* and *Pp1*. We should point out the *Ocflo* clock gene *CK2*, which functions as a core

clock gene and a photoreceptor in the model fungi *Neurospora*, shows a significant upregulation throughout the disease progression, both at the halfway mark as well as the manipulated biting stage (discussed in more details in Chapter three). If this finding suggests a direct interaction of the fungal-ant clocks during disease or not remains unclear, but the possibility remains. In comparison, at halfway through both diseases, the rhythmic module C21 containing core clock genes *Per* and *Clk* show a high degree of preservation, highlighting that host genes that tightly co-express with its core clock components are likely essential for host survival, and as such remain unaltered as the parasite incubates inside its host.

Most of the ant genes significantly up-regulated during *Ocflo*-infection were located in one module only (C22), and the same module contained most of the genes down-regulated during *Beauveria*-infection. In comparison, ant genes significantly downregulated during *Ocflo* infections were overrepresented in three modules (C1, C8, and C9), all of which also showed overrepresentation for genes upregulated in *Beauveria*-infected ants. This reconfirms our conclusion about the DEGs as discussed in the previous section. There seems to exist a core set of genes that are differentially expressed during both diseases (disease-associated DEGs). What distinguishes one infectious disease from another is the direction of this differential expression. As we have discussed above, our prior meta-analyses revealed that *Ocflo* might be inducing differential expression of the same set of ant genes that underlie behavioral plasticity (DEGs between foragers and nurses). So, we wanted to check if the disease-associated DEGs we have identified in this study significantly overlap with the behavioral plasticity genes. Mapping the behavioral plasticity genes on to our ant GCN, we found that the genes downregulated in foragers (versus nurses; for-DOWN) were mostly located in module C1 whereas genes upregulated in foragers (for-UP) were located primarily in module C22 (Supp. Fig. 4A-B), the

same modules that show overrepresentation for disease-associated DEGs. Therefore, it appears that expression levels of C1 and C22 genes are associated with behavioral plasticity as well as parasite-specific disease outcomes. More specifically, genes in module C22, usually upregulated in foragers (versus nurses), show an even stronger upregulation during *Ocflo* infection. Whereas, during *Beauveria* infection, the same cluster of genes show a significant downregulation (Supp. Fig.). To understand what function such upregulation of C22 (or downregulation of C1) might be serving in *Ocflo*-infected ants, we first need to discuss the possible links between differential gene expression and differential rhythmicity as evidenced by our annotated GCN.

We found that module C22, that contains the majority of *Ocflo*-DOWN, *Beauveria*-UP, and for-UP genes, is connected to all three of the rhythmic modules (C18, C20, C21) in our ant GCN (Fig. 15). However, we did not find any edges connecting module C1 to any of the rhythmic modules. Therefore, it seems that module C22 might be functioning as a regulatory switch in ants that modulates the rhythmic properties of the clock and its output. When we mapped, respectively, the genes that show caste-associated and disease-associated differential rhythmicity on to the GCN, we found that both sets of genes showed a significant overlap with only one module: C21. Therefore, it appears that drastic changes (up/down-regulation) in the expression of C22 could induce differential rhythmicity of C21 genes which contains essential clock genes and modulators. To summarize the results of the network analyses, we have shown that (1) molecular links between behavioral plasticity and rhythmic genes that we found for ant brains also exist at the scale of whole heads, (2) not only *Ocflo*, but also *Beauveria*, significantly affects the expression of modules overrepresented for behavioral plasticity genes, (3) the direction of the effect (up or downregulation) on these behavioral plasticity genes is exactly the opposite for infections by *Ocflo* and *Beauveria*, and (4) disease associated changes to the

expression of host genes regulating behavior plasticity (forager v. nurse) is correlated with differential rhythmicity (synchronized changes) in clock components including *Period*, *Clock*, *Ck2a*, and *Pp1b*. All the results from the network analyses are provided as a supplementary file (Additional Files 18).

CHAPTER THREE:
FUNGAL CLOCKS

Introduction

Several parasites have evolved the ability to adaptively change its host's behavior to facilitate their own survival and transmission. Examples of manipulating parasites and their hosts are found across several taxa [257-259]. Among parasitic manipulators, the *Ophiocordyceps* fungi that infect ants are emerging as a powerful model system. *Ophiocordyceps*-ant systems are highly species-specific; one species of *Ophiocordyceps* is able to successfully manipulate behavior of only one species of ant. This is consistent with the fact that these parasite-host pairs seem to have coevolved for millions of years [260]. Although these parasite-host systems show species-specificity, the disease phenotype is similar across all *Ophiocordyceps*-ant systems. In the final stages of the disease, *Ophiocordyceps* infected ants tend to show stereotypical behavioral changes that are adaptive to the parasite: social isolation from the colony, phototactic summiting, and eventual attachment at vantage points that promote fungal development and transmission. Furthermore, the manipulated biting seems to be highly synchronized to a specific time-of-day. Field observations in Thailand showed that the biting happens primarily around solar noon [36], and a similar time-of-day synchronized biting was observed in controlled lab studies with two completely different *Ophiocordyceps*-ant pairs [34, 35]. The conserved nature of timely host manipulation across *Ophiocordyceps*-ant pairs strongly suggest an underlying role of biological clocks. Our findings from Chapter two demonstrated that at least the host's clock is involved. For example, at the halfway mark in disease, *Ophiocordyceps camponoti-floridani* infected ants showed synchronized changes in the daily expression of several clock-controlled

genes previously found to show caste-associated differential rhythmicity (Chapter one). Such alteration to the host's rhythmic processes have also been found in other manipulating parasite-host systems. For example, baculoviruses are known to manipulate infected caterpillars to show a phototactic summiting behavior prior to death. Transcriptomic evidence suggested that this phototactic behavior is likely due to disease-associated alteration in host's phototransduction and circadian entrainment pathways [44, 45].

What remains less clear is the precise role of the parasite's clock in inducing timely changes to host rhythms. A previous study by de Bekker and colleagues has shown that *Ophiocordyceps,* like most fungi, has homologs of known core clock components that make up the transcription-translation feedback loop [30]. Using time-course RNASeq, the authors also showed that the daily expression of several secreted enzymes, proteases, toxins and small bioactive compounds show robust 24h-rhythms. However, it is not yet known to what degree the disease outcome – differential rhythmicity in host clock-controlled genes as found in chapter two – is driven by the parasite's clock. Furthermore, if the clock of *Ophiocordyceps* is important for inducing timely manipulation of ant behavior, it would be worth investigating how the clock of a manipulating fungus functionally differs from that of other fungal entomopathogens that do not manipulate host behavior. The latter question is important to address because, although studies of plant pathogens have demonstrated a role of fungal clocks in regulating virulence, we do not know much about the role clocks play for the success of fungal entomopathogens in general, let alone for behavior modifying fungi [42, 43]. Therefore, to understand the mechanisms via which *Ophiocordyceps* clock might enable manipulation of ant behavior, we need to disentangle the role of fungal clocks in host manipulation from its role in parasite's growth and survival. In this study, we aimed to characterize the clock and clock-controlled processes of the behavior

manipulating fungi *Ophiocordyceps* in comparison to a generalist, non-manipulating entomopathogen, to shed light on the role of fungal clocks in inducing timely changes to host's clock-controlled processes, including rhythmic behavior.

Using time-course RNASeq and comparative network analyses, we compared the daily transcriptome of *Ophiocordyceps camponoti-floridani* (*Ocflo*) and *Beauveria bassiana* (*Beauveria*; synonymous to *Cordyceps bassiana*), both of which are known to successfully infect the Florida carpenter ant *Camponotus floridanus*. More specifically, we aimed to characterize the similarities and differences in how the clocks of these two fungal parasites temporally segregate their biological processes as they grow in their blastospore stage in controlled liquid media, outside the ant host. Additionally, we discuss how clock-controlled gene expression changes for the manipulating parasite, *Ocflo*, while it grows inside the ant head at the halfway mark in disease (data was obtained from chapter two). Finally, we use network analyses to identify potential mechanisms via which the *Ocflo* clock might be either interacting with the host's clock or regulating aspects of timekeeping in its infected host.

Methods

Fungal culturing and circadian entrainment

To culture *Ocflo* and *Beauveria*, we used the same protocol and fungal strains (Arb2 and BB0062, respectively) as described in Chapter two. To reiterate the process briefly, we grew both *Ocflo* and *Beauveria* in their blastospore stage in Grace's Insect Medium (Gibco, Thermo Fisher Scientific) supplemented with 2.5% FBS (Gibco) using established protocols (de Bekker et al., 2017; Will et al., 2020; Ying & Feng, 2006). As for entraining fungal samples for time-course RNASeq, we closely followed the protocol described in de Bekker et al. (2017). We decided to entrain the fungal cultures using the same entrainment protocol that I have used to entrain their host (ants) in my prior experiments (in Chapter one and two): strict 12h:12h light-dark cycles while keeping the temperature and relative humidity constant. To ensure that the fungi entrained to the new light-dark regime readily, we kept fungal cultures under constant light conditions for 48 hours (constant temperature and relative humidity as well) before moving them to strict 12h:12h light-dark cycles. We allowed the fungal cultures to entrain to light-dark cycles for five days before harvesting them for RNASeq. To perform time-course RNASeq, however, we needed to harvest fungal blastospores at multiple time points throughout the day. To do so, for each fungal species, we split the original (source) culture undergoing entrainment into 18 separate fungal cultures (12 for sampling and 6 as backup), on day four of light-dark entrainment. More specifically, we reseeded 250 µL of source fungal culture (OD at 660nm = 1.089) into 15 mL of fresh media. Providing blastospores with fresh media also ensured that the fungal cells didn't experience starvation conditions during sampling. Following the split, all

fungal cultures demarcated for sampling were left undisturbed under the light-dark entrainment conditions until sampling day.

Harvesting fungal samples over a day under 12:12 LD

We harvested both fungal samples, simultaneously, on day six of the light-dark entrainment period. Starting at ZT2 (two hours after lights were turned on), we harvested fungal blastospores every 2h, over a 24h period. At a given sampling time point, for each species, we pelleted the fungal cells by spinning down 2 mL of the fungal culture for 3 min at 10,000 rpm. The supernatant was discarded, and the process was repeated twice for *Ocflo*, and thrice for *Beauveria* to obtain comparable size of fungal pellets (condensed blastospores). We then added two ball bearings to each pellet, and flash froze the samples in liquid nitrogen and kept them at -80 ºC until further processing for RNASeq. In total, we obtained twenty-four fungal samples from the two species, harvested across 12 time points throughout the 24h day.

RNA extraction, library preparation and RNASeq

We extracted total RNA from the frozen fungal samples and prepared the cDNA libraries for RNASeq using exactly the same protocol described in Chapter two. All twenty-four cDNA libraries were sequenced as 50 bp single-end reads on an Illumina HiSeq1500 at the Laboratory for Functional Genome Analysis (Ludwig-Maximilians-Universitat Gene Center, Munich). Raw read data will be uploaded to the relevant NCBI database prior to submitting this study for publication.

Pre-processing sequencing data

Similar to what we have done in Chapter one and two, we first removed sequencing adapters and low-quality reads from our RNASeq data using BBDuk (parameters: qtrim = rl, trimq = 10, hdist = 1, k = 23) [124]. Post-trimming, we used HISAT2 [125] to map transcripts to the relevant genomes (*O. camponoti-floridani* (NCBI ID: 91520; Will et al. 2020) and *B. bassiana* (ARSEF 2860; Xiao et al. 2012)). Finally, we obtained normalized gene expression from the mapped reads as Fragments Per Kilobase of transcript per Million (FPKM) using Cuffdiff [127].

Rhythmicity and Overrepresentation analyses

To perform functional enrichment analyses, we used an updated version of the custom enrichment function that performs hypergeometric test (previously used in [34] and [226]). The function "check_enrichment" is now publicly available for use via the timecourseRnaseq package on GitHub (https://github.com/biplabendu/timecourseRnaseq) [235]. For a given set of genes, we identified overrepresented Gene Ontology (GO) terms or PFAM domains using the check_enrichment function, and significance was inferred at 5% FDR. If not mentioned otherwise, for functional enrichment tests, we used all genes that were found to be "expressed" (≥ 1 FPKM expression for at least one sample) in the ant heads, for each treatment, as the background geneset. We only tested terms annotated for at least 5 protein coding genes. To cluster a set of genes according to their daily expression, we used an agglomerative hierarchical clustering framework (method = complete linkage) using the 'hclust' function in the stats package for R. To determine differentially expressed genes, we used the linear modelling framework proposed in LimoRhyde [132], but without an interaction between treatment and time. A gene was considered significantly differentially expressed if treatment was found to be a

significant predictor (at 5% FDR) and the gene showed at least a two-fold change in mean diel expression between the two treatment groups (abs($\log_2$-fold-change) ≥ 1).

All data analyses, including statistical tests and graphical visualizations, were performed in RStudio [136] using the R programming language v3.5.1 [137]. Heatmaps were generated using the pheatmap [138] and viridis [139] packages. Upset diagrams, used to visualize intersecting gene sets, were made using the UpsetR package [140]. We used a Fisher's exact test for identifying if two genesets showed significant overlap (significance was inferred at 5% FDR). We visualized the results of multiple pairwise Fisher's exact test using the GeneOverlap package [141]. All figures were generated using the ggplot2 package [236].

Network analyses

To build the annotated gene co-expression network (GCN), we used the exact protocol detailed in de Bekker and Das (2022) [225] (Additional File). The clustering of genes into co-expressed modules was performed using functions from the WGCNA package [237-239], the gene-gene and module-module correlations were calculated using Kendall's tau-b correlation [240], and the global connectivity patterns of the GCN was visualized using the igraph package [241]. The significance of pairwise overlaps were calculated using Fisher's exact tests and visualized using the GeneOverlap package [141].

Results and Discussion

General patterns of daily gene expression

To identify the putative genes and processes that are under clock control in *O. camponoti-floridani* and *B. bassiana*, and to characterize the differences in their daily timekeeping, we performed RNA-Seq on 12h:12h light-dark entrained fungal cultures that were harvested every 2h, over a 24h period. For each time point, we collected the two fungal species, simultaneously, in their yeast-like blastospore stage which is the primary life stage of the fungi inside their infected ant host (Wang and Wang 2017).

We classified fungal genes as "expressed" if their mRNA levels were greater than 1 FPKM for at least one of the 12 sampling time points during the 24h period. Of the 7455 protein-coding genes annotated in the *O. camponoti-floridani* (*Ocflo*) genome, 94% (6998 genes) were expressed, whereas only 2.5% (190 genes) showed no expression (FPKM = 0 at all time points). As for *B. bassiana* (Beau), 9006 (87%) of the 10364 protein-coding genes were expressed at some point during the 24h day, and 756 (7.3%) were not expressed at all. The non-expressed genes for *Ocflo*, but not *Beauveria*, showed overrepresentation of heat-labile enterotoxin genes (five out of the 34 annotated in the genome) putatively involved in pathogenesis and interspecies interaction between organisms (Fig. 16), of which some have been hypothesized to be involved in behavioral manipulation (de Bekker et al., 2015; de Bekker et al., 2017; Will et al., 2020). Among these five *Ocflo* genes, two copies of heat-labile enterotoxin A subunit did not show any expression (FPKM = 0) even inside ant hosts at halfway through disease progression (also referred to as "infection" throughout this manuscript). Whereas, two putative enterotoxins and a

FAD-binding domain-containing protein showed only a low expression (0 < FPKM < 1) during infection.

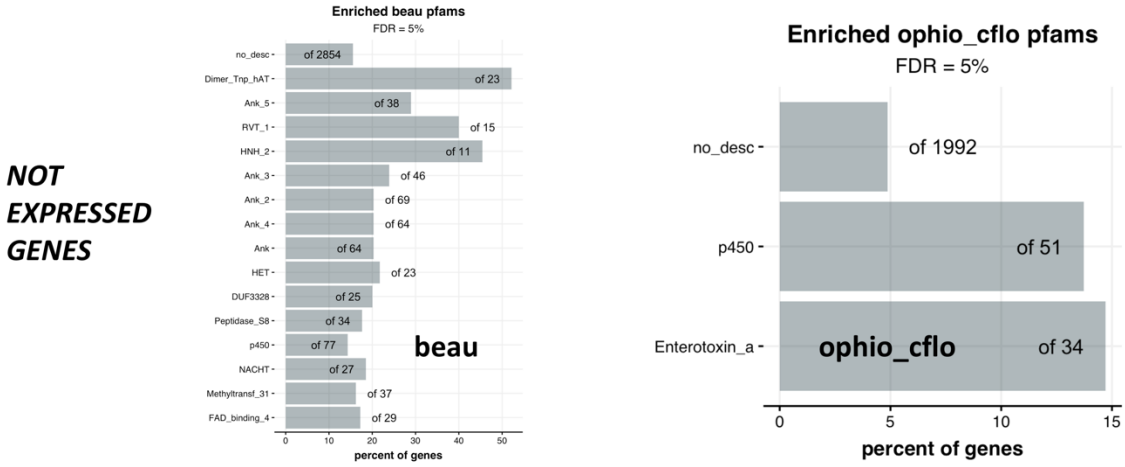

Figure 16: Functions of fungal genes not expressed in their blastospore stage while they grow in controlled conditions outside the host body.

The two panels show the pfam domains overrepresented in the set of genes that show no expression (FPKM=0) in (left) *Ocflo* and (right) *Beauveria* during their blastospore growth stage in controlled conditions. The bars represent the percent of genes annotated with a given pfam domain that is found in the test gene set (in this case, non-expressed genes) as compared to all such genes found in the background gene set (in this case, all genes in the ant genome). Unless mentioned otherwise, all subsequent enrichment plots used in this manuscript have the same meaning. Also, beau represents data for *Beauveria bassiana* and ophio_cflo represents data for *Ophiocordyceps camponoti-floridani*.

Daily rhythms in gene expression – Ocflo

We identified significant daily rhythms in fungal gene expression using the non-parametric algorithm empirical JTK Cycle (eJTK) [129, 130]. Of the 6889 *O. camponoti-floridani* genes expressed in their blastospore stage, 33% (2285 genes) showed significant 24h-rhythms in daily

expression. Identifying how the clock in *Ocflo* temporally budgets its biological processes would be useful to understand how closely related the parasite's daily expression profile is to its host, and how this host-parasite comparison differs between *Ocflo* and *Beauveria*. The ability of incubating parasites to synchronize their development to host metabolic rhythms has been observed in malaria [261]. Work by Reece and colleagues also demonstrated that malaria parasites that have developmental rhythms asynchronous to their host's metabolic rhythm readily re-synchronized their development to host metabolic rhythms by changing the periodicity of the parasite's developmental cycles [262]. This highlights that synchronicity of host-parasite rhythms likely is an essential component of successful infections, and the degree of synchronization, therefore, can correlate with disease severity and outcome. In the case of ants infected by two fungal parasites with distinct disease outcomes, we could hypothesize that the more than three-week long incubation (or growth) period of *Ocflo* inside its ant host involves a relatively higher synchronization of the clock-controlled processes of the parasite to its host, which might not occur for *Beauveria*-ant interactions.

We used hierarchical clustering of rhythmic genes identified in *Ocflo* to tease apart different clusters of genes that show the same (or similar) phase of daily expression (i.e., synchronized to a specific time of day). To identify potentially day, night, dusk, and dawn peaking genes, we decided to split the rhythmic genes into four clusters upon hierarchical clustering (Fig. 17A-B). We identified a set of 354 genes (Fig. 17A-B, cluster-3) that showed clear day-peaking activity with more than 50% (172 genes) of genes oscillating with a phase at ZT2, two hours after lights were turned on. It is hard to say if the peak activity at ZT2 for these processes is driven by the endogenous clock (anticipatory) or a synchronized response to light (reactive) since the transition from dark to light happens at exactly ZT0. Next, we identified

another set of 633 putative day-active genes (cluster-4) that showed a more distributed phase of daily expression as compared to cluster-3 genes (Fig. 17A). The majority of cluster-4 genes (45% of 633 genes) showed a peak expression between ZT10 and ZT12. The latter – ZT12 – is the time at which the fungus experiences light to dark transition. Prior to and during harvesting samples for RNASeq, we kept the fungal cultures under strict 12h:12h light-dark cycles without any ramping of light intensity. Given that we sampled right at the transition of light-dark, and that we harvested samples fairly quickly, we cannot dismiss the peaks of daily gene expression observed at the transition periods (ZT12 or ZT24) as a response to changes in light. Therefore, genes peaking prior to and at the light-dark transitions are most likely clock-controlled anticipatory peaks. Similar to cluster-4, we found that most genes in cluster-2 (465 genes) showed a peak activity at the transition from dark to light (ZT24), whereas genes in cluster-3 (833 genes) showed anticipatory peaks between ZT20 and ZT24, a few hours before lights turned on (Fig. 16 A-B). Taken together, our data suggests that *Ocflo* entrained to strict 12h:12h light-dark cycle is able to anticipate light-dark (and dark-light) transitions while the majority of their rhythmic genes show an anticipatory peak prior to or at the light-dark transitions. Light, therefore, seems to be a strong zeitgeber (entrainment cue) for the endogenous clock of *Ocflo*. This is not surprising given that for most fungi and animals studied so far, daily fluctuations in light-dark seems to be one of the prominent abiotic cues that synchronize an organism's clock (reviewed in [263, 264]). However, we should also point out that in the presence of conflicting or non-synchronous entrainment cues, the choice of the primary zeitgeber is dependent on the species' life history. For example, social cues such as colony volatiles seem to be a stronger zeitgeber than light in highly social insect societies, whereas multiple studies in animals and fungi provide some evidence for the presence of a metabolic oscillator that is coupled to, but

independent from, the transcription-translation feedback loop that is usually thought to be the primary oscillator that drives an organism's clock-controlled processes. In the next two sections, we will discuss how the temporal division of clock-controlled genes, and the processes they regulate, in *Ocflo* compares with that of *Beauveria*.

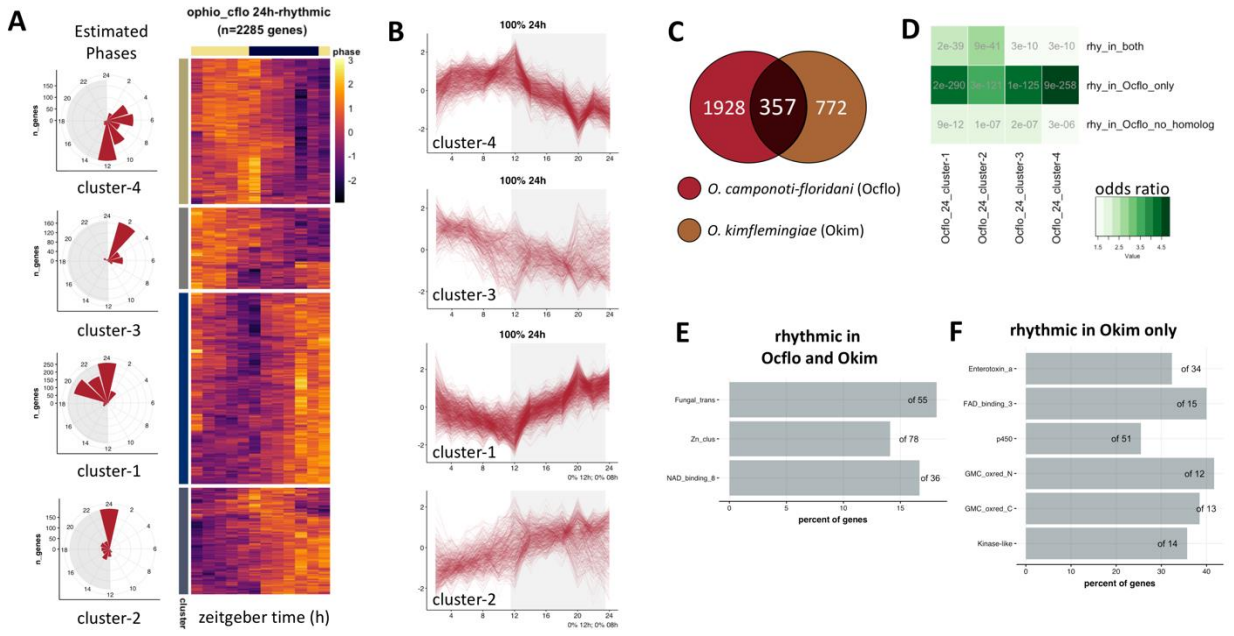

Figure 17: Temporal division of clock-controlled processes in Ophiocordyceps.

The heatmap in panel (A) shows the daily expression (z-score) patterns of the genes identified as significantly oscillating every 24h in *Ocflo* blastospores grown in controlled liquid cultures. Each row represents a single gene and each column represents the Zeitgeber Time (ZT) at which the sample was collected, shown in chronological order from left to right (from ZT2 to ZT24, every 2 h). These 2285 rhythmic genes were hierarchically clustered into four groups based on their daily expression profiles, and the cluster identity of each gene is indicated in the cluster annotation column on the left of the heatmap. Additionally, the distribution of phases (peak time of expression) for rhythmic genes belonging to each of the clusters are shown on the left of the heatmap. In panel (B), we have presented the stacked zplots for all genes in a given cluster. For stacked zplots of a given cluster, each line represents the daily expression of one single gene in that cluster. Panel (C) shows the overlap between the genes classified as significantly rhythmic in two *Ophiocordyceps* species (data for *O. kimflemingiae* (*Okim*) was obtained from de Bekker et al. (2021) [30] and to be consistent across the two species, rhythmicity analyses was re-run using eJTK; see Methods for more details). Panel (D) shows the results of pairwise Fisher's exact test that we have performed to find if certain sets of *O. camponoti-floridani* (*Ocflo*) genes significantly overlapped with either of the four distinct clusters identified in (A). The abbreviations used in the panel have the following meaning: (i) rhy_in_both = homologous genes between *Ocflo* and *Okim* classified as 24h-rhythmic in both,

(ii) rhy_in_*Ocflo*_only = homologous genes classified as rhythmic in *Ocflo* but not in *Okim*, and (iii) rhy_in_*Ocflo*_no_homolog = genes that are classified as rhythmic in *Ocflo* but lack a homolog in *Okim*. Finally, panels (E) and (F), respectively, shows the overrepresented pfam domains found in the set of homologous genes classified as rhythmic in both *Ocflo* and *Okim*, and the homologous genes rhythmic in *Okim* but not in *Ocflo*.

Daily rhythms in gene expression – Ocflo vs. Okim.

Before conducting the comparison between two very different fungal species with drastically different infection strategies and disease outcomes, we compared how the clock-controlled genes and processes compared between two more closely related *Ophiocordyceps* species, that have both evolved with their respective ant hosts and have the ability to induce timely behavioral manipulations in their hosts. In a previous time-course transcriptomics study, de Bekker et al. (2017) described the daily rhythms in gene expression for *O. kimflemingiae* (*Okim*), a closely related species of our focal *O. camponoti-floridani* (*Ocflo*), that infects and manipulates behavior of a different carpenter ant *C. castaneus*. Therefore, we set out to test if the identity and functions of clock-controlled genes in these two *Ophiocordyceps* species are similar or not.

Of the 8441 genes annotated in the genome of *Okim*, 6867 were found to have a unique homolog in *Ocflo*. Among these homologs, 357 genes, including the fungal core clock gene *Frequency*, showed significant 24h rhythms in both *Ocflo* and *Okim* (Fig. 17C). Furthermore, the overlap between rhythmic genes identified in *Ocflo* and in *Okim* was significant (Fisher's exact test; odds-ratio = 1.2, p-value = 0.04). This finding indicates that in both *Ophiocordyceps* species, the clock drives daily rhythms in similar genes and molecular functions. Next, we wanted to see if these conserved rhythmic genes showed any time-of-day preference in *Ocflo* (i.e., are these genes primarily day-peaking or night-peaking?). To do so, we tested if the set of 357 rhythmic genes showed a significant overlap with any one of the four clusters that we

identified for rhythmic *Ocflo* genes (discussed in previous section). We found that these 357 rhythmic genes (rhy_in_both) were fairly well distributed among the four clusters of *Ocflo* rhythmic genes, as can be seen from the results of our pairwise Fisher's exact tests shown in Fig. 17D. Next, we explored the functions of these seemingly conserved clock-controlled genes in *Ophiocordyceps*. To do so, we performed functional enrichment analyses on the 357 homologous genes that seem to be under clock-control in both *Ophiocordyceps* species. The conserved rhythmic genes were enriched for the pfam domains, fungal-specific transcription factor, Zn(2)-Cys(6) binuclear cluster domain, and NAD(P)-binding Rossmann-like domain, and were putatively involved in several metabolic and biosynthetic processes (Fig. 17E). Taken together, it appears that the clock of both *Ophiocordyceps* species drive daily rhythms in a core set of genes involved in transcriptional regulation and metabolic processes, but these seemingly conserved clock-controlled processes do not show a characteristic time-of-day preference, at least in *Ocflo*.

It is known that *Ophiocordyceps*-ant interactions are highly species-specific; usually one species of fungi is able to successfully manipulate behavior of only one species of ant [35]. However, it is not known how differences in the fungal clock functioning, especially the identity and function of the clock-controlled genes, play a role in such host-specificity. To get a first glimpse, we wanted to compare the homologous genes that showed significant daily rhythms in one species but not the other. Given that in the previous transcriptomics study *Okim* samples were collected every 4h over a 48h period [30], as compared to every 2h over a 24h period for *Ocflo* in our study, genes classified as rhythmic in *Ocflo* but not in *Okim* might be due to a lower sampling resolution used for the latter. However, oscillating genes in *Okim* that were not significantly rhythmic in *Ocflo* might be worth investigating since the sampling resolution and sequencing depth we used for *Ocflo* should have allowed us to identify more of the cycling genes

[265]. We found 772 genes that were classified as rhythmic in *Okim* but not in *Ocflo*, and these genes showed significant overrepresentation in several pfam domains, including heat-labile enterotoxin, cytochrome p450, and kinase-like protein coding genes (Fig. 17F). We should note, however, that none of these pfam domains were enriched in the homologous genes uniquely rhythmic in *Ocflo*. In summary, our findings seem to suggest that although several key biological processes (transcription and metabolism) are under clock control in both *Ophiocordyceps* species, species-specific differences exist in the repertoire of clock-controlled genes and processes, some of which (e.g., enterotoxins) are hypothesized to be important for *Ophiocordyceps'* ability to successfully manipulate its specific ant host [30, 34].

Daily rhythms in gene expression - Ocflo vs. Beauveria

Part One

The behavior-manipulating fungal parasite *O. camponoti-floridani* and the non-manipulating generalist entomopathogen *B. bassiana* have vastly different disease progressions inside their ant host, *C. floridanus*. A clear difference can be found in the survival times of the infected host; in controlled lab conditions, ants infected with *O. camponoti-floridani* can live up to three to four weeks, whereas *B. bassiana*-infected ants die within a week [116, 227]. Since *B. bassiana* functions as a generalist parasite that kills and consumes its host within a matter of days upon infection, without the need to induce pathogen-adaptive behavior in its host, its lifestyle can be classified as necrotrophic. On the contrary, *O. camponoti-floridani*, which has co-evolved with and highly specialized to infect one host, *C. floridanus*, spends more time in a seemingly symbiotic relationship with its host before killing it. Such a parasitic lifestyle can be classified as hemibiotrophic (reviewed in [228]). Here we discuss the similarities and differences in the

functioning of the biological clock of *Beauveria* as compared to *Ocflo*. The comparison between *Beauveria* and *Ocflo* fits multiple, non-mutually exclusive, contexts: (1) a necrotroph versus a hemibiotroph, (2) a generalist versus a specialist, and finally (3) a non-manipulating versus behavior manipulating parasite.

To enable comparison between the two fungal species, we first identified the one-to-one orthologs between *Ocflo* and *Beauveria*. Of the 7455 protein coding genes annotated in *Ocflo* genome and 10364 genes annotated in *Beauveria* genome, 5274 genes show a one-to-one orthology. Of the 9006 genes expressed in *Beauveria*, 1872 displayed a significant 24h rhythm in daily expression, among which 701 oscillating genes lacked an ortholog in *Ocflo*. Similarly, in *Ocflo*, 485 of the 2285 rhythmic genes did not have an ortholog in *Beauveria*. To get a glimpse at the differences in clock-controlled genes and processes among these two fungal species, we explored the identity and function of these non-orthologous rhythmic genes in either species. The 485 non-orthologous rhythmic genes in *Ocflo* were enriched in heat-labile enterotoxin genes and methyltransferases (Fig. 18). Neither of these two pfams were overrepresented in the set of non-orthologous, rhythmic *Beauveria* genes; instead, they showed significant enrichment for fungal-specific transcription factors, genes containing both, catalytic domain of alcohol dehydrogenase and zinc binding domain, beta-lactamases, NACHT domain containing genes, and zinc finger containing transcription factors (Fig. 18). Beta-lactamase enzymes, usually produced by bacteria, are well known in enabling bacterial resistance against beta-lactam antibiotics such as penicillin [266]. However, several fungal species are also known to encode beta-lactamases (reviewed in Dawe and Kharwar, 2017). The functions of fungal lactamases seem to be more diverse than mere resistance against beta-lactam antibiotics. For example, fungal lactamases seem to enhance fungal detoxification of xenobiotic compounds or act as a fungal pathogenicity factor that is

recognized by the host's immune system [266]. The daily oscillations we find in expression of beta-lactamase encoding genes in *Beauveria*, therefore, could either suggest a prophylactic response to daily fluctuations in circulating xenobiotic compounds or an indicator for daily fluctuations in *Beauveria* pathogenicity to its host. On the other hand, the finding that non-orthologous rhythmic genes in *Ocflo* comprises mostly of enterotoxin genes lines up with our previous knowledge of the role enterotoxins play in manipulating host behavior. Additionally, the rhythmic expression of *Ocflo* enterotoxins suggests that daily fluctuations in enterotoxin activity can potentially elicit rhythmic detoxification response from its host. And if so, it would be worth exploring how the detoxification pathways in the host are coupled to its core clock and clock output pathways. There is some evidence that oxidoreductase activity shows daily rhythms in animals, and this rhythmicity in detoxification is not just a byproduct of an oscillating clock but a component that feeds back into the clock (REF).

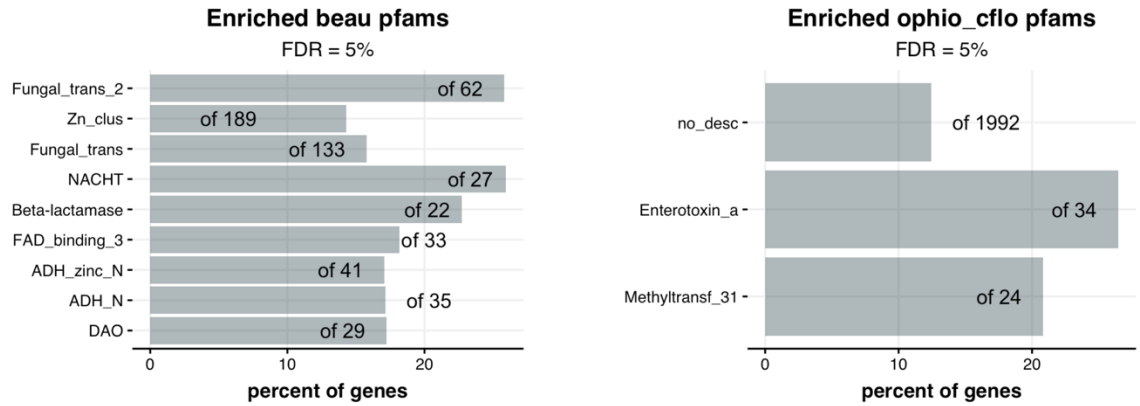

Figure 18 Functions of non-orthologous rhythmic genes in Ocflo and Beauveria.

The overrepresented pfam domains found in the subset of rhythmic genes in (left) *Beauveria* and (right) *Ocflo* that lack a one-to-one ortholog in the other species are shown. The bars and numbers in the enrichment plot has the same meaning as before.

Daily rhythms in gene expression - Ocflo v. Beauveria

Part Two

Having identified the orthologous genes between *Ocflo* and *Beauveria* that show robust daily rhythms, we can now ask if certain clusters of genes oscillate in both fungi but with a characteristic difference in time-of-day preference. In other words, are certain clock-controlled genes day-peaking in *Ocflo* but night-peaking in *Beauveria*? This is useful to explore since we hypothesized earlier that the long incubation period of *Ocflo*, as compared to *Beauveria*, in their ant hosts is likely due to a relatively higher degree of synchronization of the parasite-host clock-controlled processes. However, a higher degree of parasite-host synchronization of daily rhythms can also be detrimental for the host. For example, synchronization of the parasite's daily peak of pathogenicity to the host's resting phase has been seen to result in increased virulence and disease severity (REF). However, as we pointed out earlier, not much is known about the role of parasite-host synchronization in disease severity for either of our focal diseases. Therefore, in this section, we aimed to characterize the similarities and differences in the clock-controlled gene expression of *Ocflo* versus *Beauveria* hoping to get a glimpse into the links between fungal clock functioning and disease outcomes.

Of the 5274 orthologous genes between *Ocflo* and *Beauveria*, 1790 genes in *Ocflo* and 1171 genes in *Beauveria* were classified as significantly 24h-rhythmic (433 were classified as rhythmic in both, and 2519 genes were rhythmic in at least one fungal species). Since we aimed to identify synchronized changes in the daily expression of rhythmic gene clusters across the two species, we performed hierarchical clustering on all 2519 genes that were significantly rhythmic in at least one of the two fungal species (Fig. 19A). We obtained four clusters upon hierarchical

clustering with the aim to identify potentially day, night, dusk, and dawn peaking clusters. Comparing the daily expression of these four clusters in the two fungal species, two primary observations stand out. First, the orthologous genes in cluster-1 and cluster-2 displayed a similar pattern of daily oscillations in the two fungal species. For example, genes in Cluster-1 showed a putative day-time peak around ZT08-Z12 in both fungi, whereas Cluster-2 peaked during the subjective night around ZT20-24. Second, genes in cluster-3 and cluster-4 showed a reversal in their phase of daily expression in the two fungal species, as is evident from their stacked z-plots shown in Fig. 19B. More careful observation revealed that Cluster-3 genes in *Ocflo* showed daily expression patterns similar to night-peaking Cluster-2 genes, but the same genes in *Beauveria* showed a day-time peak. Whereas, in *Ocflo,* Cluster-4 genes showed daily fluctuations similar to the day-peaking Cluster-1, but in *Beauveria* the same Cluster-4 genes showed a seemingly night-time peak. This difference in the time-of-day of peak activity – which we call differential rhythmicity – of the same clock-controlled genes might explain, at least partly, the differences we observe in the two fungi's life history, mode of operation inside the ant host, and the eventual disease outcome. Therefore, as a next step, we explored the identity of these differentially rhythmic genes and the molecular functions they perform in fungi.

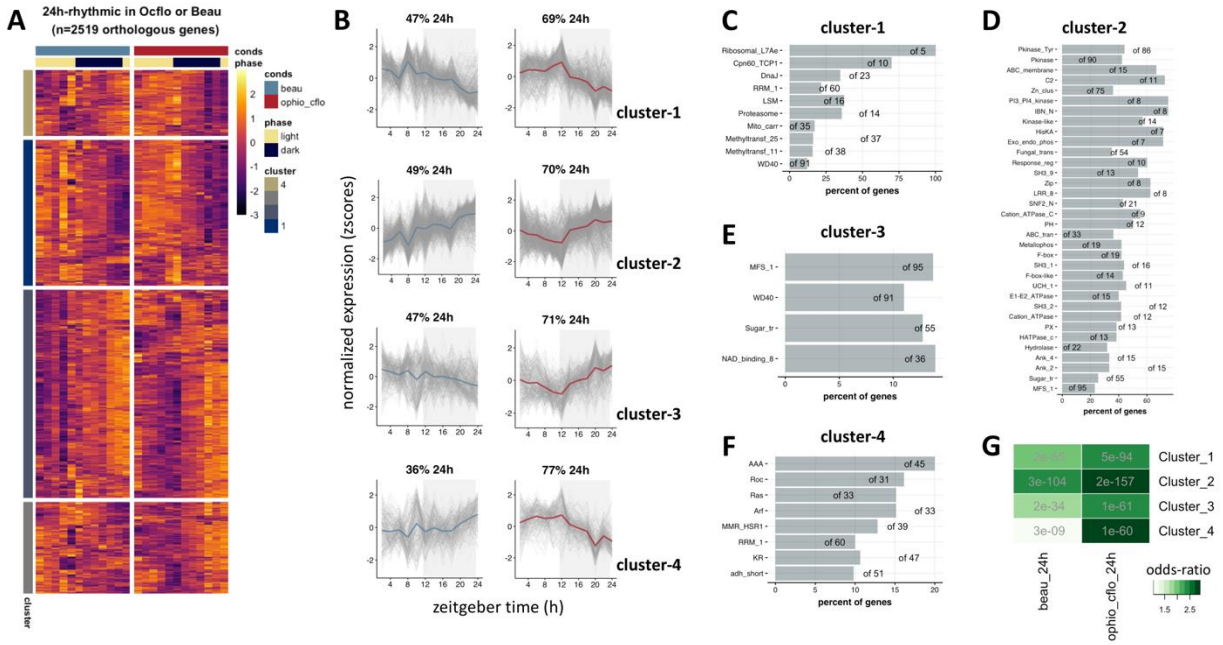

Figure 19 Orthologous rhythmic genes in Ocflo and Beauveria show species-specific differences in daily timing.

The heatmap in panel (A) shows the daily expression (z-score) patterns of the orthologous genes between *Ocflo* and *Beauveria* that were classified as significantly 24h-rhythmic in either *Ocflo* or *Beauveria*. Each row represents a single gene and each column represents the Zeitgeber Time (ZT) at which the sample was collected, shown in chronological order from left to right (from ZT2 to ZT24, every 2 h). These 2519 genes were hierarchically clustered into four groups based on their daily expression profiles in both the fungi, and the cluster identity of each gene is indicated in the cluster annotation column on the left of the heatmap. In panel (B), we have presented the stacked zplots showing the daily expression of the orthologous genes in a given cluster for *Beauveria* and *Ocflo*. For a given cluster, the solid colored line represents the median daily expression of all genes in that cluster. For each stacked zplot, the number on top indicates the percentage of genes in that cluster that were classified by eJTK as significantly rhythmic as per our p-value threshold ($p < 0.05$). Panesl (C) through (F) shows the overrepresented pfam domains found in each of the four clusters identified in (A). The bars and numbers of the enrichment plot have the same meaning as before. Finally, in panel (G), we report our results of pair-wise Fishers' exact test that we performed to check which of the four clusters identified in (A) show a significant overrepresentation for genes identified as rhythmic in *Beauveria* (beau_24h) and *Ocflo* (ophio_cflo_24h).

The differentially rhythmic genes in Cluster-3 showed overrepresentation for genes encoding Major Facilitator Superfamily (MFS_1 domain) of membrane proteins, some of which function as glucose transporters (Sugar_tr domain), including a probable aflatoxin efflux pump

AFLT and an MFS drug transporter. Additionally, this cluster showed enrichment for genes containing NAD(P)-binding Rossmann-like (NAD_binding_8) domain and WD-40 repeats (WD40 domain). The latter is implicated in signal transduction and transcriptional regulation [267]. Scanning through the entire list of Cluster-3 genes revealed other genes of interest such as two copies of *protein tyrosine phosphatase* (candidate effector of parasitic manipulation of host behavior; reviewed in [258]), a *D-3-phosphoglycerate dehydrogenase* and an *alanine--glyoxylate aminotransferase* (putative regulators of ant behavioral plasticity, see Chapter one), and *arrestin* (involved in photoreceptor maintenance and olfactory perception in *Drosophila*). In comparison, Cluster-4 showed enrichment for genes containing ATPase associated with diverse cellular activities (AAA) domain which included several DNA replication factors, a DNA helicase, a chromosome transmission fidelity protein, and a cell division control protein. Also overrepresented in this cluster were NAD- or NADP-dependent oxidoreductases (adh_short domain), genes encoding GTP-binding (MMR_HSR1, Roc, Arf, and Ras domains) and RNA-binding proteins (RRM_1). Apart from the overrepresented functional groups, this differentially rhythmic cluster also contained *will die slowly* (histone modification gene in flies), *Nicotinamide N-methyltransferase* (mediates genome-wide epigenetic and transcriptional change, and also implicated in xenobiotic detoxification), *Superoxide dismutase* (detoxifies reactive oxygen species), and a *glutathione S-transferase* (GST) protein coding gene (GSTs are involved in detoxification and hypothesized to be core regulators of insect olfaction; [268]). Finally, we should note that among all the pfam domains enriched across the two differentially rhythmic clusters (3 and 4), only a few (MFS_1, Sugar_tr, and WD40, RRM_1) were also found to be overrepresented in the non-differentially rhythmic clusters (1 and 2) (Fig. 19C-F). This latter finding suggests that these two sets of clock-controlled genes perform distinct functions in fungi.

The differences in the time-of-day at which these clock-controlled processes peak in the two fungal entomopathogen might be key determinants of how each disease progresses in its nocturnal host ant. Future studies focused on functionally testing the role of a few of these differentially rhythmic fungal genes, especially the ones that have been linked to behavioral plasticity in ants, will be important next steps.

Differentially expressed Ocflo genes during infection

Thus far, we have discussed the differences in the pattern of daily gene expression of *Ocflo* and *Beauveria* blastospores, both of which were grown in controlled liquid cultures outside the host. Although blastospores represent the fungal life stage in which it exists inside infected ant hosts, we expect the fungal daily gene expression profiles to change substantially as the fungus grows inside the host's body and is subjected to a completely different set of entrainment cues and a newfound competition against host's microbiota and immune repertoire. In Chapter two, we sampled *Ocflo*-infected ant heads at halfway through its disease progression using the same sampling resolution and entrainment cues used in this study to harvest fungal blastospores. This is the timepoint in disease progression at which infected ants appear to lose their daily activity rhythms (Chapter two) [116]. At every 2h, over a 24h period, we pooled extracted RNA from three infected ant heads to prepare the cDNA libraries for sequencing (see Methods in Chapter two for more details). Performing RNASeq on the entire ant head, instead of the brain, allowed us to obtain a mixed transcriptome containing both ant and fungal mRNA, and eventually, normalized gene expression data for both host and parasite.

At the halfway mark in the disease, two primary changes in parasite's gene expression are of interest to us. First, identifying the drastic changes in gene expression (differential

expression) will allow us to understand which fungal genes and processes show an early activation/deactivation and their relevance to *Ocflo*'s disease progression in the ant host. And, second, identifying synchronized changes in the daily expression of *Ocflo* rhythmic genes will provide support for the parasite's ability to show disease-associated plasticity in its clock-controlled rhythms. However, to confidently characterize the changes to the fungal daily gene expression profiles during disease, sufficient sequencing reads for each timepoint of sampling was necessary. Although, on an average, we obtained 8.1 (± 1.8) million reads per sample (timepoint) that mapped uniquely to the *Ocflo* genome, the pooled sample we collected at ZT6 displayed a relatively low read depth (1.1 million reads). As a consequence, we were unable to confidently run the rhythmicity analyses for *Ocflo* daily transcriptomes during disease since the sharp peaks or troughs we observed at ZT6 could easily be due to low sequencing depth of the sample and not biologically relevant. Therefore, we decided against interpreting the rhythmic properties of fungal daily gene expression at halfway through disease. However, our data still allowed us to identify the *Ocflo* genes that showed significantly different expression levels, throughout the day. In this section, therefore, we highlight the *Ocflo* genes that were differentially expressed at the halfway mark in disease as compared to their expression in liquid culture. Subsequently, we will discuss how these DEGs might be regulating (or be regulated by) the rhythmic output of the fungal clock, especially focusing on potential cross-talk between DEGs and the genes that seem to be differentially rhythmic between *Ocflo* and *Beauveria*.

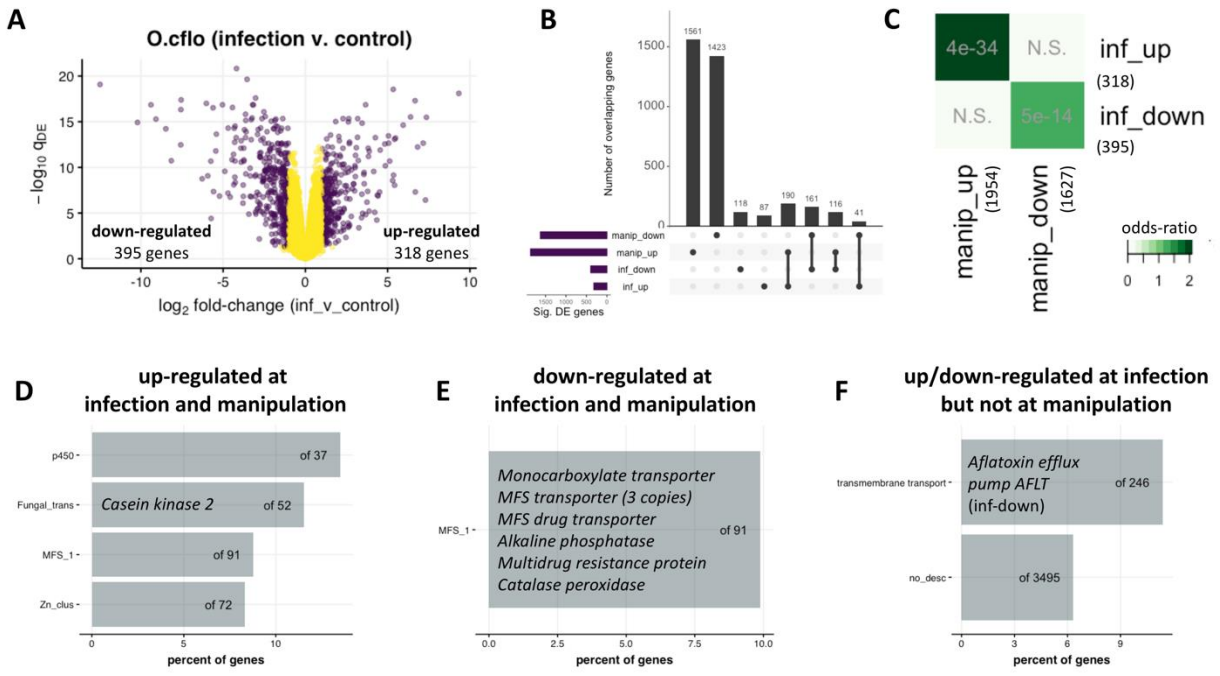

Figure 20 Differentially expressed genes in Ocflo at halfway through disease progression (infection) as compared to late-stage of the disease (manipulation).

The volcano plot in panel (A) shows the results of differential gene expression analysis for *Ocflo* sampled from within the host ant's head, at halfway through disease progression (infection), as compared to blastospores grown in liquid media outside the host. Panel (B) shows the intersections between four sets of *Ocflo* DEGs (manip_down/up represents genes down/up regulated in *Ocflo* at the manipulated biting stage as compared to controls, and inf_down/up represents genes down/up regulated in *Ocflo* at infection as compared to controls). Panel (C) shows the results from the pairwise Fisher's exact test we performed to check for significant overlap between the four sets of DEGs discussed in (B). In the next three panels, we show the overrepresented pfam domains we found in the set of genes (D) up regulated at both *Ocflo* infection and manipulation, as compared to controls, (E) down-regulated at both *Ocflo* infection and manipulation, as compared to controls, and (F) up or down-regulated at infection, but not differentially expressed at manipulation, as compared to controls. The bars and numbers of the enrichment plots have the same meaning as before. The text overlaid on top of the bars highlight some of the *Ocflo* genes that contributed to the respective pfam enrichments.

At the halfway mark in disease (referred to as "infection" from here on), we found that 318 genes were upregulated, and 395 genes were downregulated in *Ocflo* as compared to liquid culture controls (fold-change ≥ 2, q-value < 0.05) (Fig. 20A). In comparison, a previous study by Will and colleagues found that at the final stages of the disease ("manipulation"; infected ants biting into a substrate with locked jaws prior to death), 1867 genes were upregulated, and 1625

genes were downregulated in *Ocflo* versus time-matched controls (Fig. 20B; manipulation data obtained from REF). Around 60% (190) of genes upregulated at infection were also upregulated at manipulation, whereas 41% (161) of genes downregulated during infection also were downregulated at manipulation, and both the overlaps were significant (STATS? You give them everywhere else so also here!) (Fig. 20C). To try and understand the role of DEGs in mediating the characteristic hemibiotrophic life style of *Ocflo* as it grows inside the ant host, we decided to look at three biologically relevant subsets of these DEGs, (1) genes that are significantly up/down-regulated at infection as well as manipulation, and (2) genes that are up/down-regulated only at infection but not at manipulation, and (3) genes that are downregulated at infection but upregulated at manipulation.

The genes that showed a consistent up/down-regulation at both infection and manipulation are likely involved in general growth and survival of the fungus inside the host. For genes upregulated at both infection and manipulation, we found overrepresentation for fungal specific transcription factors including the clock gene *Casein kinase 2* (Fig 19D). *Ck2* seems to play a key role in temperature compensation of fungal [268]and plant [269] circadian clocks, which provides the ability of the biological oscillator to function normally under different temperatures. In flies, the catalytic subunit of CK2 is required for maintaining the near 24h periodicity of the circadian clock [155]. Given that CK2 plays an important role in mediating the response to ultraviolet light, it has been hypothesized that the conserved role for CK2 across plants, fungi, and animals is driven by the organism's need to avoid mutagenic ultraviolet light. It has previously been shown that several manipulating parasites, including *Ocflo*, seem to affect the host's response to light, usually turning the infected hosts to become light-seekers [37, 270]. Therefore, future studies exploring the role of CK2 as a candidate parasitic effector in

modulating the host's phototactic behavior will be important. In addition to transcription factors, the up-regulated genes throughout *Ocflo* infection were also overrepresented for cytochrome p450 genes (oxidoreductase activity), fungal transcriptional regulatory proteins involved in zinc-dependent binding of DNA (Zn_clus domain), and membrane proteins belonging to major facilitator superfamily (transmembrane transport activity). The latter, MFS family of membrane proteins, was also overrepresented in fungal genes down-regulated throughout the disease, both at infection and manipulation. These downregulated MFS membrane proteins contained several transporters of interest (e.g., an *MFS drug transporter* and a *Multidrug resistance protein*). In addition, the genes downregulated throughout disease also contained two putative *enterotoxins* and a copy of *protein tyrosine phosphatase*.

Next, we reasoned that the second set of 205 genes that are differentially expressed (118 upregulated and 87 downregulated) only at infection but not at manipulation might be important for maintaining parasite-host homeostasis, maybe via temporal synchronization of biological functions, to ensure that the infected ant host can survive the long incubation period necessary for *Ocflo* to complete its life cycle. These 205 genes differentially expressed only at infection were enriched for transmembrane transport activity and contained the *Aflatoxin efflux pump AFLT* (downregulated at infection) (Fig. 19F). This set of DEGs contained several other toxin-related genes: three enterotoxins (two *heat-labile enterotoxins* were upregulated, and a *putative enterotoxin* was downregulated), a *protoplast regeneration and killer toxin resistance protein* (downregulated), a *gliotoxin biosynthesis protein GliK* (upregulated). Gliotoxin, a known fungal virulence factor, has been implicated in assisting host tissue penetration [271]. We are compelled to speculate if a higher production of gliotoxin at the halfway mark in disease might be necessary for an efficient delivery of the fungal enterotoxins into the host tissues, especially in the brain.

Therefore, future research on the role of toxins in *Ocflo*-induced manipulation of ant behavior would benefit from including gliotoxin as a candidate fungal effector. In addition to the toxins, this subset of two hundred odd DEGs also contained the two core clock genes *Frequency* (upregulated) and *Vivid* (synonymous to *Envoy*; downregulated). In addition to be an important component of the fungal circadian clock, *Vivid* is known to be essential for sensing and adapting to light in the model fungi *Neurospora crassa* [272] [273]. Light regulates a plethora of different fungal processes, including phototropism, secondary metabolism, and pathogenicity (reviewed in [273]. It remains unclear to what degree the light seeking behavior of manipulated ant hosts is in fact an extended phenotype of the light-seeking fungal parasite growing within. But, given that we find differential expression of light-sensing components of the fungal clock (*Vivid* and *CK2*) at the halfway mark, it seems possible that the altered host response to light, at least at this disease stage, is regulated by components of the parasite's clock.

Finally, the third set of genes that are downregulated at the halfway mark but upregulated at manipulation likely contains fungal effectors that are necessary to induce successful manipulation of host behavior (death-grip), but harmful to the host otherwise. We did not find any enriched pfams or GO terms for these 43. Although not enriched for a specific biological process, these genes might be functioning as key regulatory components in the fungal gene expression network (e.g., highly connected nodes in the network). In the next section, we map the several genes of interest that we have identified so far on to the gene expression network of *Ocflo* and discuss how they undergo co-regulation in order to successfully grow inside the ant host for an extended period of time.

Changes to the gene expression network of Ocflo during infection

In this section, similar to Chapter two, we took a systems approach to (1) build a daily gene co-expression network (GCN) of *Ocflo* as observed in control (culture) conditions, (2) annotate the *Ocflo* GCN by identifying the location of differentially rhythmic genes, especially the ones that show evidence of differential rhythmicity between *Ocflo* and *Beauveria* (Clusters 3 and 4, Fig. 19), and (3) identify which modules of the *Ocflo* GCN show a drastic change in their expression (differential expression) at the halfway mark in its disease progression.

The construction and annotation of the gene co-expression network (GCN) of *Ocflo* was done as per the protocol detailed in de Bekker and Das (2022) (Additional File 17). We built the GCN of *Ocflo* using the 6874 genes that were expressed (≥1 FPKM) for at least half of all sampled time points in their blastospore stage grown in controlled liquid media (i.e., "controls"). We wanted to use the gene expression network of controls as the background to see what changes occur in the parasite's network during infection. These 6874 *Ocflo* genes were then clustered into 16 modules based on their degree of co-expression and named accordingly (OC1 to OC16). The global connectivity patterns of the *Ophiocordyceps* GCN are shown in Figure 20A, where nodes represent the modules or clusters of highly co-expressed genes (Kendall's tau-b correlation ≥ 0.7), and edges between modules indicate a similarity of module-module expression (Kendall's tau-b correlation of at least 0.6 between a module's eigengene expression with another).

To understand how the different genes-of-interest we have identified so far regulate each other, we annotated the *Ocflo* GCN by identifying where in the network our genes of interest are located. To annotate the *Ocflo* GCN, we identified the module(s) that showed a significant

overlap with *Ocflo* genes displaying (1) robust 24h-rhythms in *Ocflo* controls (rhy24h-*Ocflo*), (2) genes classified as significantly rhythmic in both *Ocflo* and *Okim* (rhy24-*Ocflo*-*Okim*), (3) two clusters of genes that showed differential rhythmicity between *Ocflo* and *Beauveria* (rhy24-*Ocflo*|Beau-cluster3 and rhy24-*Ocflo*|Beau-cluster4, Fig. 19), (4) genes that were significantly upregulated at infection as well as manipulation (*Ocflo*-inf-manip-UP), (5) genes that were significantly downregulated at infection as well as manipulation (*Ocflo*-inf-manip-DOWN), (6) genes that were differentially expressed only at infection but not at manipulation (*Ocflo*-DEGs-inf-only), and (7) genes that were downregulated at infection but upregulated at manipulation (*Ocflo*-inf-DOWN-manip-UP).

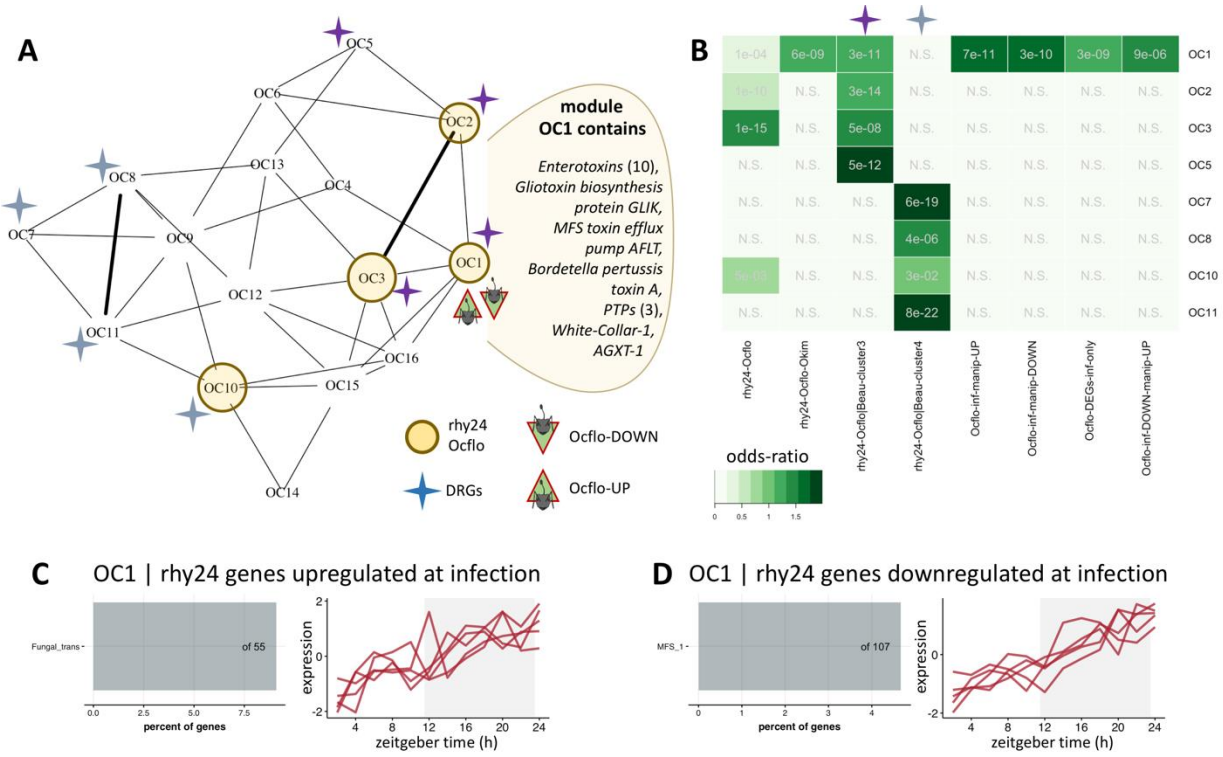

Figure 21 Annotated gene co-expression network of O. camponoti-floridani identifies a single cluster that potentially regulates the parasitic processes necessary to manipulate host behavior.

Panel (A) shows the annotated gene co-expression network (GCN) of the manipulating fungal parasite *Ocflo* as observed during growth in controlled liquid media outside the host. The annotations in the network shows the different modules of interest that we have identified as being putatively important for the interplay of fungal rhythmicity, disease-associated plasticity, and its ability to manipulate host behavior. The nodes represent modules of highly co-expressed genes that are clustered together, and the edges represent co-expression of connected modules. Thick edges indicate module-module correlations ≥ 0.8, thinner edges indicate correlations between 0.6 and 0.8, and no edges indicate correlations <0.6. The abbreviations have the following meaning: (i) rhy24-*Ocflo* indicate modules that show an overrepresentation for *Ocflo* genes that were classified as significantly rhythmic in controls, (ii) DRGs indicate the modules that show overrepresentation of orthologous genes, between *Ocflo* and *Beauveria*, that show differential rhythmicity between the two species (clusters 3 and 4, Fig. 19). The two colors of the DRG symbol indicate overrepresentation for different clusters of the differentially rhythmic genes between *Ocflo* and *Beauveria*, as indicated in panel (B), and (iii) *Ocflo*-DOWN/UP identifies the one module in *Ocflo* GCN that shows significant overrepresentation for several subsets of disease-associated differentially expressed genes in *Ocflo* as compared to controls. Panel (B) shows the results of the pairwise Fisher's exact test that was performed to identify the modules of interest in (A). Panel (C) shows the pfam domain overrepresented in the *Ocflo* genes belonging to module OC1 that were identified as rhythmic in control conditions but upregulated at halfway through infection (referred to as "infection"). Also shown alongside is the daily expression of these *Ocflo* genes in controls, as stacked zplots. In panel (D) we show the same information provided in (C) but for *Ocflo* genes in module OC1 that were classified as rhythmic in controls but show a downregulation at infection.

We found that most of the 24h oscillating genes in *Ocflo* controls were primarily located in four modules (OC1, OC2, OC3 and OC10; Fig. 21A-B). To validate these module annotations, we looked at the identity of the genes in these putatively rhythmic modules. As expected, we found that they contained known fungal clock components. Module OC1 contained the two core fungal clock genes *white collar 1* and *white collar 2* that form the positive arm of the transcription-translation feedback loop (TTFL). However, two of the other fungal core clock genes *frequency* and *vivid* that make up the negative arm of TTFL were located in module OC8, which did not show an overrepresentation for clock-controlled genes. Module OC8, however, showed an overrepresentation of genes identified as differentially rhythmic between *Ocflo* and *Beauveria* (rhy24-*Ocflo*|Beau-cluster-4; Fig. 21A-B). In addition to module OC8, the differentially rhythmic genes (DRGs) between the fungal species were also found to be overrepresented in six other modules, which included all of the four rhythmic modules (OC10,

OC1, OC2, and OC3). Taken together, this finding suggests that fungal genes that show the opposite pattern of daily expression in the two entomopathogens (e.g. day-peaking in *Ocflo* but night-peaking in *Beauveria*) are fairly well distributed throughout the gene expression network of *Ocflo*. Furthermore, the presence of these DRGs in all of the rhythmic modules of *Ocflo,* some of which contain putative core clock genes, likely highlights an inherent difference in how the two fungal clocks temporally segregate the various biological processes it regulates. Future studies that functionally test the role of some of these DRGs, especially the ones found in the rhythmic modules, might uncover some of the mechanistic links that exist between a parasite's clock-controlled rhythmicity and its disease outcomes.

Next, we mapped the different subsets of *Ocflo* genes that showed a disease-associated differential expression. All of the different subsets of DEGs – both upregulated and downregulated genes – mapped to only one module in the *Ocflo* GCN: module OC1. This finding suggests a difference in how the parasite's clock and disease-associated genes co-regulate, as compared the host. In the host ant's GCN, as observed in the head and in the brain, disease-associated host DEGs were consistently found in a non-rhythmic module, which was connected to the rhythmic module that contained the majority of the genes that undergo synchronized changes in their daily expression during *Ocflo* infections (see Chapter 2). Furthermore, this disease-associated DEG module of the host contained the majority of the behavioral plasticity genes (caste-associated DEGs). In summary, the data from Chapter two provided support for our hypothesis that *Ocflo* likely targets this inherent molecular link between ant behavioral plasticity and plasticity of its clock. The fact that we found that the disease-associated DEGs in *Ocflo* are located in the rhythmic module that contained the fungal core clock genes (*wc1* and *wc2*), shows that regulatory links between DEGs and clock-controlled

processes exist in both the manipulating parasite and its ant host. However, the finding also highlights a major difference in how the putative regulation works in the manipulating parasite, as compared to the host. First, the host ant genes that were up and down regulated during *Ocflo* infection cluster separately into distinct modules, and it appears that only the down-regulated module could induce changes to the rhythmic modules. Whereas in case of the parasite, genes differentially expressed in *Ocflo* during infection were all clustered in one module (OC1) which contained fungal core clock components and several clock-controlled genes. Although it is unclear what the function of having all of these parasitic genes of interest in one co-expressed rhythmic module might be, one could argue that the co-occurrence likely allows the parasite to rapidly adapt its clock-controlled processes in response to changes in its local environment (host's disease state). If this co-occurrence has an adaptive value for the parasite's ability to manipulate host behavior or not remains to be seen. However, we did find evidence suggesting that, at the very least, module OC1 plays a central role even in the final stages of *Ocflo* infection, during the manipulated biting. When we mapped all the *Ocflo* DEGs at manipulated biting (Will et al., 2020) on to our GCN, we found that the up-regulated genes again were overrepresented in module OC1, while the down-regulated genes were primarily located in module OC3 and OC1. As such, it appears that during the manipulated biting stage, the differentially expressed genes in *Ocflo* show a host-like modular separation; during manipulation, the fungal up and down regulated genes are no longer located in the same module. This hints at the possibility that the gene co-expression network of the *Ocflo* might undergo substantial rewiring during the ultimate manipulated biting stage, as compared to the halfway mark.

To summarize our findings from the network analyses, we have shown that a single cluster (module OC1) in the gene expression network of *Ocflo* contains not only genes that are

under clock control, but also genes that are differentially expressed in the parasite during disease, at the halfway mark as well as in the final stages during active manipulation. We wondered, therefore, if such a regulatory cluster might be a hallmark of behavior manipulating parasites, at least in the genus *Ophiocordyceps.* To begin to ask this question, we located the genes that were classified as rhythmic in both *Ocflo* and *Okim*. Again, the only module that showed overrepresentation for these conserved rhythmic genes was module OC1, which suggests that, at least the behavior manipulating fungi of the genus *Ophiocordyceps* might have a regulatory cluster that connects daily rhythms with infection and manipulation. Since OC1 is seemingly important to the infection biology of the hemibiotroph *Ophiocordyceps*, we further investigated the function of some putative fungal effectors that might be mediating the cross-talk between disease-associated differential expression and changes to clock-controlled rhythms. Of the 1144 genes in module OC1, 42 showed daily rhythms in *Ocflo* controls, and an upregulation during infection (halfway mark in disease). These 42 genes were overrepresented for fungal-specific transcription factors, including the nitrogen assimilation transcription factor *nirA* which functions as a regulator of nitrate assimilation in fungi [274] (Fig. 21C). In the dinoflagellate *Lingulodinium polyeadra*, extracellular nitrate has been shown to act as a light-independent zeitgeber, and in turn the clock regulates nitrate metabolism via control of nitrate reductase concentrations [275, 276] (REFS). Such clock-controlled nitrate metabolism has also been found in green algae, whereas in plants nitrate transport seem to be under clock control (reviewed in [277]). More relevant to our findings, rhythmic nitrate metabolism has been observed in a *frq*-less *Neurospora* in which the transcription-translation feedback loop (TTFL) was dysfunctional, suggesting that rhythms in nitrate metabolism are not dependent on the fungal TTFL. Given that we observed a significant differential expression of the clock components *frq* (upregulated) and

vvd (downregulated) during infection, but not for either of the *white-collar* genes, it is possible that the *Ocflo* might be employing non-TTFL means to maintain rhythmic gene expression while inside its host, at least at the halfway mark in disease. In comparison to upregulation of several rhythmic transcription factors during infection, *Ocflo* seems to be simultaneously downregulating several rhythmic membrane transporters of the Major Facilitator Superfamily (MFS_1 domain). This functional enrichment encompassed several genes that we have already discussed previously including a *multidrug resistance protein* (GQ602_006511) and an *MFS drug transporter* (GQ602_004931). In addition to having highlighted a few candidate genes that show functional enrichments in the identified module of interest, OC1, we included the full results of our network analyses as a supplementary file (Additional file 19).

GENERAL DISCUSSION

Parasites that have evolved the ability to manipulate host behavior have fascinated humans for a long time. This dissertation explores one such parasite-host system: the fungal parasite *Ophiocordyceps camponoti-floridani* that manipulates the behavior of its carpenter ant host *Camponotus floridanus*. More specifically, using this parasite-host system as a model, we wanted to understand to what degree do the biological clocks of the host and the parasite play a role in driving this disease outcome. We started our investigation with the apriori hypothesis that *O. camponoti-floridani* most likely targets the internal timekeeping machinery – the clock – of the infected ant to induce the observed time-of-day specific changes in host behavior. In order to test this hypothesis, we first needed to demonstrate that there exists a certain degree of plasticity in the host's clock that is corruptible, and that the plasticity of the clock is linked to its behavior.

Using time-course transcriptomics, the first chapter of the dissertation provides a first look at the clock-controlled pathways in the ant host, *C. floridanus*, that regulates their caste-associated behavioral plasticity. We found a reduced number of 24h oscillating genes in nurses as compared to foragers, consistent with the results of a previous microarray study done in honeybees. This indicates that a difference in 24h-rhythmic gene repertoire between foragers and nurses could be a more general phenomenon within eusocial Hymenoptera. Moreover, many genes that oscillated every 24h in forager brains were expressed in an ultradian manner in nurses – every 8h – instead of being entirely arrhythmic. Among these caste-associated differentially rhythmic genes (DRGs) were essential components of the core and auxiliary feedback loops that form the endogenous clock of insects, as well as genes involved in metabolism, cellular communication and protein modification. This ability of core clock and clock-controlled genes in

ants to oscillate at different harmonics of the circadian rhythm shows an inherent plasticity of the host that could be targeted by its manipulating parasite.

In the second chapter, we tested if the manipulating parasite *O. camponoti-floridani* can induce such synchronized changes to the rhythmic genes of its host *C. floridanus.* Additionally, we also wanted to know if such changes to the host's clock-controlled rhythms are a general hallmark of infectious diseases, or if this is specific to parasites that have evolved to manipulate ant behavior. To answer this, we compared the changes that occur to the daily transcriptome of *C. floridanus* while infected with the manipulating parasite *O. camponoti-floridani* versus a generalist, non-manipulating fungi *Beauveria bassiana*. Using time-course transcriptomics and comparative network analyses, we found that synchronized changes to the host's daily gene expression are a general hallmark of infectious disease as both fungal parasites induced differential rhythmicity in the same set of rhythmic host genes. Furthermore, we found that the disease-associated DRGs significantly overlapped with the caste-associated DRGs that we identified in chapter one, suggesting that both parasites likely affect the behavioral state of the infected ant. However, the pattern of the synchronized changes to the host rhythms during disease showed parasite-specific differences. Although disease-associated DRGs in the host showed synchronized changes during both infections, ants infected by the manipulating parasite maintained the phase of these DRGs similar to uninfected controls. In comparison, *Beauveria*-infected ants did not show any clear peaks of daily expression for these DRGs. It appears this difference has a regulatory basis. The results of the network analyses demonstrate that the host genes that are upregulated during infection by the manipulating parasite reside in a module that is connected to the disease-associated DRGs. The same module that contains the upregulated host genes during *Ocflo* infection, is downregulated during *Beauveria* infections. This suggests

that the DEG module might be functioning as a regulatory switch which is activated (upregulated) by the manipulating parasite and deactivated (downregulated) by the non-manipulating one. Taken together, it appears that although the inherent plasticity of the host clock (caste-associated DRGs) are targeted by the manipulating parasite, it does so to maintain the phase of these rhythmic genes.

In the third, and final, chapter of this dissertation, we focused on the characterizing the timekeeping machinery of the manipulating parasite and how it might differ from that of a non-manipulating generalist. We did so to identify potential regulatory mechanisms via which the clock of the manipulating fungi might be inducing the changes to the host clock that we observed in chapter two. We found that similar to their host's gene expression network, there seems to be potential cross-talk between *Ocflo* genes that are differentially expressed during infection and the genes that are under clock control. However, a primary difference exists between the host and the parasite. In the gene expression network of the manipulating fungi, the genes that are upregulated at both the halfway mark in disease as well as at the manipulated biting stage are both located in one primary module, one that shows a significant overrepresentation for rhythmic genes including fungal core clock components and fungal-specific transcription factors. Assuming that the *Ocflo* genes differentially expressed during infection or manipulation play a role in its ability to manipulate ant behavior, we can conclude that the clock of *Ocflo* seems to be tightly linked to this ability since genes co-localized in a module are highly co-expressed.

This dissertation, at the least, has provided some validation to the hypothesis we started off with, that *O. camponoti-floridani* targets the internal timekeeping machinery of the infected ant in order to induce timely changes in its host ant's behavior. Furthermore, this dissertation puts forward several hypotheses for the regulatory mechanisms via which the parasite clocks

might be inducing changes to the host's clock or clock output, including clock-controlled behavior. Functionally testing the role of even a single gene of interest is a challenging task and requires considerable amount of time and resources for non-model systems such as *Ophiocordyceps*. The consistent regulatory patterns and genes of interest that we have identified throughout the dissertation can serve as a data-driven repository of candidate fungal effectors and host ant targets that are involved in the manipulation of host behavior, at least for *Ophiocordyceps*-ant systems.

APPENDIX A:
COPYRIGHT PERMISSION LETTER FOR CHAPTER ONE

The findings of the study presented in CHAPTER ONE, authored by Biplabendu Das and Charissa de Bekker, have already been published in a peer-reviewed journal under a Creative Commons Attribution 4.0 International license. The details of the publication are provided below, along with a copy of the Creative Commons license for the article.

Das, Biplabendu, *de Bekker, Charissa* Time-course RNASeq of *Camponotus floridanus* forager and nurse ant brains indicate links between plasticity in the biological clock and behavioral division of labor. *BMC Genomics* **23,** 57 (2022).

2/25/22, 6:49 PM Rightslink® by Copyright Clearance Center

CCC RightsLink®

? Help | Email Support

SPRINGER NATURE

Time-course RNASeq of Camponotus floridanus forager and nurse ant brains indicate links between plasticity in the biological clock and behavioral division of labor

Author: Biplabendu Das et al
Publication: BMC Genomics
Publisher: Springer Nature
Date: Jan 15, 2022

Copyright © 2022, The Author(s)

Creative Commons

This is an open access article distributed under the terms of the Creative Commons CC BY license, which permits unrestricted use, distribution, and reproduction in any medium, provided the original work is properly cited.

You are not required to obtain permission to reuse this article.
CC0 applies for supplementary material related to this article and attribution is not required.

APPENDIX B:
ADDITIONAL FILES FOR CHAPTER ONE

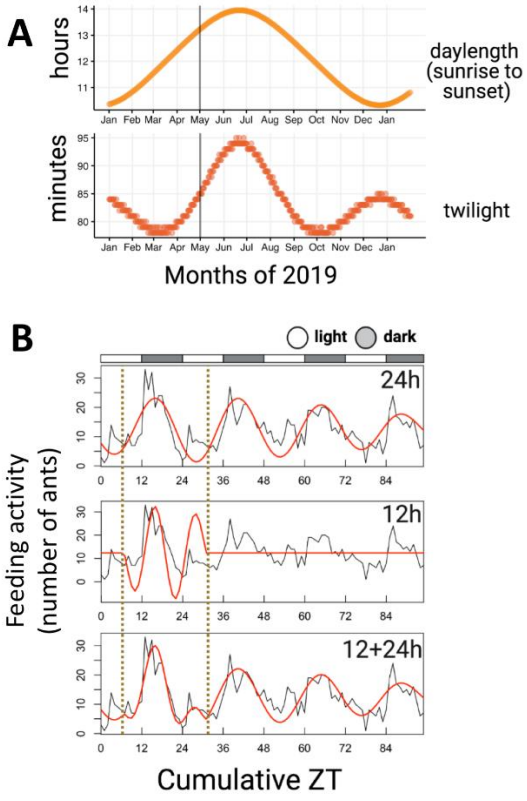

Additional File 1: Ultradian rhythms in colony behavior.

(**A)** The length of day (daylength in hours, top) and dusk (twilight in minutes, bottom) in Orlando, for every single day in 2019, is shown. Data was obtained from www.timeanddate.com. The vertical grey line indicates the time-of-year (May 2019) during which the *C. floridanus* colony was collected and all experiments were performed. (**B)** Recreated activity profiles of feeding bouts (shown in red lines) using decomposed 24h, 12h, and both (12h+24h) waveforms plotted on top of the observed activity data (black lines). The vertical dashed lines indicate the time period during which the 12h rhythms were found to be significant. The x-axis shows the Cumulative ZT (in hours) since mark-and-recapture. The y-axis indicates colony feeding activity as the number of ants present on the feeding stage at a given time point. The 12h:12h light-dark cycles are indicated in white (lights on) and grey (lights off) at the top. (PNG, 466 KB)

Additional File 2: General patterns of gene expression in forager and nurse ants.

The excel file contains four worksheets. (**Sheet 1**) The excel worksheet contains list of genes that displayed "no expression" (FPKM = 0) and "low expression" (0 < FPKM < 1) in the brains of *C. floridanus* foragers and nurses. In addition to the gene symbols (column: gene_name), the blast annotation (column: blast_annotation) and expression data for foragers (column: X2F to X24F) and nurses (column: X2N to X24N) are also provided. (**Sheet 2**) Results of GO enrichment analyses for genes that show "no expression" and "low expression". (**Sheet 3**) List of genes that are expressed only in forager brains or nurse brains. (**Sheet 4**) Results of GO enrichment analyses for genes expressed only in forager brains or nurse brains. (XLS, 1.7 MB)
Link to file: https://doi.org/10.1186/s12864-021-08282-x

Additional File 3: Diurnal gene expression in forager and nurse brains.

The excel file contains five worksheets. (**Sheet 1**) eTJK output for all tested genes in forager brains, including their gene number and normalized expression levels for each time point, sorted based on significance. (**Sheet 2**) eTJK output for all tested genes in nurse brains, including their gene number and normalized expression levels for each time point, sorted based on significance. (**Sheet 3**) List of genes that show significant 24h rhythms in forager brains, their cluster identity (corresponding to Fig. 3B), and normalized gene expression for all forager samples. (**Sheet 4**) List of genes that show significant 24h rhythms in nurse brains, their cluster identity (corresponding to Fig. 3C), and normalized gene expression for all nurse samples. (**Sheet 5**) GO enrichment results for diurnal genes in foragers (for-24h) and nurses (nur-24h) that peak during the day (day-peaking clusters) and night (night-peaking clusters). Also includes the enrichment results for day-peaking cluster of overlapping for-24h and nur-24h genes (for-24h-nur-24h). (XLS, 12.6 MB)
Link to file: https://doi.org/10.1186/s12864-021-08282-x

Additional File 4: Core clock and clock-controlled genes in C. floridanus.

The excel worksheet contains the list of fly- and mammalian-like core clock genes and clock-controlled genes identified in *C. floridanus*, along with the hmmersearch results. (XLS, 39 KB)
Link to file: https://doi.org/10.1186/s12864-021-08282-x

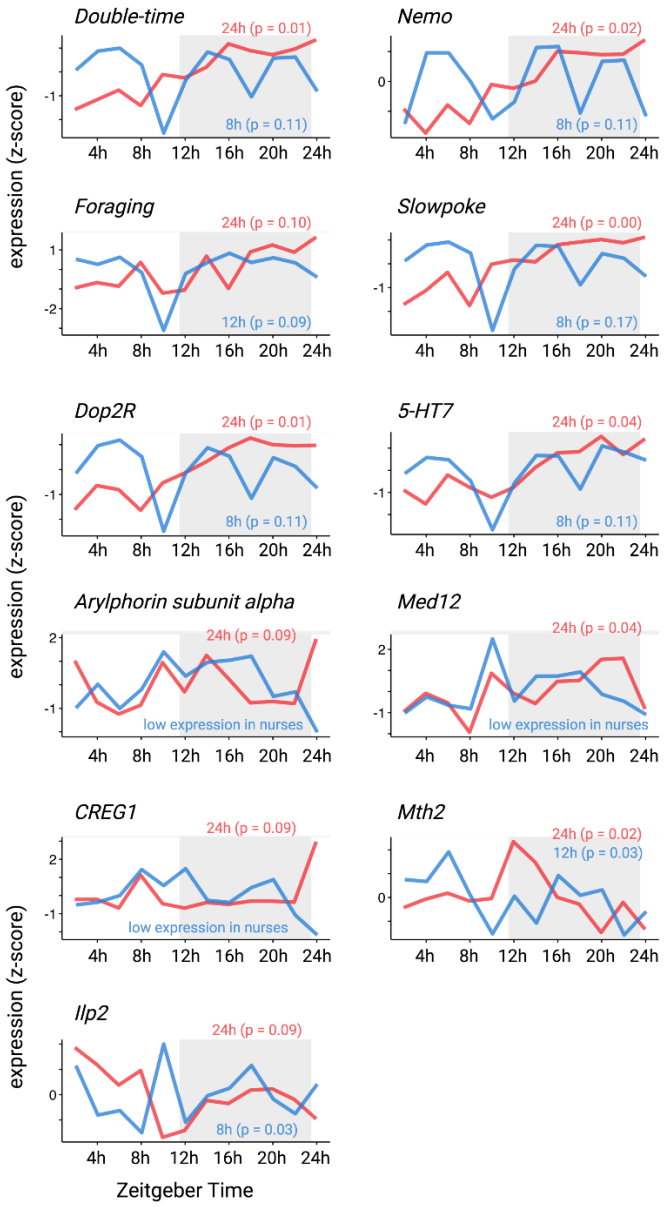

Additional File 5: Daily expression patterns of genes of interest.

The figure shows the expression patterns of several genes with a rhythmic trend that are discussed in the text. The forager expression is shown in red and nurse expression in blue. For each gene, the periodicity of rhythmic expression tested in forager and nurse brains are shown along with p-values obtained from eJTK (in parenthesis). The y-axis shows gene expression (z-score) and the x-axis shows the Zeitgeber Time (in hours). Dark phase of the 12h:12h light-dark cycle is represented in grey (dark phase begins at ZT12). (PNG, 1.1 MB)

Additional File 6: Ultradian gene expression in forager and nurse brains.

The excel file contains four worksheets. (**Sheet 1**) Results of eTJK testing for significant 12h periodicity in forager brain gene expression. (**Sheet 2**) Results of eTJK testing for significant 12h periodicity in nurse brain gene expression. (**Sheet 3**) Results of eTJK testing for significant 8h periodicity in forager brain gene expression. (**Sheet 4**) Results of eTJK testing for significant 8h periodicity in nurse brain gene expression. (XLS, 14.1 MB)
Link to file: https://doi.org/10.1186/s12864-021-08282-x

Additional File 7: Differentially rhythmic genes.

The excel file contains two worksheets. (**Sheet 1**) List of genes that cycle every 24h in forager brains but every 8h in nurses (for-24h-nur-8h). In addition to gene symbol, gene annotations and normalized expression, the cluster identity of each gene upon hierarchical clustering is provided. (**Sheet 2**) GO enrichment results for "for-24h-nur-8h" genes belonging to cluster 1 that also contains the *Per* gene. (XLS, 251 KB)
Link to file: https://doi.org/10.1186/s12864-021-08282-x

Additional File 8: Genes differently expressed between forager and nurse brains.

The excel file contains three worksheets. (**Sheet 1**) LimoRhyde results for all genes tested for differential gene expression. (**Sheet 2**) GO enrichment results for genes significantly higher expressed in nurse brains as compared to forager brains. (XLS, 1.9 MB)
Link to file: https://doi.org/10.1186/s12864-021-08282-x

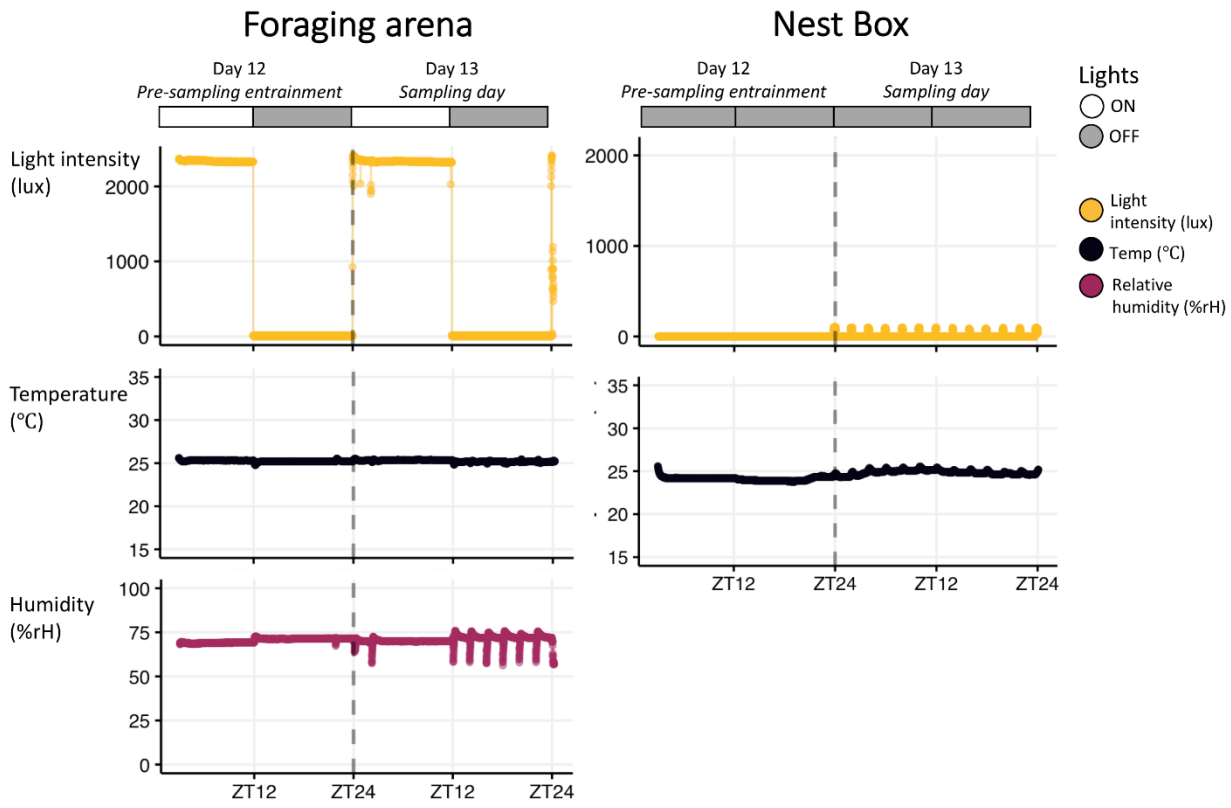

Additional File 9: Abiotic conditions in the experimental foraging arena and the nest box.

The figure shows the data for light intensity, temperature and humidity in the foraging arena and the nest box of the experimental setup, collected using HOBO data loggers. Data is shown for Day 12 and Day 13 of the experiment. (PNG, 600 KB)

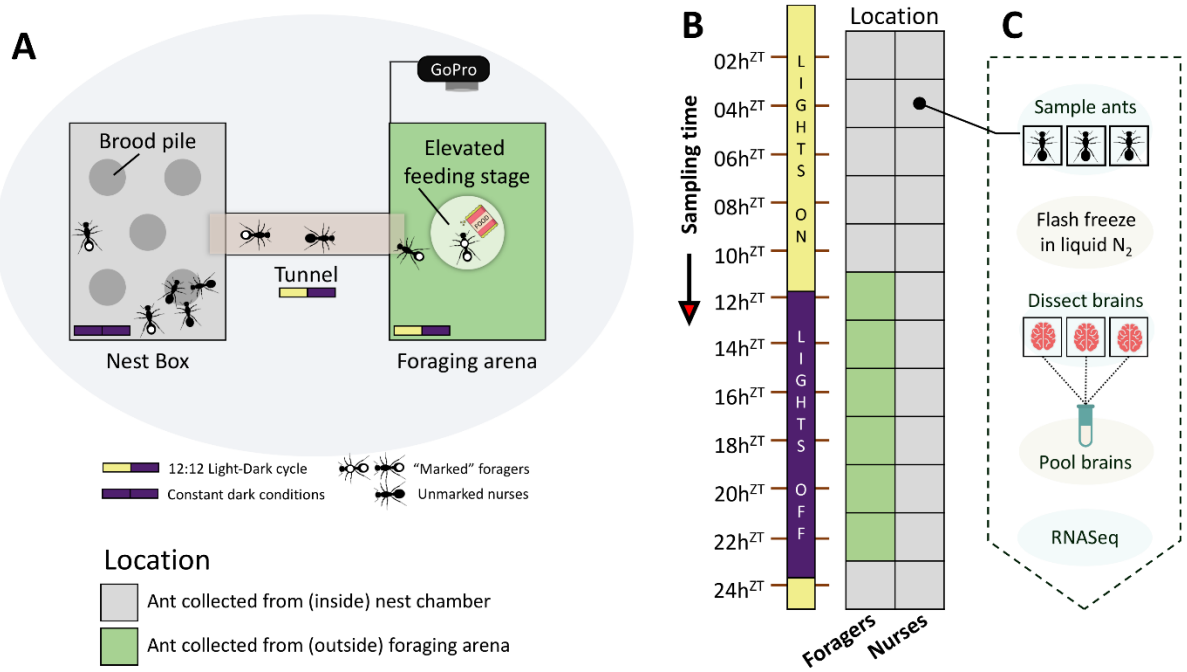

Additional File 10: Ant colony setup and experimental design.

(**A**) The figure shows the ant colony setup used for the experiment. The scheme for sampling ants from the colony is shown in (**B**) and several of the key steps from sampling to RNASeq are shown in (**C**). (PNG, 777 KB)

Additional File 11: Colony foraging and feeding activity data.

The excel worksheet contains the number of ants observed on the feeding stage (FS = feeding activity) and involved in general foraging activity (FA = foraging activity). Total activity (Total) was defined as the sum of feeding and foraging. Experimental phases: Initial entrainment (Entrain-I), Mark-and-recapture (Painting), Pre-sampling entrainment (Entrain-II), Sampling, and Post-sampling entrainment (Entrain-III). (CSV, 45 KB)
Link to file: https://doi.org/10.1186/s12864-021-08282-x

Additional File 12: Results of differential rhythmicity (in phase or amplitude) analysis.

The file contains the output from the LimoRhyde analysis to identify genes that show significantly different phase or amplitude. A 5% FDR (adj.P.Val < 0.05) was used to infer significance. (CSV, 86 KB)
Link to file: https://doi.org/10.1186/s12864-021-08282-x

APPENDIX C:
ADDITIONAL FILES FOR CHAPTER TWO

Additional File 13: Mortality data.

The zipped folder contains two files, each containing the mortality data for ants infected with *Beauveria* (BB62_surv_data) and *Ocflo* (Arb2_surv_data), and their corresponding control groups. *Link to file:* Can be provided upon request.

Additional File 14: Environmental data for the entrainment conditions in the foraging arena.

The zipped folder contains four files, two containing the climatic conditions of the foraging arena for ants infected with *Beauveria* (Billu_TC7_BB62_Incubator_FA.csv) and *Ocflo* (Billu_TC7_Ophio_right_incubator_28Apr21_1551hrs.csv), and the other two for the controls run in parallel to the infections (Billu_TC7_BB62_Controls_Incubator_FA.csv and Billu_TC7_Ophio_control_incubator_22Apr21_1411hrs.csv). *Link to file:* Can be provided upon request.

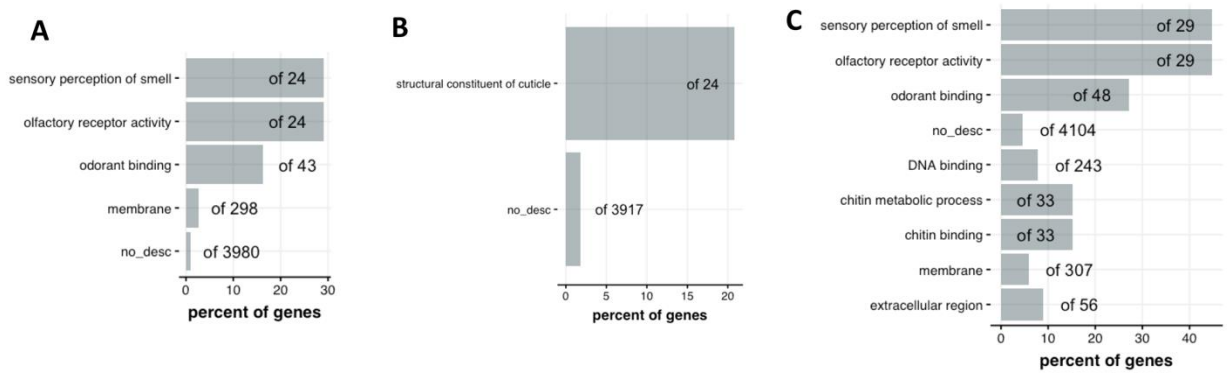

Additional File 15: Enriched GO terms for genes not expressed in ant heads.

The enrichment plots have the same meaning as the figures presented in the main text. Enriched GO terms shown for (A) genes not expressed in uninfected control heads, (B) genes expressed in *Beau*-infected ants but not in uninfected controls, and (C) genes expressed in *Ocflo*-infected ants but not in controls. *Link to file:* Can be provided upon request.

Additional File 16: Rhythmic genes in ant heads.

This excel file contains three sheets, each one contains the list of *C. floridanus* genes that were classified as significantly 24h-rhythmic in the heads of (sheet 1) uninfected controls, (sheet 2) ophio-infected foragers, and (sheet 3) beau-infected foragers. The functional annotations for the genes, including results of the functional enrichment analyses are also provided. *Link to file:* Can be provided upon request.

Additional File 17: Protocol for constructing and annotating gene co-expression networks from timecourse RNASeq data.

Link to file:
https://github.com/biplabendu/deBekker_and_Das_2021/blob/master/manuscript/pim12909-sup-0001-supinfo.pdf

Additional File 18: Results of the network analyses

The csv file contains the results from the network analysis and includes the list of all ant genes used to build the gene co-expression network, their module identity, functional annotations, and all relevant information that is necessary to follow the main text.
Link to file:
https://github.com/biplabendu/Das_et_al_2022a/blob/master/manuscript/99_dissertation/07_Cflo_forager_head_GCN_results.csv

APPENDIX D:
ADDITIONAL FILES FOR CHAPTER THREE

Additional File 19: Results of the network analyses.

The csv file contains the results from the network analysis and includes the list of all ant genes used to build the gene co-expression network, their module identity, functional annotations, and all relevant information that is necessary to follow the main text.
Link to file:
https://github.com/biplabendu/Das_et_al_2022a/blob/master/manuscript/99_dissertation/07_*Ocflo*_GCN_results.csv

LIST OF REFERENCES

1. Paranjpe DA, Sharma VK: **Evolution of temporal order in living organisms.** *J Circadian Rhythms* 2005, **3:**7.
2. Yerushalmi S, Green RM: **Evidence for the adaptive significance of circadian rhythms.** *Ecol Lett* 2009, **12:**970-981.
3. Hurley JM, Loros JJ, Dunlap JC: **Circadian oscillators: around the transcription-translation feedback loop and on to output.** *Trends Biochem Sci* 2016, **41:**834-846.
4. Stafford KM, Moore SE, Fox CG: **Diel variation in blue whale calls recorded in the eastern tropical Pacific.** *Animal Behaviour* 2005, **69:**951-958.
5. Andreani TS, Itoh TQ, Yildirim E, Hwangbo DS, Allada R: **Genetics of circadian rhythms.** *Sleep Med Clin* 2015, **10:**413-421.
6. Hardin PE: **The circadian timekeeping system of Drosophila.** *Curr Biol* 2005, **15:**R714-722.
7. Dunlap JC: **Molecular bases for circadian clocks.** *Cell* 1999, **96:**271-290.
8. Glossop NR, Hardin PE: **Central and peripheral circadian oscillator mechanisms in flies and mammals.** *Journal of Cell Science* 2002, **115:**3369-3377.
9. Stanewsky R: **Genetic analysis of the circadian system in Drosophila melanogaster and mammals.** *Journal of neurobiology* 2003, **54:**111-147.
10. Dunlap JC, Loros JJ: **How fungi keep time: circadian system in Neurospora and other fungi.** *Current opinion in microbiology* 2006, **9:**579-587.

11. Zordan MA, Rosato E, Piccin A, Foster R: **Photic entrainment of the circadian clock: from Drosophila to mammals.** In *Seminars in cell & developmental biology*. Elsevier; 2001: 317-328.

12. Yamazaki S, Numano R, Abe M, Hida A, Takahashi R-i, Ueda M, Block GD, Sakaki Y, Menaker M, Tei H: **Resetting Central and Peripheral Circadian Oscillators in Transgenic Rats.** *Science* 2000, **288:**682.

13. Bennett MM, Rinehart JP, Yocum GD, Doetkott C, Greenlee KJ: **Cues for cavity nesters: investigating relevant zeitgebers for emerging leafcutting bees, Megachile rotundata.** *Journal of Experimental Biology* 2018, **221**.

14. Fuchikawa T, Eban-Rothschild A, Nagari M, Shemesh Y, Bloch G: **Potent social synchronization can override photic entrainment of circadian rhythms.** *Nature communications* 2016, **7:**1-10.

15. Siehler O, Bloch G: **Colony Volatiles and Substrate-borne Vibrations Entrain Circadian Rhythms and Are Potential Cues Mediating Social Synchronization in Honey Bee Colonies.** *Journal of Biological Rhythms* 2020, **35:**246-256.

16. Fischer D, Lombardi DA, Marucci-Wellman H, Roenneberg T: **Chronotypes in the US–influence of age and sex.** *PloS one* 2017, **12:**e0178782.

17. Horne JA, Östberg O: **A self-assessment questionnaire to determine morningness-eveningness in human circadian rhythms.** *International Journal of Chronobiology* 1976, **4:**97-110.

18. Roenneberg T, Wirz-Justice A, Merrow M: **Life between Clocks: Daily Temporal Patterns of Human Chronotypes.** *Journal of Biological Rhythms* 2003, **18:**80-90.

19. Nikhil KL, Ratna K, Sharma VK: **Life-history traits of Drosophila melanogaster populations exhibiting early and late eclosion chronotypes.** *BMC Evolutionary Biology* 2016, **16:**46.

20. Fujioka H, Abe MS, Fuchikawa T, Tsuji K, Shimada M, Okada Y: **Ant circadian activity associated with brood care type.** *Biology letters* 2017, **13:**20160743.

21. Mildner S, Roces F: **Plasticity of daily behavioral rhythms in foragers and nurses of the ant *Camponotus* rufipes: influence of social context and feeding times.** *PloS one* 2017, **12:**e0169244.

22. Moore D, Rankin MA: **Circadian locomotor rhythms in individual honeybees.** *Physiological Entomology* 1985, **10:**191-197.

23. Moore D, Angel JE, Cheeseman IM, Fahrbach SE, Robinson GE: **Timekeeping in the honey bee colony: integration of circadian rhythms and division of labor.** *Behavioral Ecology and Sociobiology* 1998, **43:**147-160.

24. Rijo-Ferreira F, Carvalho T, Afonso C, Sanches-Vaz M, Costa RM, Figueiredo LM, Takahashi JS: **Sleeping sickness is a circadian disorder.** *Nature communications* 2018, **9:**1-13.

25. Westwood ML, O'Donnell AJ, de Bekker C, Lively CM, Zuk M, Reece SE: **The evolutionary ecology of circadian rhythms in infection.** *Nat Ecol Evol* 2019, **3:**552-560.

26. de Bekker C, Merrow M, Hughes DP: **From behavior to mechanisms: an integrative approach to the manipulation by a parasitic fungus (*Ophiocordyceps* unilateralis s.l.) of its host ants (*Camponotus* spp.).** *Integr Comp Biol* 2014, **54:**166-176.

27. Scheiermann C, Kunisaki Y, Frenette PS: **Circadian control of the immune system.** *Nature Reviews Immunology* 2013, **13:**190-198.

28. Carvalho Cabral P, Olivier M, Cermakian N: **The Complex Interplay of Parasites, Their Hosts, and Circadian Clocks.** *Front Cell Infect Microbiol* 2019, **9:**425.

29. Rijo-Ferreira F, Acosta-Rodriguez VA, Abel JH, Kornblum I, Bento I, Kilaru G, Klerman EB, Mota MM, Takahashi JS: **The malaria parasite has an intrinsic clock.** *Science* 2020, **368:**746-753.

30. de Bekker C, Will I, Hughes DP, Brachmann A, Merrow M: **Daily rhythms and enrichment patterns in the transcriptome of the behavior-manipulating parasite *Ophiocordyceps* kimflemingiae.** *PLoS One* 2017, **12:**e0187170.

31. Prior KF, O'Donnell AJ, Rund SSC, Savill NJ, van der Veen DR, Reece SE: **Host circadian rhythms are disrupted during malaria infection in parasite genotype-specific manners.** *Scientific Reports* 2019, **9:**10905.

32. Adamo SA, Webster JP: **Neural parasitology: how parasites manipulate host behaviour.** *J Exp Biol* 2013, **216:**1-2.

33. Adamo SA: **Turning your victim into a collaborator: exploitation of insect behavioral control systems by parasitic manipulators.** *Curr Opin Insect Sci* 2019, **33:**25-29.

34. Will I, Das B, Trinh T, Brachmann A, Ohm RA, de Bekker C: **Genetic Underpinnings of Host Manipulation by *Ophiocordyceps* as Revealed by Comparative Transcriptomics.** *G3: Genes|Genomes|Genetics* 2020**:**g3.401290.402020.

35. de Bekker C, Ohm RA, Loreto RG, Sebastian A, Albert I, Merrow M, Brachmann A, Hughes DP: **Gene expression during zombie ant biting behavior reflects the**

complexity underlying fungal parasitic behavioral manipulation. *BMC Genomics* 2015, **16:**620.

36. Hughes DP, Andersen SB, Hywel-Jones NL, Himaman W, Billen J, Boomsma JJ: **Behavioral mechanisms and morphological symptoms of zombie ants dying from fungal infection.** *BMC ecology* 2011, **11:**13.

37. Andriolli FS, Ishikawa NK, Vargas-Isla R, Cabral TS, de Bekker C, Baccaro FB: **Do zombie ant fungi turn their hosts into light seekers?** *Behavioral Ecology* 2019, **30:**609-616.

38. Loreto RG, Elliot SL, Freitas ML, Pereira TM, Hughes DP: **Long-term disease dynamics for a specialized parasite of ant societies: a field study.** *PloS one* 2014, **9:**e103516.

39. Andersen SB, Gerritsma S, Yusah KM, Mayntz D, Hywel-Jones NL, Billen J, Boomsma JJ, Hughes DP: **The life of a dead ant: the expression of an adaptive extended phenotype.** *The American Naturalist* 2009, **174:**424-433.

40. de Bekker C: ***Ophiocordyceps*-ant interactions as an integrative model to understand the molecular basis of parasitic behavioral manipulation.** *Curr Opin Insect Sci* 2019, **33:**19-24.

41. Kamita SG, Nagasaka K, Chua JW, Shimada T, Mita K, Kobayashi M, Maeda S, Hammock BD: **A baculovirus-encoded protein tyrosine phosphatase gene induces enhanced locomotory activity in a lepidopteran host.** *Proceedings of the National Academy of Sciences of the United States of America* 2005, **102:**2584-2589.

42. Hevia MA, Canessa P, Müller-Esparza H, Larrondo LF: **A circadian oscillator in the fungus Botrytis cinerea regulates virulence when infecting Arabidopsis thaliana.** *Proceedings of the National Academy of Sciences* 2015, **112:**8744-8749.

43. Veloso J, van Kan JA: **Many shades of grey in Botrytis–host plant interactions.** *Trends in plant science* 2018, **23:**613-622.

44. van Houte S, van Oers MM, Han Y, Vlak JM, Ros VID: **Baculovirus infection triggers a positive phototactic response in caterpillars to induce 'tree-top' disease.** *Biology Letters* 2014, **10**.

45. Bhattarai UR, Li F, Katuwal Bhattarai M, Masoudi A, Wang D: **Phototransduction and circadian entrainment are the key pathways in the signaling mechanism for the baculovirus induced tree-top disease in the lepidopteran larvae.** *Sci Rep* 2018, **8:**17528.

46. Trinh T: **Getting Lost: The Fungal Hijacking Of Ant Foraging Behavior In Space And Time.** University of Central Florida, Department of Biology; 2020.

47. Tong S-M, Zhang A-X, Guo C-T, Ying S-H, Feng M-G: **Daylight length-dependent translocation of VIVID photoreceptor in cells and its essential role in conidiation and virulence of *Beauveria* bassiana.** *Environmental Microbiology* 2018, **20:**169-185.

48. Ortiz-Urquiza A, Keyhani N: **Molecular genetics of *Beauveria* bassiana infection of insects.** In *Advances in genetics. Volume* 94: Elsevier; 2016: 165-249

49. Sharma VK: **Adaptive significance of circadian clocks.** *Chronobiology International* 2003, **20:**901-919.

50. Bell-Pedersen D, Cassone VM, Earnest DJ, Golden SS, Hardin PE, Thomas TL, Zoran MJ: **Circadian rhythms from multiple oscillators: lessons from diverse organisms.** *Nature Reviews Genetics* 2005, **6:**544-556.

51. Johnson CH, Stewart PL, Egli M: **The cyanobacterial circadian system: from biophysics to bioevolution.** *Annual review of biophysics* 2011, **40:**143-167.

52. Rund SSC, O'Donnell AJ, Gentile JE, Reece SE: **Daily rhythms in mosquitoes and their consequences for malaria transmission.** *Insects* 2016, **7**.

53. Helfrich-Förster C: **The *Drosophila* clock system.** In *Biological timekeeping: Clocks, rhythms and behaviour.* Springer; 2017: 133-176

54. Häfker NS, Meyer B, Last KS, Pond DW, Hüppe L, Teschke M: **Circadian clock involvement in zooplankton diel vertical migration.** *Current Biology* 2017, **27:**2194-2201.e2193.

55. Eelderink-Chen Z, Bosman J, Sartor F, Dodd AN, Kovács ÁT, Merrow M: **A circadian clock in a nonphotosynthetic prokaryote.** *Science Advances* 2021, **7:**eabe2086.

56. McCluskey ES: **Circadian rhythms in male ants of five diverse species.** *Science* 1965, **150:**1037-1039.

57. Roces F, Núñez JA: **Brood translocation and circadian variation of temperature preference in the ant *Camponotus mus*.** *Oecologia* 1989, **81:**33-37.

58. Falibene A, Roces F, Rössler W, Groh C: **Daily thermal fluctuations experienced by pupae via rhythmic nursing behavior increase numbers of mushroom body microglomeruli in the adult ant brain.** *Frontiers in behavioral neuroscience* 2016, **10:**73.

59. Sharma VK, Lone SR, Goel A, Chandrashekaran M: **Circadian consequences of social organization in the ant species *Camponotus compressus*.** *Naturwissenschaften* 2004, **91:**386-390.

60. Ingram KK, Kutowoi A, Wurm Y, Shoemaker D, Meier R, Bloch G: **The molecular clockwork of the fire ant *Solenopsis invicta*.** *PLoS One* 2012, **7:**e45715.

61. Bloch G: **The social clock of the honeybee.** *J Biol Rhythms* 2010, **25:**307-317.

62. Rodriguez-Zas SL, Southey BR, Shemesh Y, Rubin EB, Cohen M, Robinson GE, Bloch G: **Microarray analysis of natural socially regulated plasticity in circadian rhythms of honey bees.** *J Biol Rhythms* 2012, **27:**12-24.

63. Levine JD, Funes P, Dowse HB, Hall JC: **Resetting the circadian clock by social experience in *Drosophila melanogaster*.** *Science* 2002, **298:**2010-2012.

64. Rensing L, Ruoff P: **Temperature effect on entrainment, phase shifting, and amplitude of circadian clocks and its molecular bases.** *Chronobiology International* 2002, **19:**807-864.

65. Helfrich-Förster C: **Light input pathways to the circadian clock of insects with an emphasis on the fruit fly *Drosophila melanogaster*.** *Journal of Comparative Physiology A* 2019**:**1-14.

66. Lewis P, Oster H, Korf HW, Foster RG, Erren TC: **Food as a circadian time cue — evidence from human studies.** *Nature Reviews Endocrinology* 2020, **16:**213-223.

67. Fujioka H, Abe MS, Okada Y: **Ant activity-rest rhythms vary with age and interaction frequencies of workers.** *Behavioral ecology and sociobiology* 2019, **73:**30.

68. Bloch G, Toma DP, Robinson GE: **Behavioral rhythmicity, age, division of labor and period expression in the honey bee brain.** *Journal of Biological Rhythms* 2001, **16:**444-456.

69. Ingram KK, Krummey S, LeRoux M: **Expression patterns of a circadian clock gene are associated with age-related polyethism in harvester ants, *Pogonomyrmex occidentalis*.** *BMC Ecol* 2009, **9:**7.

70. Ingram KK, Gordon DM, Friedman DA, Greene M, Kahler J, Peteru S: **Context-dependent expression of the foraging gene in field colonies of ants: the interacting roles of age, environment and task.** *Proc Biol Sci* 2016, **283**.

71. Zhang Y, Emery P: **Molecular and neural control of insect circadian rhythms.** In *Insect molecular biology and biochemistry.* Elsevier; 2012: 513-551

72. Sandrelli F, Costa R, Kyriacou CP, Rosato E: **Comparative analysis of circadian clock genes in insects.** *Insect Molecular Biology* 2008, **17:**447-463.

73. Partch CL, Green CB, Takahashi JS: **Molecular architecture of the mammalian circadian clock.** *Trends Cell Biol* 2014, **24:**90-99.

74. Top D, Young MW: **Coordination between differentially regulated circadian clocks generates rhythmic behavior.** *Cold Spring Harbor Perspectives in Biology* 2018, **10:**a033589.

75. Horne JA, Östberg O: **A self-assessment questionnaire to determine morningness-eveningness in human circadian rhythms.** *International journal of chronobiology* 1976.

76. Maury C, Serota MW, Williams TD: **Plasticity in diurnal activity and temporal phenotype during parental care in European starlings, *Sturnus vulgaris*.** *Animal Behaviour* 2020, **159:**37-45.

77. Weinert D: **Age-dependent changes of the circadian system.** *Chronobiology International* 2000, **17:**261-283.

78. Gil K-E, Park C-M: **Thermal adaptation and plasticity of the plant circadian clock.** *New Phytologist* 2019, **221:**1215-1229.

79. van der Vinne V, Riede SJ, Gorter JA, Eijer WG, Sellix MT, Menaker M, Daan S, Pilorz V, Hut RA: **Cold and hunger induce diurnality in a nocturnal mammal.** *Proceedings of the National Academy of Sciences* 2014, **111:**15256.

80. Randler C: **Sleep, sleep timing and chronotype in animal behaviour.** *Animal Behaviour* 2014, **94:**161-166.

81. Schwartz WJ, Helm B, Gerkema MP: **Wild clocks: preface and glossary.** The Royal Society; 2017.

82. Dominoni DM, Helm B, Lehmann M, Dowse HB, Partecke J: **Clocks for the city: circadian differences between forest and city songbirds.** *Proceedings of the Royal Society B: Biological Sciences* 2013, **280:**20130593.

83. Graham JL, Cook NJ, Needham KB, Hau M, Greives TJ: **Early to rise, early to breed: a role for daily rhythms in seasonal reproduction.** *Behavioral Ecology* 2017, **28:**1266-1271.

84. Sharma VK, Lone SR, Goel A: **Clocks for sex: loss of circadian rhythms in ants after mating?** *Naturwissenschaften* 2004, **91:**334-337.

85. Tripet F, Nonacs P: **Foraging for work and age-based polyethism: the roles of age and previous experience on task choice in ants.** *Ethology* 2004, **110:**863-877.

86. Moore D: **Honey bee circadian clocks: behavioral control from individual workers to whole-colony rhythms.** *Journal of Insect Physiology* 2001, **47:**843-857.

87. Bloch G, Robinson GE: **Reversal of honeybee behavioural rhythms.** *Nature* 2001, **410:**1048-1048.

88. Sharma VK, Lone SR, Mathew D, Goel A, Chandrashekaran MK: **Possible evidence for shift work schedules in the media workers of the ant species *Camponotus compressus*.** *Chronobiology International* 2004, **21:**297-308.

89. Eban-Rothschild A, Shemesh Y, Bloch G: **The colony environment, but not direct contact with conspecifics, influences the development of circadian rhythms in honey bees.** *Journal of biological rhythms* 2012, **27:**217-225.

90. Ito H, Mutsuda M, Murayama Y, Tomita J, Hosokawa N, Terauchi K, Sugita C, Sugita M, Kondo T, Iwasaki H: **Cyanobacterial daily life with Kai-based circadian and diurnal genome-wide transcriptional control in *Synechococcus elongatus*.** *Proceedings of the National Academy of Sciences* 2009, **106:**14168.

91. Rund SS, Hou TY, Ward SM, Collins FH, Duffield GE: **Genome-wide profiling of diel and circadian gene expression in the malaria vector *Anopheles gambiae*.** *Proc Natl Acad Sci U S A* 2011, **108:**E421-430.

92. Hughes ME, Grant GR, Paquin C, Qian J, Nitabach MN: **Deep sequencing the circadian and diurnal transcriptome of *Drosophila* brain.** *Genome Res* 2012, **22:**1266-1281.

93. Rund SSC, Gentile JE, Duffield GE: **Extensive circadian and light regulation of the transcriptome in the malaria mosquito *Anopheles gambiae*.** *BMC Genomics* 2013, **14:**218.

94. Zhang R, Lahens NF, Ballance HI, Hughes ME, Hogenesch JB: **A circadian gene expression atlas in mammals: implications for biology and medicine.** *Proceedings of the National Academy of Sciences* 2014, **111:**16219-16224.

95. Hurley JM, Dasgupta A, Emerson JM, Zhou X, Ringelberg CS, Knabe N, Lipzen AM, Lindquist EA, Daum CG, Barry KW: **Analysis of clock-regulated genes in *Neurospora* reveals widespread posttranscriptional control of metabolic potential.** *Proceedings of the National Academy of Sciences* 2014, **111:**16995-17002.

96. Ferrari C, Proost S, Janowski M, Becker J, Nikoloski Z, Bhattacharya D, Price D, Tohge T, Bar-Even A, Fernie A, et al: **Kingdom-wide comparison reveals the evolution of diurnal gene expression in Archaeplastida.** *Nature Communications* 2019, **10:**737.

97. Hughes ME, Abruzzi KC, Allada R, Anafi R, Arpat AB, Asher G, Baldi P, De Bekker C, Bell-Pedersen D, Blau J: **Guidelines for genome-scale analysis of biological rhythms.** *Journal of biological rhythms* 2017, **32:**380-393.

98. Laloum D, Robinson-Rechavi M: **Methods detecting rhythmic gene expression are biologically relevant only for strong signal.** *PLoS computational biology* 2020, **16:**e1007666.

99. Hansen LD, Klotz JH: *Carpenter ants of the United States and Canada.* Cornell University Press; 2005.

100. Gronenberg W, Heeren S, Hölldobler B: **Age-dependent and task-related morphological changes in the brain and the mushroom bodies of the ant *Camponotus floridanus*.** *Journal of Experimental Biology* 1996, **199:**2011-2019.

101. Feldhaar H, Straka J, Krischke M, Berthold K, Stoll S, Mueller MJ, Gross R: **Nutritional upgrading for omnivorous carpenter ants by the endosymbiont *Blochmannia*.** *BMC Biology* 2007, **5:48:**11 p.

102. Simola DF, Ye C, Mutti NS, Dolezal K, Bonasio R, Liebig J, Reinberg D, Berger SL: **A chromatin link to caste identity in the carpenter ant *Camponotus floridanus*.** *Genome Res* 2013, **23:**486-496.

103. Gupta SK, Kupper M, Ratzka C, Feldhaar H, Vilcinskas A, Gross R, Dandekar T, Forster F: **Scrutinizing the immune defence inventory of *Camponotus floridanus* applying total transcriptome sequencing.** *BMC Genomics* 2015, **16:**540.

104. Simola DF, Graham RJ, Brady CM, Enzmann BL, Desplan C, Ray A, Zwiebel LJ, Bonasio R, Reinberg D, Liebig J, Berger SL: **Epigenetic (re)programming of caste-specific behavior in the ant *Camponotus floridanus*.** *Science* 2016, **351:**aac6633.

105. Kay J, Menegazzi P, Mildner S, Roces F, Helfrich-Förster C: **The circadian clock of the ant *Camponotus floridanus* is localized in dorsal and lateral neurons of the brain.** *Journal of biological rhythms* 2018, **33:**255-271.

106. LeBoeuf AC, Cohanim AB, Stoffel C, Brent CS, Waridel P, Privman E, Keller L, Benton R: **Molecular evolution of juvenile hormone esterase-like proteins in a socially exchanged fluid.** *Sci Rep* 2018, **8:**17830.

107. Shields EJ, Sheng L, Weiner AK, Garcia BA, Bonasio R: **High-quality genome assemblies reveal long non-coding RNAs expressed in ant brains.** *Cell Rep* 2018, **23:**3078-3090.

108. Will I, Das B, Trinh T, Brachmann A, Ohm RA, de Bekker C: **Genetic underpinnings of host manipulation by *Ophiocordyceps* as revealed by comparative transcriptomics.** *G3: Genes|Genomes|Genetics* 2020**:**g3.401290.402020.

109. Ferguson ST, Park KY, Ruff AA, Bakis I, Zwiebel LJ: **Odor coding of nestmate recognition in the eusocial ant *Camponotus floridanus*.** *Journal of Experimental Biology* 2020.

110. LeBoeuf AC, Waridel P, Brent CS, Gonçalves AN, Menin L, Ortiz D, Riba-Grognuz O, Koto A, Soares ZG, Privman E: **Oral transfer of chemical cues, growth proteins and hormones in social insects.** *Elife* 2016, **5:**e20375.

111. Gautrais J, Theraulaz G, Deneubourg J-L, Anderson C: **Emergent polyethism as a consequence of increased colony size in insect societies.** *Journal of theoretical biology* 2002, **215:**363-373.

112. Jeanson R, Fewell JH, Gorelick R, Bertram SM: **Emergence of increased division of labor as a function of group size.** *Behavioral Ecology and Sociobiology* 2007, **62:**289-298.

113. Dornhaus A, Powell S, Bengston S: **Group size and its effects on collective organization.** *Annual review of entomology* 2012, **57:**123-141.

114. Klotz J, Greenberg L, Reid B, Davis Jr L: **Spatial distribution of colonies of three carpenter ants, *Camponotus pennsylvanicus, Camponotus floridanus, Camponotus laevigatus* (Hymenoptera: Formicidae).** *Sociobiology (USA)* 1998.

115. Hakala SM, Meurville M-P, Stumpe M, LeBoeuf AC: **Biomarkers in a socially exchanged fluid reflect colony maturity, behavior and distributed metabolism.** *eLife* 2021, **10:**e74005.

116. Trinh T, Ouellette R, de Bekker C: **Getting lost: the fungal hijacking of ant foraging behaviour in space and time.** *Animal Behaviour* 2021, **181:**165-184.

117. Kwapich CL, Tschinkel WR: **Demography, demand, death, and the seasonal allocation of labor in the Florida harvester ant (*Pogonomyrmex badius*).** *Behavioral Ecology and Sociobiology* 2013, **67:**2011-2027.

118. Kwapich CL, Tschinkel WR: **Limited flexibility and unusual longevity shape forager allocation in the Florida harvester ant (*Pogonomyrmex badius*).** *Behavioral ecology and sociobiology* 2016, **70:**221-235.

119. Sendova-Franks AB, Franks NR: **Spatial relationships within nests of the ant *Leptothorax unifasciatus* (Latr.) and their implications for the division of labour.** *Animal Behaviour* 1995, **50:**121-136.

120. Mersch DP, Crespi A, Keller L: **Tracking individuals shows spatial fidelity is a key regulator of ant social organization.** *Science* 2013, **340:**1090-1093.

121. Jeanson R: **Long-term dynamics in proximity networks in ants.** *Animal Behaviour* 2012, **83:**915-923.

122. Li J, Grant GR, Hogenesch JB, Hughes ME: **Considerations for RNA-seq analysis of circadian rhythms.** *Methods Enzymol* 2015, **551:**349-367.

123. de Bekker C, Bruning O, Jonker MJ, Breit TM, Wösten HA: **Single cell transcriptomics of neighboring hyphae of *Aspergillus niger*.** *Genome biology* 2011, **12:**R71.

124. Bushnell B: **BBMap short-read aligner, and other bioinformatics tools.**; 2018.

125. Kim D, Langmead B, Salzberg S: **HISAT2: graph-based alignment of next-generation sequencing reads to a population of genomes.** 2017.

126. Shields EJ, Sheng L, Weiner AK, Garcia BA, Bonasio R: **High-quality genome assemblies reveal long non-coding RNAs expressed in ant brains.** *Cell reports* 2018, **23:**3078-3090.

127. Trapnell C, Roberts A, Goff L, Pertea G, Kim D, Kelley DR, Pimentel H, Salzberg SL, Rinn JL, Pachter L: **Differential gene and transcript expression analysis of RNA-seq experiments with TopHat and Cufflinks.** *Nature protocols* 2012, **7:**562-578.

128. Rösch A, Schmidbauer H: **WaveletComp 1.1: A guided tour through the R package.** *URL: http://wwwhsstatcom/projects/WaveletComp/WaveletComp_guided_tourpdf* 2016.

129. Hutchison AL, Allada R, Dinner AR: **Bootstrapping and empirical bayes methods improve rhythm detection in sparsely sampled data.** *J Biol Rhythms* 2018, **33:**339-349.

130. Hutchison AL, Maienschein-Cline M, Chiang AH, Tabei SM, Gudjonson H, Bahroos N, Allada R, Dinner AR: **Improved statistical methods enable greater sensitivity in rhythm detection for genome-wide data.** *PLoS Comput Biol* 2015, **11:**e1004094.

131. Hughes ME, Hogenesch JB, Kornacker K: **JTK_CYCLE: an efficient nonparametric algorithm for detecting rhythmic components in genome-scale data sets.** *J Biol Rhythms* 2010, **25:**372-380.

132. Singer JM, Hughey JJ: **LimoRhyde: A flexible approach for differential analysis of rhythmic transcriptome data.** *J Biol Rhythms* 2019, **34:**5-18.

133. Romanowski A, Garavaglia MJ, Goya ME, Ghiringhelli PD, Golombek DA: **Potential conservation of circadian clock proteins in the phylum Nematoda as revealed by bioinformatic searches.** *PLoS One* 2014, **9:**e112871.

134. Eddy SR: **Accelerated profile HMM searches.** *PLoS computational biology* 2011, **7**.

135. Lechner M, Findeiß S, Steiner L, Marz M, Stadler PF, Prohaska SJ: **Proteinortho: detection of (co-) orthologs in large-scale analysis.** *BMC bioinformatics* 2011, **12:**124.

136. Team R: **RStudio: Integrated development for R [Computer software].** *URL http://wwwrstudiocom/ Boston, MA: RStudio, Inc* 2016.

137. Team RC: **R: A language and environment for statistical computing.** 2013.

138. Kolde R: **Pheatmap: Pretty Heatmaps (version 1.0. 12).** 2019.

139. Garnier S, Ross N, Rudis B, Sciaini M, Scherer C: **viridis: Default Color Maps from 'matplotlib'.** *R package version 05* 2018, **1**.

140. Conway JR, Lex A, Gehlenborg N: **UpSetR: an R package for the visualization of intersecting sets and their properties.** *Bioinformatics* 2017, **33:**2938-2940.

141. Shen L: **GeneOverlap: An R package to test and visualize gene overlaps.** *R Package* 2014.

142. Mikheyev AS, Linksvayer TA: **Genes associated with ant social behavior show distinct transcriptional and evolutionary patterns.** *Elife* 2015, **4:**e04775.

143. McArthur AJ, Hunt AE, Gillette MU: **Melatonin action and signal transduction in the rat suprachiasmatic circadian clock: activation of Protein Kinase C at dusk and dawn.** *Endocrinology* 1997, **138:**627-634.

144. Benloucif S, Dubocovich ML: **Melatonin and light induce phase shifts of circadian activity rhythms in the C3H/HeN mouse.** *Journal of Biological Rhythms* 1996, **11:**113-125.

145. Yasuo S, Yoshimura T, Ebihara S, Korf H-W: **Melatonin transmits photoperiodic signals through the MT1 melatonin receptor.** *The Journal of Neuroscience* 2009, **29:**2885.

146. Sancar C, Sancar G, Ha N, Cesbron F, Brunner M: **Dawn- and dusk-phased circadian transcription rhythms coordinate anabolic and catabolic functions in *Neurospora*.** *BMC Biology* 2015, **13:**17.

147. Bloch G, Barnes BM, Gerkema MP, Helm B: **Animal activity around the clock with no overt circadian rhythms: patterns, mechanisms and adaptive value.** *Proc Biol Sci* 2013, **280:**20130019.

148. Senthilan Pingkalai R, Piepenbrock D, Ovezmyradov G, Nadrowski B, Bechstedt S, Pauls S, Winkler M, Möbius W, Howard J, Göpfert Martin C: ***Drosophila* auditory organ genes and genetic hearing defects.** *Cell* 2012, **150:**1042-1054.

149. Sokabe T, Chen H-C, Luo J, Montell C: **A switch in thermal preference in *Drosophila* larvae depends on multiple rhodopsins.** *Cell reports* 2016, **17:**336-344.

150. Leung NY, Montell C: **Unconventional roles of opsins.** *Annual review of cell and developmental biology* 2017, **33:**241-264.

151. Kirchner W: **Acoustical communication in honeybees.** *Apidologie* 1993, **24:**297-307.

152. Kirchner W: **Acoustical communication in social insects.** In *Orientation and communication in arthropods.* Springer; 1997: 273-300

153. Fuchs S: **An informational analysis of the alarm communication by drumming behavior in nests of carpenter ants (*Camponotus*, Formicidae, Hymenoptera).** *Behavioral Ecology and Sociobiology* 1976, **1:**315-336.

154. Fuchs S: **The response to vibrations of the substrate and reactions to the specific drumming in colonies of carpenter ants (*Camponotus*, Formicidae, Hymenoptera).** *Behavioral Ecology and Sociobiology* 1976, **1:**155-184.

155. Lin J-M, Kilman VL, Keegan K, Paddock B, Emery-Le M, Rosbash M, Allada R: **A role for casein kinase 2α in the Drosophila circadian clock.** *Nature* 2002, **420:**816-820.

156. Lin J-M, Schroeder A, Allada R: ***In vivo* circadian function of casein kinase 2 phosphorylation sites in *Drosophila* PERIOD.** *Journal of Neuroscience* 2005, **25:**11175-11183.

157. Szabó Á, Papin C, Zorn D, Ponien P, Weber F, Raabe T, Rouyer F: **The CK2 kinase stabilizes CLOCK and represses its activity in the *Drosophila* circadian oscillator.** *PLoS Biol* 2013, **11:**e1001645.

158. Top D, Harms E, Syed S, Adams EL, Saez L: **GSK-3 and CK2 kinases converge on timeless to regulate the master clock.** *Cell reports* 2016, **16:**357-367.

159. Ananthasubramaniam B, Diernfellner A, Brunner M, Herzel H: **Ultradian rhythms in the transcriptome of *Neurospora crassa*.** *Iscience* 2018, **9:**475-486.

160. Biscontin A, Martini P, Costa R, Kramer A, Meyer B, Kawaguchi S, Teschke M, De Pittà C: **Analysis of the circadian transcriptome of the Antarctic krill *Euphausia superba*.** *Scientific reports* 2019, **9:**1-11.

161. Connor KM, Gracey AY: **Circadian cycles are the dominant transcriptional rhythm in the intertidal mussel *Mytilus californianus*.** *Proceedings of the National Academy of Sciences* 2011, **108:**16110-16115.

162. Hughes ME, DiTacchio L, Hayes KR, Vollmers C, Pulivarthy S, Baggs JE, Panda S, Hogenesch JB: **Harmonics of circadian gene transcription in mammals.** *PLoS Genet* 2009, **5:**e1000442.

163. Payton L, Perrigault M, Hoede C, Massabuau J-C, Sow M, Huvet A, Boullot F, Fabioux C, Hegaret H, Tran D: **Remodeling of the cycling transcriptome of the oyster *Crassostrea gigas* by the harmful algae *Alexandrium minutum*.** *Scientific reports* 2017, **7:**1-14.

164. Satoh A, Terai Y: **Circatidal gene expression in the mangrove cricket *Apteronemobius asahinai*.** *Scientific reports* 2019, **9:**1-7.

165. Schnytzer Y, Simon-Blecher N, Li J, Ben-Asher HW, Salmon-Divon M, Achituv Y, Hughes M, Levy O: **Tidal and diel orchestration of behaviour and gene expression in an intertidal mollusc.** *Scientific reports* 2018, **8:**1-13.

166. Payton L, Hüppe L, Noirot C, Hoede C, Last KS, Wilcockson D, Ershova E, Valière S, Meyer B: **Widely rhythmic transcriptome in *Calanus finmarchicus* during the high Arctic summer solstice period.** *iScience* 2021, **24**.

167. Toma DP, Bloch G, Moore D, Robinson GE: **Changes in period mRNA levels in the brain and division of labor in honey bee colonies.** *Proceedings of the National Academy of Sciences* 2000, **97:**6914-6919.

168. Abruzzi KC, Rodriguez J, Menet JS, Desrochers J, Zadina A, Luo W, Tkachev S, Rosbash M: ***Drosophila*** **CLOCK target gene characterization: implications for circadian tissue-specific gene expression.** *Genes & development* 2011, **25:**2374-2386.

169. Martinek S, Inonog S, Manoukian AS, Young MW: **A role for the segment polarity gene *shaggy*/GSK-3 in the *Drosophila* circadian clock.** *Cell* 2001, **105:**769-779.

170. Ko HW, Kim EY, Chiu J, Vanselow JT, Kramer A, Edery I: **A hierarchical phosphorylation cascade that regulates the timing of PERIOD nuclear entry reveals novel roles for proline-directed kinases and GSK-3β/SGG in circadian clocks.** *The Journal of Neuroscience* 2010, **30:**12664.

171. Kloss B, Price JL, Saez L, Blau J, Rothenfluh A, Wesley CS, Young MW: **The *Drosophila* clock gene *double-time* encodes a protein closely related to human Casein Kinase Iε.** *Cell* 1998, **94:**97-107.

172. Price JL, Blau J, Rothenfluh A, Abodeely M, Kloss B, Young MW: ***double-time*** **is a novel *Drosophila* clock gene that regulates PERIOD protein accumulation.** *Cell* 1998, **94:**83-95.

173. Cyran SA, Yiannoulos G, Buchsbaum AM, Saez L, Young MW, Blau J: **The Double-Time protein kinase regulates the subcellular localization of the *Drosophila* clock protein Period.** *The Journal of Neuroscience* 2005, **25:**5430.

174. Chiu Joanna C, Ko Hyuk W, Edery I: **NEMO/NLK phosphorylates PERIOD to initiate a time-delay phosphorylation circuit that sets circadian clock speed.** *Cell* 2011, **145:**357-370.

175. Akten B, Jauch E, Genova GK, Kim EY, Edery I, Raabe T, Jackson FR: **A role for CK2 in the *Drosophila* circadian oscillator.** *Nature Neuroscience* 2003, **6:**251-257.

176. Li Y, Guo F, Shen J, Rosbash M: **PDF and cAMP enhance PER stability in *Drosophila* clock neurons.** *Proceedings of the National Academy of Sciences* 2014, **111:**E1284-E1290.

177. Fang Y, Sathyanarayanan S, Sehgal A: **Post-translational regulation of the *Drosophila* circadian clock requires Protein Phosphatase 1 (PP1).** *Genes & development* 2007, **21:**1506-1518.

178. Sathyanarayanan S, Zheng X, Xiao R, Sehgal A: **Posttranslational regulation of *Drosophila* PERIOD protein by Protein Phosphatase 2A.** *Cell* 2004, **116:**603-615.

179. Huang Y, Ainsley JA, Reijmers LG, Jackson FR: **Translational profiling of clock cells reveals circadianly synchronized protein synthesis.** *PLOS Biology* 2013, **11:**e1001703.

180. Li S, Shui K, Zhang Y, Lv Y, Deng W, Ullah S, Zhang L, Xue Y: **CGDB: a database of circadian genes in eukaryotes.** *Nucleic Acids Research* 2016**:**gkw1028.

181. Shapiro RA, Wakimoto BT, Subers EM, Nathanson NM: **Characterization and functional expression in mammalian cells of genomic and cDNA clones encoding a *Drosophila* muscarinic acetylcholine receptor.** *Proceedings of the National Academy of Sciences* 1989, **86:**9039.

182. Harrison JB, Chen HH, Blake AD, Huskisson NS, Barker P, Sattelle DB: **Localization in the nervous system of *Drosophila melanogaster* of a C-terminus anti-peptide antibody to a cloned *Drosophila* muscarinic acetylcholine receptor.** *Journal of Neuroendocrinology* 1995, **7:**347-352.

183. Inagaki HK, Panse KM, Anderson DJ: **Independent, reciprocal neuromodulatory control of sweet and bitter taste sensitivity during starvation in *Drosophila*.** *Neuron* 2014, **84:**806-820.

184. Petruccelli E, Li Q, Rao Y, Kitamoto T: **The unique Dopamine/Ecdysteroid receptor modulates ethanol-induced sedation in *Drosophila*.** *The Journal of neuroscience : the official journal of the Society for Neuroscience* 2016, **36:**4647-4657.

185. Abrieux A, Duportets L, Debernard S, Gadenne C, Anton S: **The GPCR membrane receptor, DopEcR, mediates the actions of both dopamine and ecdysone to control sex pheromone perception in an insect.** *Frontiers in behavioral neuroscience* 2014, **8:**312-312.

186. Kang X-L, Zhang J-Y, Wang D, Zhao Y-M, Han X-L, Wang J-X, Zhao X-F: **The steroid hormone 20-hydroxyecdysone binds to dopamine receptor to repress lepidopteran insect feeding and promote pupation.** *PLOS Genetics* 2019, **15:**e1008331.

187. Kamhi JF, Traniello JF: **Biogenic amines and collective organization in a superorganism: neuromodulation of social behavior in ants.** *Brain, behavior and evolution* 2013, **82:**220-236.

188. Friedman DA, Gordon DM: **Ant genetics: Reproductive physiology, worker morphology, and behavior.** *Annu Rev Neurosci* 2016, **39:**41-56.

189. Beninger RJ: **The role of dopamine in locomotor activity and learning.** *Brain Research Reviews* 1983, **6:**173-196.

190. Grippo RM, Güler AD: **Dopamine signaling in circadian photoentrainment: Consequences of desynchrony.** *The Yale journal of biology and medicine* 2019, **92:**271.

191. Liang X, Ho MC, Zhang Y, Li Y, Wu MN, Holy TE, Taghert PH: **Morning and evening circadian pacemakers independently drive premotor centers via a specific dopamine relay.** *Neuron* 2019, **102:**843-857. e844.

192. Blum ID, Zhu L, Moquin L, Kokoeva MV, Gratton A, Giros B, Storch K-F: **A highly tunable dopaminergic oscillator generates ultradian rhythms of behavioral arousal.** *Elife* 2014, **3:**e05105.

193. Zhu B, Zhang Q, Pan Y, Mace EM, York B, Antoulas AC, Dacso CC, O'Malley BW: **A cell-autonomous mammalian 12 hr clock coordinates metabolic and stress rhythms.** *Cell metabolism* 2017, **25:**1305-1319. e1309.

194. van der Veen DR, Gerkema MP: **Unmasking ultradian rhythms in gene expression.** *The FASEB Journal* 2017, **31:**743-750.

195. Roces F: **Variable thermal sensitivity as output of a circadian clock controlling the bimodal rhythm of temperature choice in the ant *Camponotus mus*.** *Journal of Comparative Physiology A* 1995, **177:**637-643.

196. Roces F, Nunez JA: **A circadian rhythm of thermal preference in the ant *Camponotus mus*: masking and entrainment by temperature cycles.** *Physiological Entomology* 1996, **21:**138-142.

197. Helfrich-Förster C: **The *period* clock gene is expressed in central nervous system neurons which also produce a neuropeptide that reveals the projections of circadian pacemaker cells within the brain of *Drosophila melanogaster*.** *Proceedings of the National Academy of Sciences* 1995, **92:**612-616.

198. Helfrich-Förster C: **Robust circadian rhythmicity of *Drosophila melanogaster* requires the presence of lateral neurons: a brain-behavioral study of disconnected mutants.** *Journal of Comparative Physiology A* 1998, **182:**435-453.

199. Renn SCP, Park JH, Rosbash M, Hall JC, Taghert PH: **A *pdf* neuropeptide gene mutation and ablation of PDF neurons each cause severe abnormalities of behavioral circadian rhythms in *Drosophila*.** *Cell* 1999, **99:**791-802.

200. Stoleru D, Peng Y, Agosto J, Rosbash M: **Coupled oscillators control morning and evening locomotor behaviour of *Drosophila*.** *Nature* 2004, **431:**862-868.

201. Majercak J, Kalderon D, Edery I: ***Drosophila melanogaster* deficient in protein kinase A manifests behavior-specific arrhythmia but normal clock function.** *Molecular and Cellular Biology* 1997, **17:**5915.

202. Petri B, Stengl M: **Pigment-dispersing hormone shifts the phase of the circadian pacemaker of the cockroach *Leucophaea maderae*.** *Journal of Neuroscience* 1997, **17:**4087-4093.

203. Peng Y, Stoleru D, Levine JD, Hall JC, Rosbash M: ***Drosophila* free-running rhythms require intercellular communication.** *PLoS Biol* 2003, **1:**e13.

204. Saifullah A, Tomioka K: **Pigment-dispersing factor sets the night state of the medulla bilateral neurons in the optic lobe of the cricket, *Gryllus bimaculatus*.** *Journal of insect physiology* 2003, **49:**231-239.

205. Singaravel M, Fujisawa Y, Hisada M, Saifullah A, Tomioka K: **Phase shifts of the circadian locomotor rhythm induced by pigment-dispersing factor in the cricket *Gryllus bimaculatus*.** *Zoological science* 2003, **20:**1347-1354.

206. Lin Y, Stormo GD, Taghert PH: **The neuropeptide pigment-dispersing factor coordinates pacemaker interactions in the *Drosophila* circadian system.** *Journal of Neuroscience* 2004, **24:**7951-7957.

207. Yoshii T, Wülbeck C, Sehadova H, Veleri S, Bichler D, Stanewsky R, Helfrich-Förster C: **The neuropeptide pigment-dispersing factor adjusts period and phase of *Drosophila*'s clock.** *Journal of Neuroscience* 2009, **29:**2597-2610.

208. Schendzielorz J, Schendzielorz T, Arendt A, Stengl M: **Bimodal oscillations of cyclic nucleotide concentrations in the circadian system of the Madeira cockroach *Rhyparobia maderae*.** *Journal of biological rhythms* 2014, **29:**318-331.

209. Liang X, Holy TE, Taghert PH: **Synchronous *Drosophila* circadian pacemakers display nonsynchronous Ca2+ rhythms in vivo.** *Science* 2016, **351:**976-981.

210. Liang X, Holy TE, Taghert PH: **A series of suppressive signals within the *Drosophila* circadian neural circuit generates sequential daily outputs.** *Neuron* 2017, **94:**1173-1189. e1174.

211. Helfrich-Förster C, Homberg U: **Pigment-dispersing hormone-immunoreactive neurons in the nervous system of wild-type *Drosophila melanogaster* and of several mutants with altered circadian rhythmicity.** *Journal of Comparative Neurology* 1993, **337:**177-190.

212. Beer K, Kolbe E, Kahana NB, Yayon N, Weiss R, Menegazzi P, Bloch G, Helfrich-Förster C: **Pigment-Dispersing Factor-expressing neurons convey circadian information in the honey bee brain.** *Open Biology*, **8:**170224.

213. Fuchikawa T, Beer K, Linke-Winnebeck C, Ben-David R, Kotowoy A, Tsang V, Warman G, Winnebeck E, Helfrich-Förster C, Bloch G: **Neuronal circadian clock protein oscillations are similar in behaviourally rhythmic forager honeybees and in arrhythmic nurses.** *Open biology* 2017, **7:**170047.

214. Robinson GE, Grozinger CM, Whitfield CW: **Sociogenomics: social life in molecular terms.** *Nature Reviews Genetics* 2005, **6:**257-270.

215. Ament SA, Corona M, Pollock HS, Robinson GE: **Insulin signaling is involved in the regulation of worker division of labor in honey bee colonies.** *Proceedings of the National Academy of Sciences* 2008, **105:**4226.

216. Alaux C, Sinha S, Hasadsri L, Hunt GJ, Guzmán-Novoa E, DeGrandi-Hoffman G, Uribe-Rubio JL, Southey BR, Rodriguez-Zas S, Robinson GE: **Honey bee aggression supports a link between gene regulation and behavioral evolution.** *Proceedings of the National Academy of Sciences* 2009, **106:**15400.

217. Chandrasekaran S, Ament SA, Eddy JA, Rodriguez-Zas SL, Schatz BR, Price ND, Robinson GE: **Behavior-specific changes in transcriptional modules lead to distinct and predictable neurogenomic states.** *Proceedings of the National Academy of Sciences* 2011, **108:**18020.

218. Manfredini F, Lucas C, Nicolas M, Keller L, Shoemaker D, Grozinger CM: **Molecular and social regulation of worker division of labour in fire ants.** *Molecular Ecology* 2014, **23:**660-672.

219. Kamita SG, Hinton AC, Wheelock CE, Wogulis MD, Wilson DK, Wolf NM, Stok JE, Hock B, Hammock BD: **Juvenile hormone (JH) esterase: why are you so JH specific?** *Insect Biochemistry and Molecular Biology* 2003, **33:**1261-1273.

220. Warner MR, Qiu L, Holmes MJ, Mikheyev AS, Linksvayer TA: **Convergent eusocial evolution is based on a shared reproductive groundplan plus lineage-specific plastic genes.** *Nature communications* 2019, **10:**1-11.

221. Amdam GV, Norberg K, Hagen A, Omholt SW: **Social exploitation of vitellogenin.** *Proceedings of the National Academy of Sciences* 2003, **100:**1799.

222. Antonio DSM, Guidugli-Lazzarini KR, Do Nascimento AM, Simões ZLP, Hartfelder K: **RNAi-mediated silencing of *vitellogenin* gene function turns honeybee (*Apis mellifera*) workers into extremely precocious foragers.** *Naturwissenschaften* 2008, **95:**953-961.

223. Hawkings C, Calkins TL, Pietrantonio PV, Tamborindeguy C: **Caste-based differential transcriptional expression of hexamerins in response to a juvenile hormone analog in the red imported fire ant (*Solenopsis invicta*).** *PLOS ONE* 2019, **14:**e0216800.

224. Andersen SB, Ferrari M, Evans HC, Elliot SL, Boomsma JJ, Hughes DP: **Disease dynamics in a specialized parasite of ant societies.** *PloS one* 2012, **7:**e36352.

225. de Bekker C, Das B: **Hijacking time: How *Ophiocordyceps* fungi could be using ant host clocks to manipulate behavior.** *Parasite Immunology* 2022**:**e12909.

226. Das B, de Bekker C: **Time-course RNASeq of *Camponotus floridanus* forager and nurse ant brains indicate links between plasticity in the biological clock and behavioral division of labor.** *BMC Genomics* 2022, **23:**57.

227. Will I, Das B, Trinh T, Brachmann A, Ohm RA, de Bekker C: **Genetic Underpinnings of Host Manipulation by *Ophiocordyceps* as Revealed by Comparative Transcriptomics.** *G3: Genes|Genomes|Genetics* 2020**:**g3.401290.402020.

228. de Bekker C, Beckerson WC, Elya C: **Mechanisms behind the Madness: How Do Zombie-Making Fungal Entomopathogens Affect Host Behavior To Increase Transmission?** *Mbio* 2021, **12:**e01872-01821.

229. Huang S, Keyhani NO, Zhao X, Zhang Y: **The Thm1 Zn (II) 2Cys6 transcription factor contributes to heat, membrane integrity and virulence in the insect pathogenic fungus *Beauveria* bassiana.** *Environmental microbiology* 2019, **21:**3153-3171.

230. Ying SH, Feng MG: **Medium components and culture conditions affect the thermotolerance of aerial conidia of fungal biocontrol agent *Beauveria* bassiana.** *Letters in applied microbiology* 2006, **43:**331-335.

231. Xiao G, Ying S-H, Zheng P, Wang Z-L, Zhang S, Xie X-Q, Shang Y, St. Leger RJ, Zhao G-P, Wang C, Feng M-G: **Genomic perspectives on the evolution of fungal entomopathogenicity in *Beauveria* bassiana.** *Scientific Reports* 2012, **2:**483.

232. MacFarland TW, Yates JM: **Kruskal–Wallis H-test for oneway analysis of variance (ANOVA) by ranks.** In *Introduction to nonparametric statistics for the biological sciences using R.* Springer; 2016: 177-211

233. Bauer DF: **Constructing confidence sets using rank statistics.** *Journal of the American Statistical Association* 1972, **67:**687-690.

234. Kassambara A, Kassambara MA: **Package 'ggpubr'.** *R package version 01* 2020, **6**.

235. Das B: **timecourseRnaseq: an R package to analyze time-course RNAseq data.** 2022.

236. Wickham H: **ggplot2.** *Wiley interdisciplinary reviews: computational statistics* 2011, **3:**180-185.

237. Langfelder P, Horvath S: **WGCNA: an R package for weighted correlation network analysis.** *BMC Bioinformatics* 2008, **9:**559.

238. Langfelder P, Horvath S: **Tutorials for the WGCNA Package.** UCLA; 2014.

239. Langfelder P, Luo R, Oldham MC, Horvath S: **Is My Network Module Preserved and Reproducible?** *PLOS Computational Biology* 2011, **7:**e1001057.

240. Samara B, Randles RH: **A test for correlation based on Kendall's tau.** *Communications in statistics-theory and methods* 1988, **17:**3191-3205.

241. Csardi MG: **Package 'igraph'.** *Last accessed* 2013, **3:**2013.

242. Mangold CA, Ishler MJ, Loreto RG, Hazen ML, Hughes DP: **Zombie ant death grip due to hypercontracted mandibular muscles.** *Journal of Experimental Biology* 2019, **222:**jeb200683.

243. Rollmann SM, Wang P, Date P, West SA, Mackay TFC, Anholt RRH: **Odorant Receptor Polymorphisms and Natural Variation in Olfactory Behavior in *Drosophila melanogaster*.** *Genetics* 2010, **186:**687-697.

244. Goettel MS, St Leger RJ, Rizzo NW, Staples RC, Roberts DW: **Ultrastructural localization of a cuticle-degrading protease produced by the entomopathogenic fungus Metarhizium anisopliae during penetration of host (Manduca sexto) cuticle.** *Microbiology* 1989, **135:**2233-2239.

245. Zhang X, Yang Y, Zhang L: **Ultrastructure of the entomopathogenic fungus Metarhizium anisopliae during cuticle penetration in the locust, Locusta migratoria (Insecta: Acrididae).** *Journal of Orthoptera Research* 2010**:**115-119.

246. Standiford DM, Davis MB, Miedema K, Franzini-Armstrong C, Emerson Jr CP: **Myosin rod protein: a novel thick filament component of Drosophila muscle.** *Journal of molecular biology* 1997, **265:**40-55.

247. Li BX, Satoh AK, Ready DF: **Myosin V, Rab11, and dRip11 direct apical secretion and cellular morphogenesis in developing Drosophila photoreceptors.** *The Journal of cell biology* 2007, **177:**659-669.

248. Viswanathan MC, Tham RC, Kronert WA, Sarsoza F, Trujillo AS, Cammarato A, Bernstein SI: **Myosin storage myopathy mutations yield defective myosin filament assembly in vitro and disrupted myofibrillar structure and function in vivo.** *Human molecular genetics* 2017, **26:**4799-4813.

249. Trujillo AS, Hsu KH, Puthawala J, Viswanathan MC, Loya A, Irving TC, Cammarato A, Swank DM, Bernstein SI: **Myosin dilated cardiomyopathy mutation S532P disrupts actomyosin interactions, leading to altered muscle kinetics, reduced locomotion, and cardiac dilation in Drosophila.** *Molecular biology of the cell* 2021, **32:**1690-1706.

250. Mecklenburg KL, Takemori N, Komori N, Chu B, Hardie RC, Matsumoto H, O'Tousa JE: **Retinophilin is a light-regulated phosphoprotein required to suppress photoreceptor dark noise in Drosophila.** *Journal of Neuroscience* 2010, **30:**1238-1249.

251. Venkatachalam K, Wasserman D, Wang X, Li R, Mills E, Elsaesser R, Li H-S, Montell C: **Dependence on a retinophilin/myosin complex for stability of PKC and INAD and termination of phototransduction.** *Journal of Neuroscience* 2010, **30:**11337-11345.

252. Lin Y-J, Seroude L, Benzer S: **Extended life-span and stress resistance in the Drosophila mutant methuselah.** *Science* 1998, **282:**943-946.

253. Min K-T, Benzer S: **Preventing neurodegeneration in the Drosophila mutant bubblegum.** *Science* 1999, **284:**1985-1988.

254. Krieger MJ, Ross KG: **Identification of a major gene regulating complex social behavior.** *Science* 2002, **295:**328-332.

255. Kim BY, Jin BR: **Molecular characterization of a venom acid phosphatase from the Asiatic honeybee Apis cerana.** *Journal of Asia-Pacific Entomology* 2016, **19:**793-797.

256. Dominguez CV, Maestro JL: **Expression of juvenile hormone acid O-methyltransferase and juvenile hormone synthesis in Blattella germanica.** *Insect science* 2018, **25:**787-796.

257. Hafer-Hahmann N: **Experimental evolution of parasitic host manipulation.** *Proceedings of the Royal Society B* 2019, **286:**20182413.

258. de Bekker C, Will I, Das B, Adams RM: **The ants (Hymenoptera: Formicidae) and their parasites: effects of parasitic manipulations and host responses on ant behavioral ecology.** *Myrmecological News* 2018, **28**.

259. Poulin R, Maure F: **Host Manipulation by Parasites: A Look Back Before Moving Forward.** *Trends in Parasitology* 2015, **31:**563-570.

260. Araújo JP, Hughes DP: **Zombie-ant fungi emerged from non-manipulating, beetle-infecting ancestors.** *Current Biology* 2019, **29:**3735-3738. e3732.

261. Prior KF, Middleton B, Owolabi AT, Westwood ML, Holland J, O'Donnell AJ, Blackman MJ, Skene DJ, Reece SE: **Synchrony between daily rhythms of malaria parasites and hosts is driven by an essential amino acid.** *Wellcome Open Research* 2021, **6**.

262. O'Donnell AJ, Greischar MA, Reece SE: **Mistimed malaria parasites re-synchronize with host feeding-fasting rhythms by shortening the duration of intra-erythrocytic development.** *Parasite Immunology* 2021**:**e12898.

263. Patke A, Young MW, Axelrod S: **Molecular mechanisms and physiological importance of circadian rhythms.** *Nature reviews Molecular cell biology* 2020, **21:**67-84.

264. Schafmeier T, Diernfellner AC: **Light input and processing in the circadian clock of Neurospora.** *FEBS letters* 2011, **585:**1467-1473.

265. Li J, Grant GR, Hogenesch JB, Hughes ME: **Considerations for RNA-seq analysis of circadian rhythms.** In *Methods in enzymology. Volume* 551: Elsevier; 2015: 349-367

266. Gao M, Glenn AE, Blacutt AA, Gold SE: **Fungal lactamases: their occurrence and function.** *Frontiers in Microbiology* 2017, **8:**1775.

267. Xu C, Min J: **Structure and function of WD40 domain proteins.** *Protein & cell* 2011, **2:**202-214.

268. Xin S, Zhang W: **Construction and analysis of the protein–protein interaction network for the olfactory system of the silkworm Bombyx mori.** *Archives of Insect Biochemistry and Physiology* 2020, **105:**e21737.

269. Portoles S, Mas P: **The functional interplay between protein kinase CK2 and CCA1 transcriptional activity is essential for clock temperature compensation in Arabidopsis.** *PLoS genetics* 2010, **6:**e1001201.

270. Han Y, van Houte S, van Oers MM, Ros VID: **Timely trigger of caterpillar zombie behaviour: temporal requirements for light in baculovirus-induced tree-top disease.** *Parasitology* 2018, **145:**822-827.

271. Reeves EP, Messina C, Doyle S, Kavanagh K: **Correlation between gliotoxin production and virulence of Aspergillus fumigatus in Galleria mellonella.** *Mycopathologia* 2004, **158:**73-79.

272. Gin E, Diernfellner AC, Brunner M, Höfer T: **The Neurospora photoreceptor VIVID exerts negative and positive control on light sensing to achieve adaptation.** *Molecular systems biology* 2013, **9:**667.

273. Yu Z, Fischer R: **Light sensing and responses in fungi.** *Nature Reviews Microbiology* 2019, **17:**25-36.

274. Burger G, Strauss J, Scazzocchio C, Lang B: **nirA, the pathway-specific regulatory gene of nitrate assimilation in Aspergillus nidulans, encodes a putative GAL4-type zinc finger protein and contains four introns in highly conserved regions.** *Molecular and cellular biology* 1991, **11:**5746-5755.

275. Ramalho CB, Hastings JW, Colepicolo P: **Circadian oscillation of nitrate reductase activity in Gonyaulax polyedra is due to changes in cellular protein levels.** *Plant physiology* 1995, **107:**225-231.

276. Roenneberg T, Rehman J: **Nitrate, a nonphotic signal for the circadian system.** *The FASEB Journal* 1996, **10:**1443-1447.

277. Wijnen H, Young MW: **Interplay of Circadian Clocks and Metabolic Rhythms.** *Annual Review of Genetics* 2006, **40:**409-448.